Proceedings of YRIS Meeting

Oct. 25-26 2007
KAGA city

Yellow River Project

Research Institute for Humanity and Nature

PREFACE

This is the final proceedings of the domestic study meeting for the Yellow River Study holding once every year by the whole members during two days on October 25-26 at Kaga City. As we didn't hold an international workshop this year, we determined to have to write our final study results in English, also. And we have decided to publish our final YRiS News Letter as Vol. 8, soon. This project is composed of seven sub-study teams, these are "Social-economical water team" under the leadership of Professor IMURA, Hidefumi who belongs to Nagoya University, "Real status of large irrigated agricultural fields in the Yellow River basin" under the leadership of Professor WATANABE, Tsugihiro, RIHN, "Observation and analysis of the boundary layer in Loess Plateau" under the leadership of Associate Professor HIYAMA, Tetsuya who belongs to Nagoya University, "Hydrological analysis of the long-term change of water budget by human activities" under the leadership of Senior Scientist SATO, Yoshinobu, RIHN, "Historical understanding of river channel changes downstream" under the leadership of Professor KINOSHITA, Tetsuya, RIHN, "Groundwater investigation downstream" under the leadership of Associate Professor TANIGUCHI, Makoto, RIHN, and "Changes of biological basic production in Bohai Sea" under the leadership of Professor YANAGI, Tetsuo who belongs to Kyushu University. I'm in charge of the role of coordination and bring each result successful conclusion. Fortunately, we have got fruitful results. These are seen in the proceedings.

I have already published a book for general readers on January 2008 and we are to publish a textbook for student and graduate student relevant to environmental sciences including not only natural sciences, but human sciences written by our members on March 2008. If possible, we wish to translate it in English version in future.

Although we have clarified a cause of the dry-up of the Yellow River begun since 1970s quantitatively, we became aware of polluted river water of the Yellow River, in the same time. But we didn't argue this issue positively. If possible, our results could contribute to Chinese countermeasures against water pollution, also.

January 29, 2008
FUKUSHIMA, Yoshihiro (RIHN)
Leader of the Yellow River Project

CONTENTS

V . Observed results of Atmospheric Boundary Layer

VI . Land use change and long term water budget

Investigation of fresh and salt water distribution by resistivity method in Yellow River Delta

Tomotoshi Ishitobi（Research Institute for Humanity and Nature）

Introduction:

Purposes of Yellow River Delta group are 1) to evaluate groundwater and river water discharges and their dissolved material transports into the Bo-Hai Sea, 2) to evaluate the effect of recent Yellow River cut-off due to changes in land utilization and water management on groundwater and Bo-Hai Sea, and 3) to evaluate the interactions between Yellow River, groundwater and Bo-Hai Sea in the delta. Therefore, we have to know the condition of present groundwater in the delta for our goal.

Yellow River Delta is expanding at a speed of about 500m/y by sedimentation (Yu 2002). However, speed of groundwater flow is very slow in general. Therefore, it is assumed that there is a possibility which paleo-seawater remains under the delta. Moreover, it is also assumed that saltwater intrusion into the subsurface under the delta occurs, because Yellow River basin has some problems concern water environment such as the cut-off of river water and over-pumping of groundwater. Therefore, purpose of this study is to clarify of fresh and salt water distribution under the land.

Methods

Study methods are resistivity measurement and conductivity measurement of groundwater. Resistivity method is the technique for understanding of subsurface construction by applying the electric current to the subsurface. Resistivity values and conductivity has negative correlation. Therefore, if we clarify the relationship between resistivity and conductivity in this delta, we can estimate the distributions of fresh and salt water in the area where there is no observation well. Additionally, measurements of stable isotope and carbon 14 dating of groundwater were done for the clarifying the origin.

Results and discussion:

Fig.1 shows groundwater levels in the Yellow River Delta. In this figure, it is seen that the flow to the Bo-hai sea from the Yellow River. Fig.2 shows spatial distributions of electric conductivity in the Yellow River Delta. We can see high concentrations of groundwater conductivity at the central part and the coastal zone of the Yellow River Delta. And related to the fig.2, fig.3 indicates the relationship between conductivity and depth of groundwater in the Yellow River Delta. There are few wells at the deeper part, and it is difficult to take the groundwater samples to measure the conductivity (in fact, there is a few wells at deeper part than 200m depth).

We apply the resistivity method to assume the conductivity of groundwater in the Yellow River Delta, because it is difficult to take the groundwater samples at deeper part. Fig.4 shows all results of resistivity measurement. In these figures, darker color indicates high resistivity values, and lighter color indicates low resistivity values. And, width and height of figure are 150m and 100m. Comparisons of resistivity and conductivity have been done to confirm whether it has negative correlation in the delta also. Comparison was done by datasets of the point where both measurements were done. For example, if groundwater was corrected from 5 to 20m depths, resistivity datasets at the same depth were used for the comparison. Fig.4 is the result of comparison. Resistivity and conductivity have the negative correlation clearly. Therefore, it is

thought that low resistivity indicates high conductivity and saltier water, and high resistivity indicates low conductivity and fresher water.

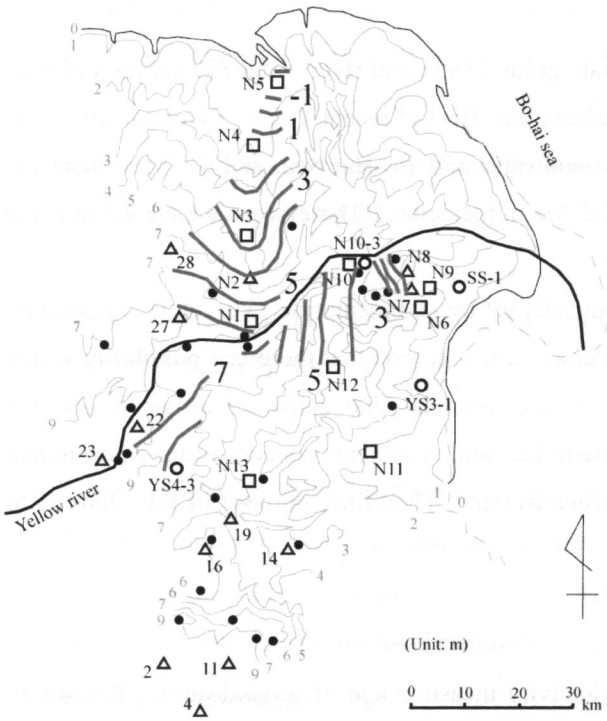

Fig.1 Spatial distributions of groundwater table

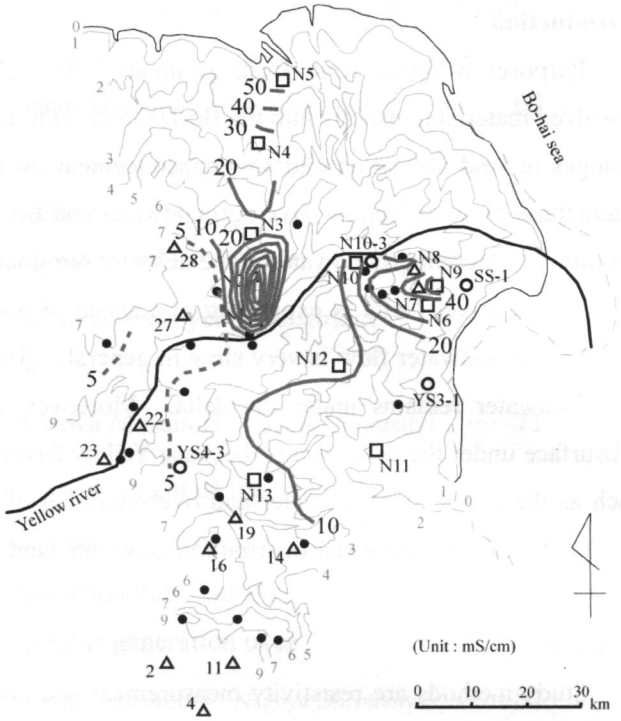

Fig.2 Spatial distributions of groundwater conductivity

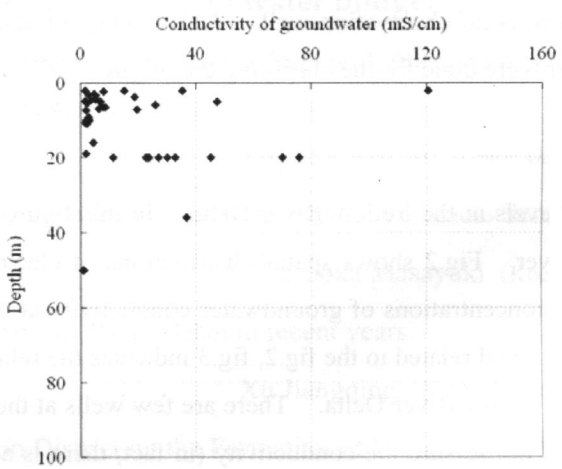

Fig.3 Conductivity of groundwater vs depth

Fig.4 indicates results of resistivity measurement. It shows several patterns of resistivity distributions under the ground. We can separate it to three patterns, first one is low resistivity regions at shallower part and high regions at deeper part (N1, YS3-2, YS4-1 and etc), second one is high regions at shallower part and low regions at deeper part (N3, N4, YS4-2, YS4-3 and etc), and last one is little change of resistivity values in the result (N4, YS3-1 and etc).

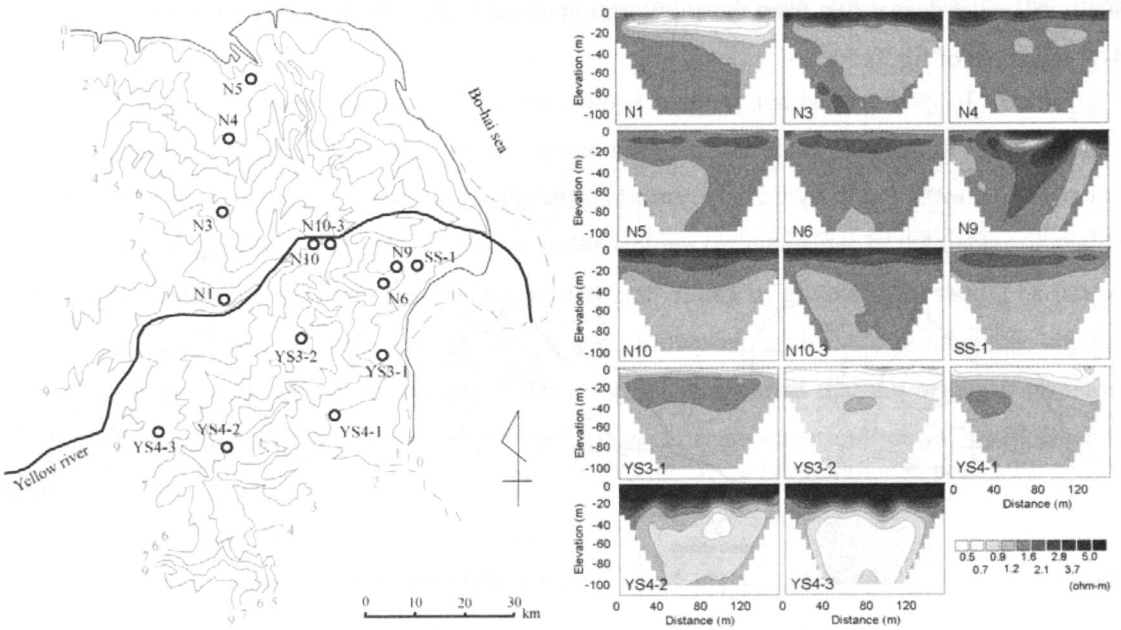

Fig.4 Results of resistivity measurement in the Yellow River delta

Fig.5 indicates conductivity of groundwater and resistivity under the ground. According to fig.5, we can see the negative correlation between conductivity and resistivity clearly. Below expression was from fig.5.

$$Cg = 44.469\ \rho^{-1.1636} \qquad (1)$$

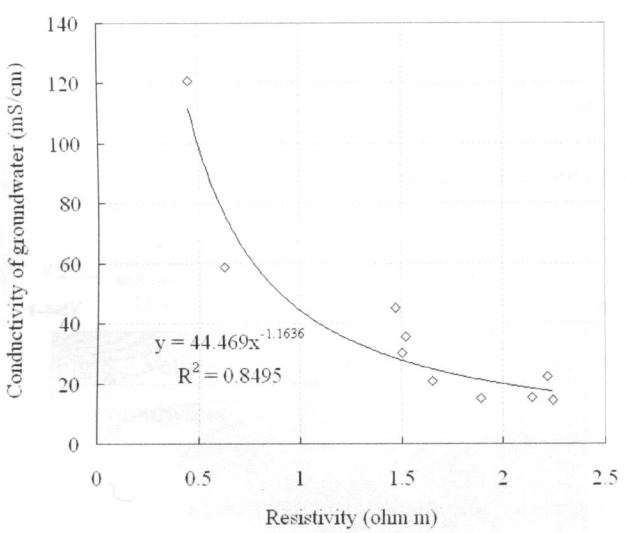

Fig.5 Conductivity of groundwater and resistivity under the ground

Therefore, we can assume the conductivity of groundwater at the point where we can not take water samples from the results of resistivity measurement and (1) expression. Spatial distributions of estimated conductivity from resistivity measurement were indicated in fig.6. From the result of 10m depth in fig.6, low conductivity values were seen in southern part (YS4-3 and N13), eastern part (N9) and northern part (N5) of the delta. On the other hand, high conductivity values were seen in center part of the delta (N1 and N12). In fact, we can see low conductivity values at YS4-3 and N13, and high conductivity values at N1 and N12 from fig.2. According to the result of 20m depth in fig.6, low conductivity values were seen at N9, YS4-3 and N13 as the result of 10m depth. It is estimated that there are saltwater widely in deeper part than 30m depth under the ground. Fig.7 shows cross sections of conductivity estimated based on fig.6. From the cross section of the Yellow river to northern part of the delta (N1 to N4, left side of fig.7), it was seen the high conductivity region near the Yellow River, and this region expands to the sea side related to the groundwater flow. On the other

hand, there is the lower conductivity groundwater recharged from the Yellow River above the high conductivity one in deeper part from the cross section of the Yellow River to eastern part of the delta (YS4-3 to YS 4-1, right side of fig.7).

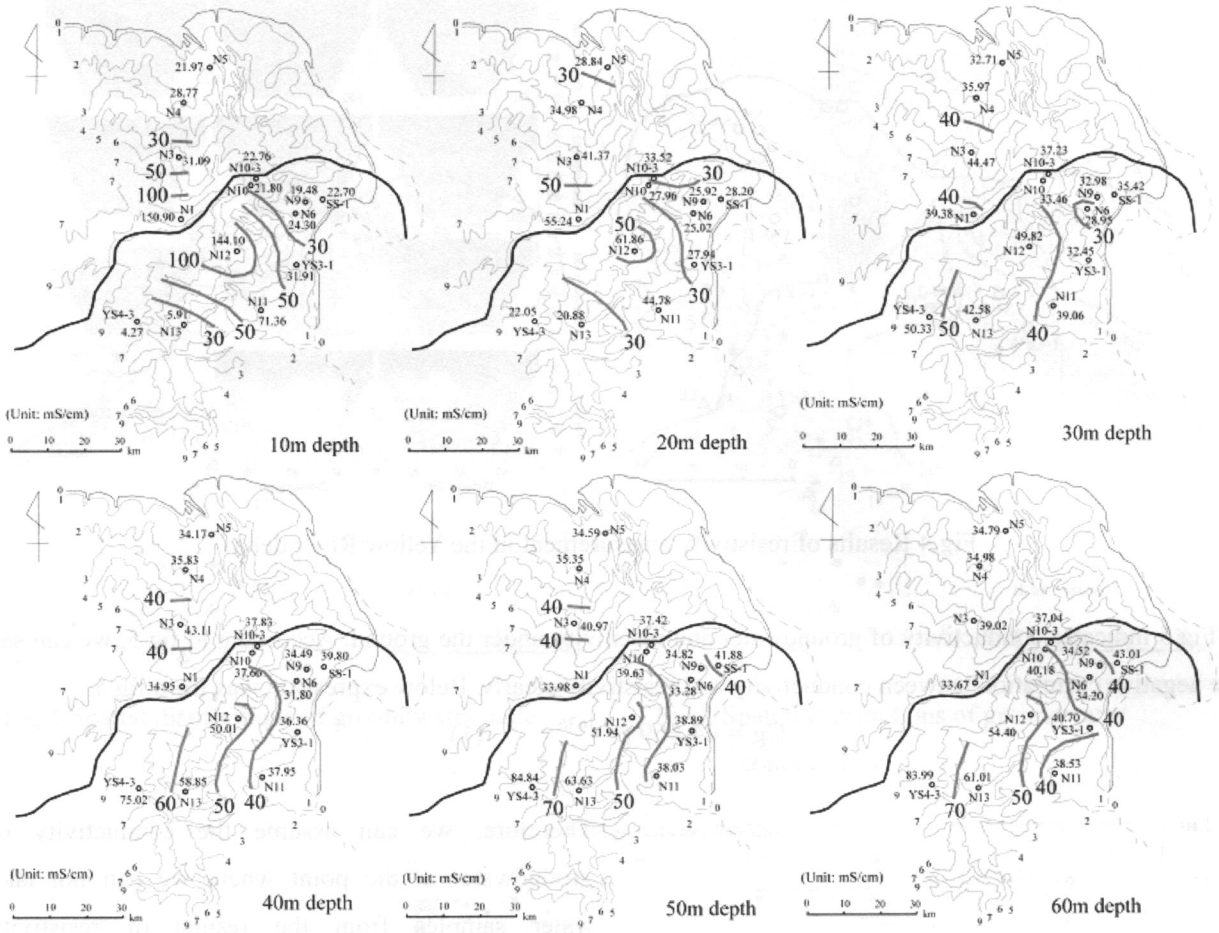

Fig.6 Spatial distributions of groundwater conductivity estimated by resistivity measurements

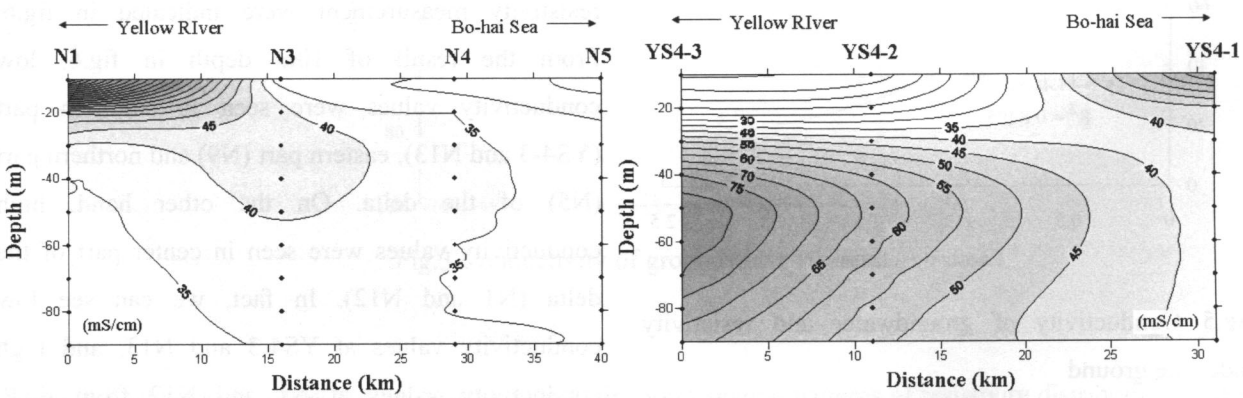

Fig.7 Cross sections of groundwater conductivity estimated by resistivity measurements
(left side – north line (N1 to N5), right side – east line (YS4-3 to YS4-1))

It was clarified that saltwater was distributed in broad area by measurements of conductivity and resistivity. Analysis of stable isotope and carbon 14 age dating of groundwater were done to clarify the origin of groundwater.

Fig.8 shows the relationship between results of stable isotope analysis and conductivity of river water from the Yellow River, seawater from the Bo-hai Sea and groundwater in the delta. Results of groundwater in 5 points could be separate two types. First one is the groundwater which has -6‰ values of stable isotope (groundwater in the coastal zone) and -3‰ values of stable isotope (groundwater in the center of the delta). If saltwater in the delta are the mixture river water and saltwater, values of groundwater should be put on the regression line from the value of river water to sea water. However, groundwater indicating about -3‰ values of stable isotope were not put on this line. Therefore, it is assumed that the origin of groundwater indicating about -3‰ values of stable isotope is not the mixture of river water and seawater and other factor should be consider.

Fig.9 shows results of age dating by carbon 14 age dating. Ages of groundwater are much differ each area. Coastal zone of the delta (N5, N9 and etc) indicate the younger age about 50yrBP. On the other hand, center of the delta (N1, N12 and etc) indicate the older age of 4000yrBP to 12000yrBP. In addition to, southern part of the delta indicate the middle age about 1000yrBP.

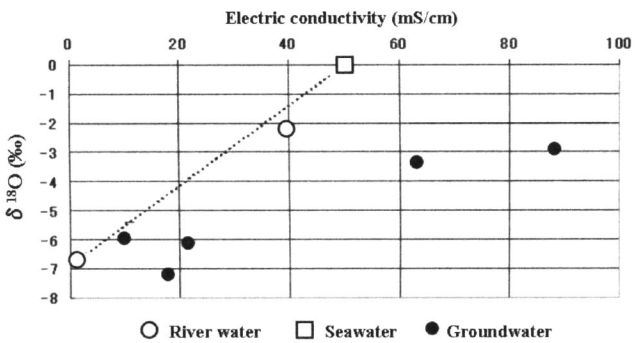

Fig.8 Values of stable isotope and conductivity of groundwater

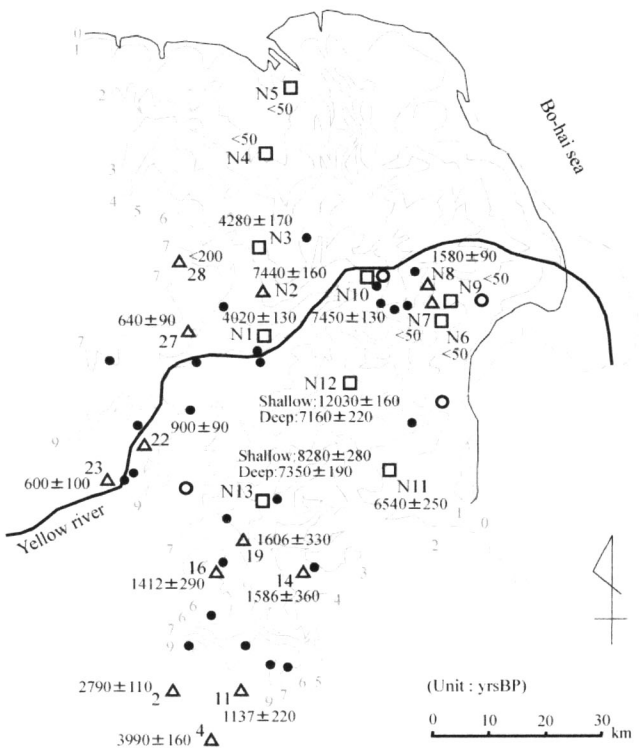

Fig.9 Results of carbon 14 age dating of the groundwater

The delta of Yellow River is expanding by the sedimentation since 1855 (fig.10). Therefore, it is assumed that there is the groundwater which has younger age and high conductivity made by caught seawater in the ground by the rapid sedimentation in the coastal zone (N5, N9 and etc).

About groundwater which has older age and high conductivity in the center of delta (N1, N12 and etc), it is assumed that groundwater made by concentration the density through remaining in this area for long-term and exists in this area. In fact, sedimentation ages are differing around N1-N12 and N5-N9.

On the other hand, groundwater which has about 1000 yrBP values exits in the southern part of delta. According to fig.2 and fig.6, it is assumed that this groundwater came from the western inland because low conductivity groundwater was confirmed in this area (Chen *et al.*, 2007).

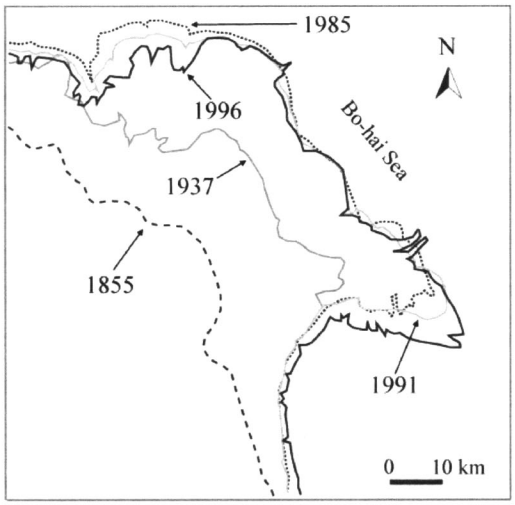

Fig.10 Change of the coastal line in the delta

From the mentioned, conditions of groundwater in the delta can be separated three types. First one is the groundwater which has younger age and high conductivity in the coastal zone, second one is the groundwater which has older age and high conductivity, and last one is the groundwater which has middle age and low conductivity.

Conclusion

1) Negative correlation between conductivity of groundwater and resistivity under the land in Yellow River Delta was confirmed by comparison of conductivity and resistivity.

2) Existence of paleo-seawater was clarified by resistivity measurements in every point.

3) Distributions of fresh and salt water were assumed by resistivity measurements.

4) Conditions of groundwater in the delta were separated three types.

References

Chen J., Taniguchi M., Liu G., Miyaoka K., Onodera S., Tokunaga T. and Fukushima Y. (2007): Nitrate pollution of groundwater in the Yellow River delta, China. *Hydrogeology Journal*, doi 10.1007/s10040-007-0196-7.

Yu L. (2002): The Huanghe (Yellow) River: a review of its development, characteristics, and future management issues, *Continental Shelf Research*, 22, 389-403.

Estimation of nutrient discharge with groundwater flow to the ocean in the Yellow river delta

Shin-ichi Onodera[1], Mitsuyo Saito [2], Makoto Taniguchi [3], Jianyao Chen[4], Kunihide Miyaoka[5], Tomotoshi Ishitobi[2], Guanqun Liu[6], Tiezhu Mu[6], Tomochika Tokunaga[7], and Yoshihiro Fukushima[2]

[1] Graduate School of Integrated Arts and Sciences, Hiroshima University, 7398521, Japan
[2] Research Institute for Humanity and Nature, Japan
[3] JSPS research fellow, Graduate student, School of Biosphere Sciences, Hiroshima University, Japan
[4] School of Geography Sciences and Planning, Zhongshan University, China
[5] Faculty of Education, Mie University, Japan
[6] College of Environmental Science and Engineering, Ocean University of China, China
[7] Graduate School of Frontier Sciences, University of Tokyo, Japan

Intorduction

As the human impact on water resource is expanding and becomes complex, we have to evaluate globally the control factors. Yellow River has kept the condition with a shortage of the river water since 1990's in the downstream area (Chen et al., 2003) by the increase of agricultural water use in the upstream area. The change in such a large river would act on the ocean environment as well as water resources, that is, on the global water and mass cycle. In addition, the Yellow river delta formed within the last 100 years has been used as agriculture land for last 20 years despite of extremely high salinity in the soil. Consequently, nitrate contamination of groundwater has been expanded there. To clarify the effect of such drastic changes on the ocean and groundwater, it is necessary to confirm the groundwater flow and nutrient transport in the delta area where the boundary of land and sea. However, the effect of human activity has not been considered in such large scale from upstream to downstream area.

The objective of this research is to confirm the effect of human activity on nutrient discharge with groundwater flow to the ocean in the Yellow river delta.

Method

In this research, we measured variations of groundwater level automatically and examined distribution of groundwater table in the area. In addition, we collected samples of river water, groundwater, soil water, and seawater. Then we estimated groundwater flux in various river runoffs, using a simple aquifer model. The major chemical component was analyzed in the laboratory.

Results and Discussion

The groundwater level distribution at the delta area indicated groundwater flow from river to ocean in both periods of wet and dry. The seasonal variations of water level were about 1m to 2m. Groundwater flux during the dry season was estimated to be about a half of that during wet season by the simple model. The relationship of groundwater flux and river runoff estimated by the model supported that groundwater discharge decreased but the nutrient flux to ocean maintained during the drought period in the river. On the other hand, it was suggested that river runoff increased in the magnitude of more than 2 orders during the wet period but groundwater flux increased only several times even in the maximum. These results indicate that groundwater discharge was dominant only during the completely draught period, but river discharge was dominant during the wet period and it is more than 100 times of groundwater. The nutrient component of river and groundwater was nitrogen rich and phosphorus and silica rich, respectively. The groundwater was also contaminated by nitrate under the agriculture land as well as river water, but the nitrate elimination occurred with groundwater flow. Therefore, it was estimated that nitrate discharge with groundwater was little. Consequently, nutrient discharge pattern was suggested that phosphorus and silica discharge were dominant during a drought period by groundwater, while nitrogen discharge was dominant during a flood period by river, respectively.

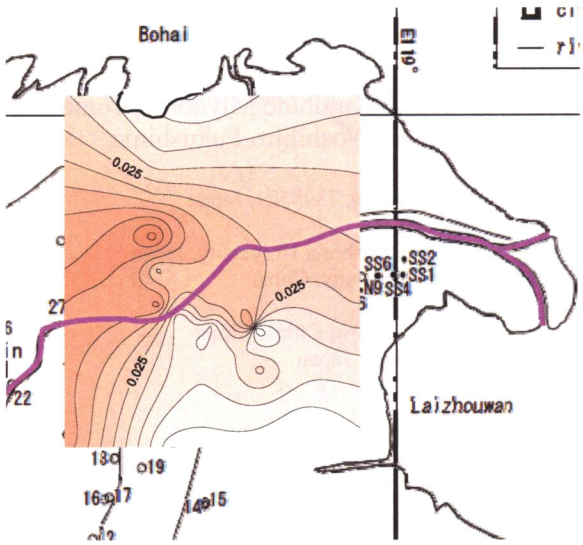

Fig.1 Inorganic nitrogen content in soil layer surface to the depth of 1m.

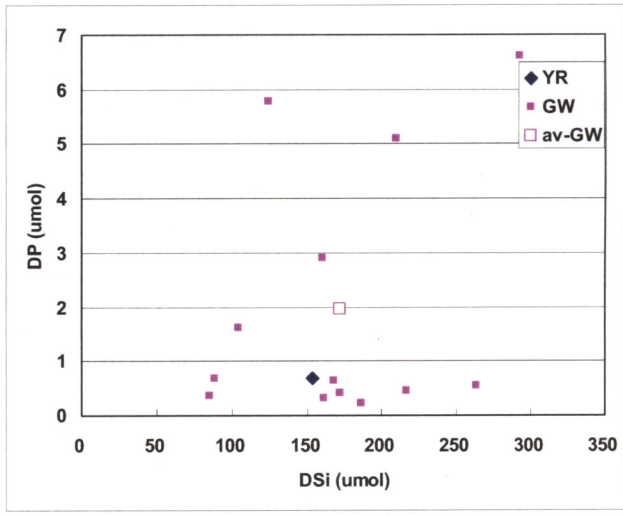

Fig.2 Dissolved Si and P of river water and groundwater in the Yellow River delt

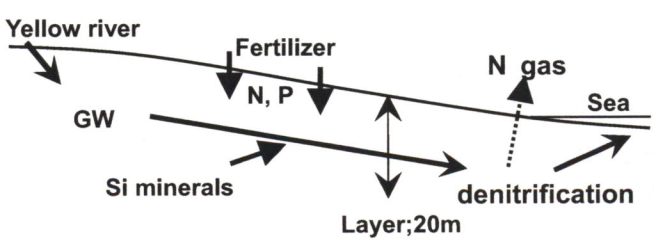

Fig.3 Solute transport model in Yellow River delta.

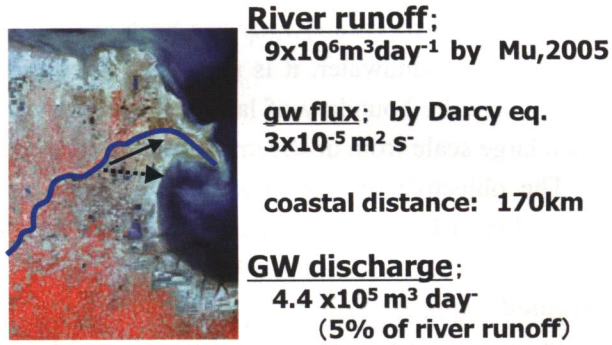

Fig.4 River runoff vs. groundwater discharge in the delta to the ocean.

	River	Groundwater
Flow	100	5
In 2005		
DTN conc.	100	50
discharge	100	2.4
Si conc.	100	1190
discharge	100	60
DTP conc.	100	1000
discharge	100	50

Fig.5 Nutrient discharge by river and groundwater

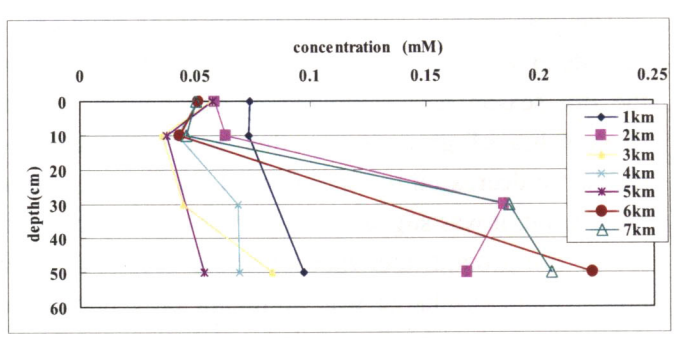

Fig.6 Dissolved nitrogen profile in pore water of seabed from the beach to 7km offshore.

Results of Groundwater Group in Yellow River delta

Makoto Taniguchi (RIHN)

1. Introduction

The roles of "groundwater group" in the Yellow River Project (PL: Yoshihiro Fukushima) are to evaluate the interaction between groundwater - river water - sea water, and to evaluate the groundwater discharge and material transports into the Bohai sea, from the points of views of "Cutoff of the Yellow River" and the effects on Bohai sea. The studies have been made from 2003 to 2007 thorough five intensive field measurements and analyses. The groundwater monitoring in the delta, measurements of the Yellow river water, and measurements of coastal water have been done. Three of five field experiments have been made with the "Bohai group". This is the final report of the results from the groundwater group.

2. Groundwater flow system in the Yellow River delta

Field experiments and analyses have been made to evaluate the groundwater flow system in the delta, hydrogeology of the aquifer, and the distribution of the saltwater and fresh water. Core sampling to evaluate hydraulic and hydrogeologic parameters, saltwater/fresh water distribution by resistivity measurements, and measurements of groundwater potential have been made. As the result, the method by use of GPS to evaluate the elevation is useful for the groundwater survey in the flat area such as

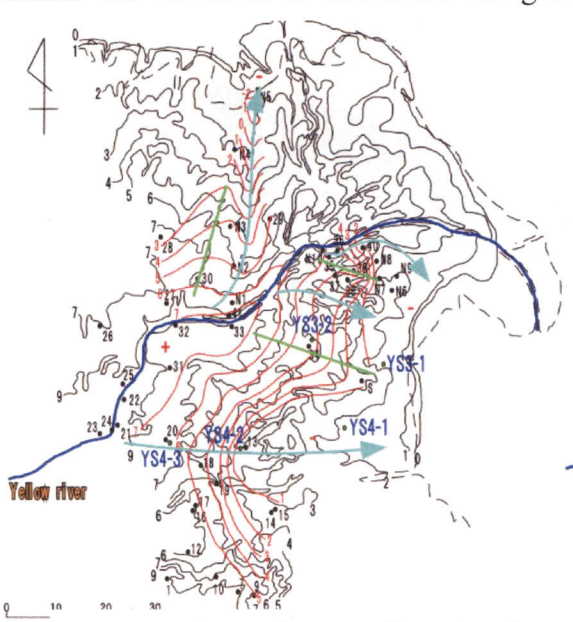

Fig. 1 : Groundwater flow in the delta (high flow, Sep. 2004).

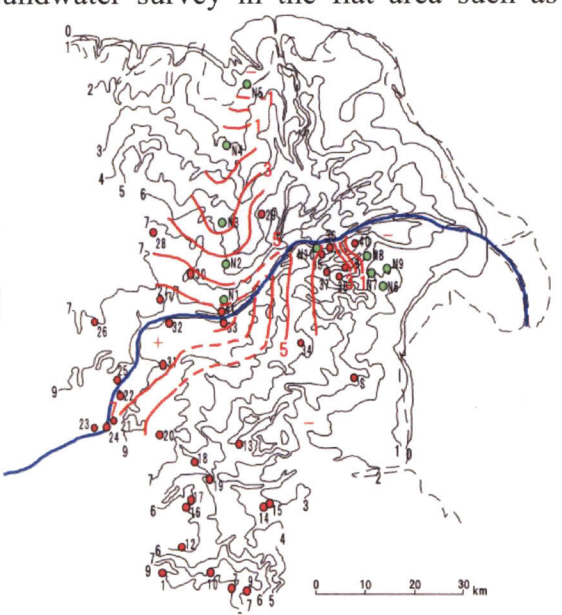

Fig.2 : Groundwater flow in the delta (low flow, May. 2005)

Yellow River delta. The Figures 1 and 2 show the groundwater table and direction of the groundwater flow on September 2004 (high flow) and May 2005 (low flow). The hydraulic gradient of the groundwater decreases during the low flow (similar to the condition of the "Cut-off of the Yellow River"), however the ratio of groundwater contribution increases during the low flow.

3. Interaction between Yellow River, groundwater and sea water

Three different waters, river water, groundwater and sea water, meat in the Yellow River delta. The magnitude and direction of the water have been examined to evaluate the effect of the cut-off of the Yellow river. As the results, the directions of the water were found to be from the Yellow River to groundwater and the groundwater to the Bohai sea (Fig.3). The replacement of the water has also been clarified from the results in the transect line from the Yellow river to the Bohai sea.(Fig. 4)

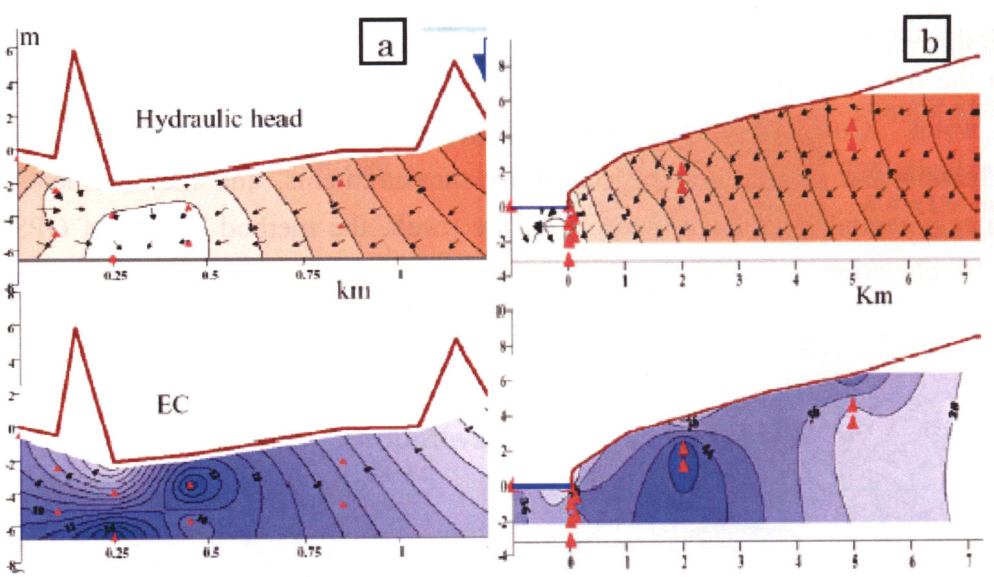

Fig. 3 Directions of the water flow,

Uppers: groundwater potential and direction

Lowers: Electric conductivity of the groundwater

Lefts (a) River-groundwater interaction (YR is located at the right side)

Rights (b): Groundwater-sea water interaction (Bohai sea is located at the left side)

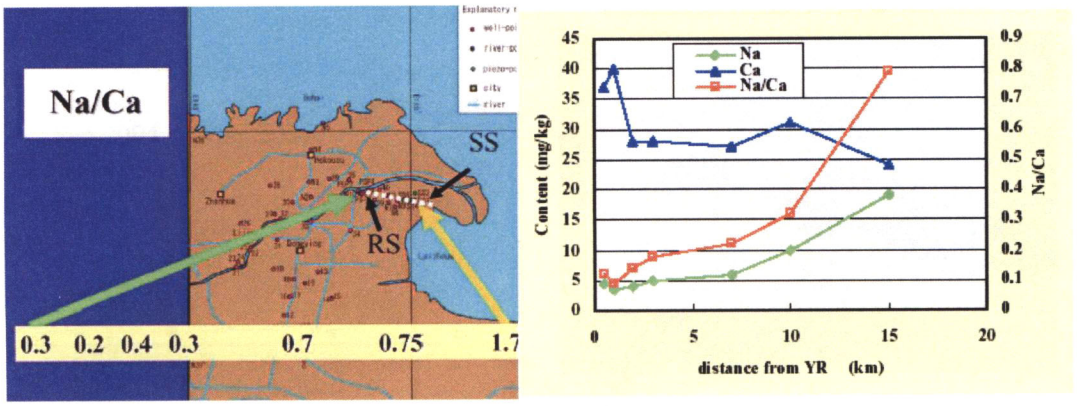

Fig 4 : Groundwater quality (Na/Ca) at RR (Yellow river) – SS (Bohai sea) line

4. Impact zone of the Yellow River

In order to evaluate the hydraulic continuity in the delta, the changes in groundwater level and discharge rate of the Yellow River have been analyzed. The correlation between the Yellow River discharge and groundwater level in the delta show that the impact zone (hydraulic continuity) of the Yellow river is more than 40 km.

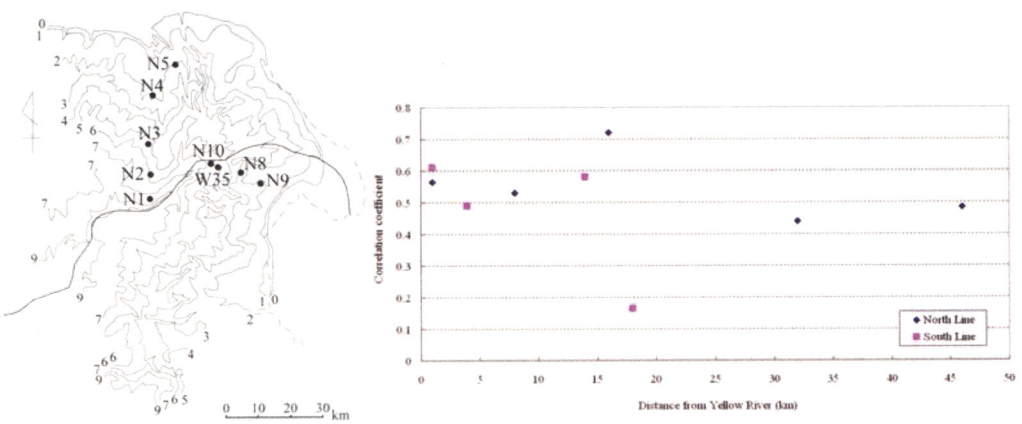

Fig5: Correlations between river discharge and groundwater level.

The analyses of the water balance in the lower reach of the Yellow River basin show that the 60 % of the water loss (total loss is 1.28 x 10^8 m^3/year) between Huayuankou and Lijin was irrigation, and that water transport through trans boundary from the Yellow river to the Qingdao and Tianjin was 20 % of the water loss.

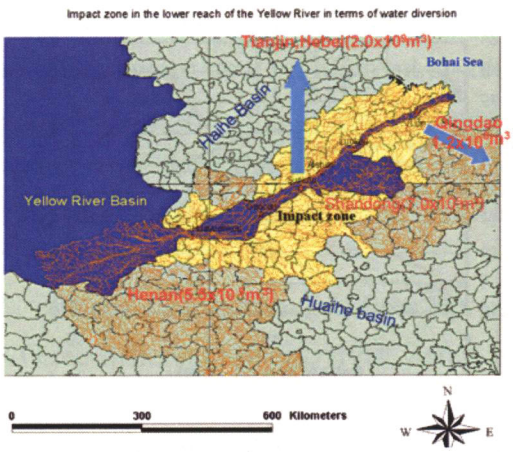

Fig.6 Irrigation area and trans boundary movement of water From the Yellow River

5. Water and dissolved material transports from the delta to the Bohai sea

Spatial and temporal variations of submarine groundwater discharge (SGD) have been evaluated by automated seepage meters from the Yellow River delta to 7 km offshore in the Bohai Sea, China (Fig.7). We identified three zones from the coast to offshore based on different relationships between tidal and SGD changes. Our results indicate that the point of maximum SGD shifted 2 km offshore from September 2004 to September 2006 (Fig.8). This spatial change is thought to be caused by sediment deposition near the coast (Fig.9).

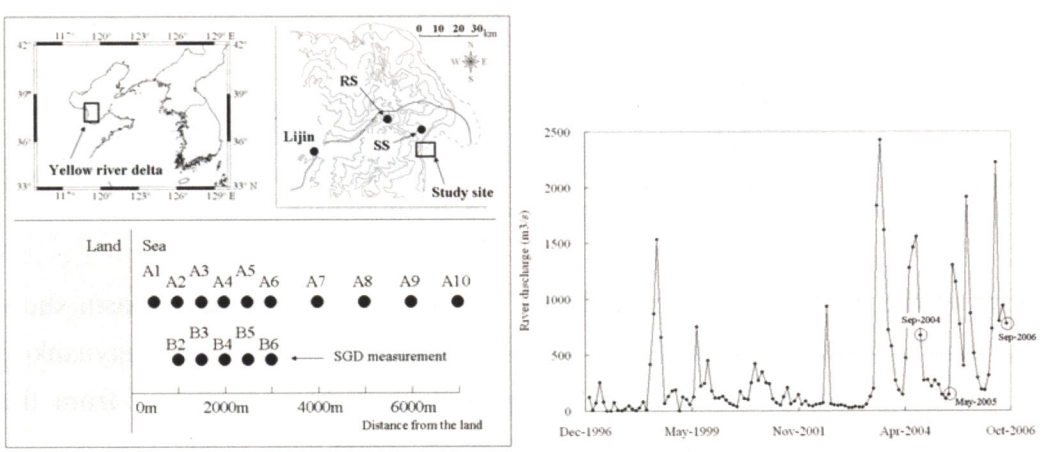

Fig.7 Locations of the seepage meters (left) and change in Yellow River discharge (right).

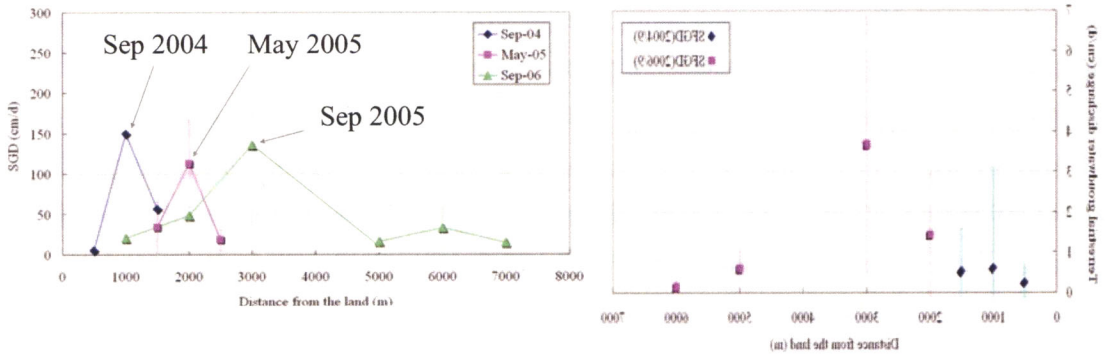

Fig.8 SGD (left) and SFGD (right) distributions

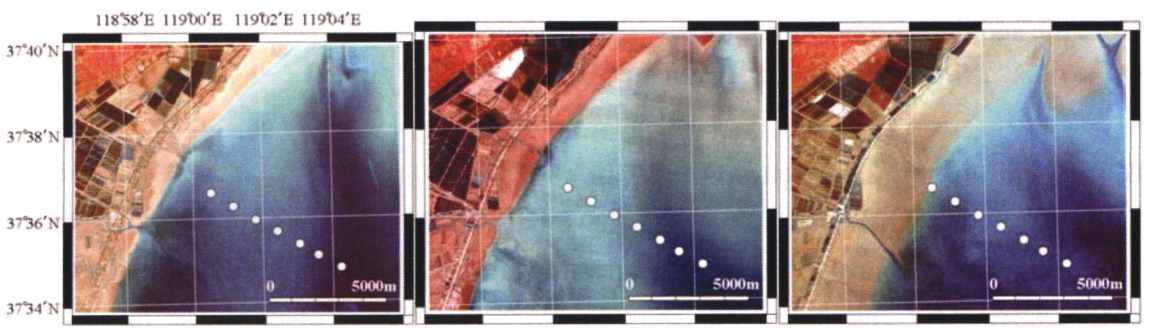

Fig.9 Locations of shoreline on Sep.2004 (left), May.2005 (middle) and Sep.2005 (right)

Assuming the seepage face extends 7 km offshore, the average integrated SGD of both the A and B lines per unit length of shoreline are estimated to be 2,300 m^3/m day and 304 m^3/m day in September 2004 and May 2005, respectively. The integrated SGD in September 2006 is estimated to be 3065 m^3/m day. Assuming the shoreline length of the Yellow River delta to be 350 km, the total SGD from the entire Yellow River delta is evaluated to be 9,300, 1,200, and 12,000 m^3/s in September 2004, May 2005, and September 2006, respectively. Since the Yellow River discharge in September 2004, May 2005, and September 2006 were 676, 145, and 778 m^3/s, respectively, the total estimated SGD from the delta are found to be 13.8, 8.5 and 16.0 times the river discharge into the Bohai Sea. Note that these numbers include both SFGD and RSGD.

Assuming the SFGD seepage face in September 2004 and September 2006 are 2 km offshore, the average SFGD in September 2004 and September 2006 are 18 and 28 m^3/m/day, respectively. Assuming the length of the coastline of the Yellow River delta to be 350 km and SFGD in the study area represents 3.6 times the average SFGD of the entire delta, SFGD is evaluated to be 110 and 170 m^3/s during September 2004 and September 2006, respectively. Therefore, SFGD represent about 4.5 % and 7.0 % of

the Yellow River discharge during September 2004 and September 2006, respectively.

Comparison of these results with global data shows that the SFGD in the Yellow River delta is smaller than global average, but SGD is larger than the average, because of gentle slope in the coastal zone of delta.

Material transports by groundwater to by Yellow river were 100:60 for Phosphate and 100:50 for Silica, though fresh water discharge (SFGD) by groundwater to by Yellow river was 100:5. Therefore, the result shows the importance of groundwater discharge for Phosphate and Silica into the Bohai sea. On the other hands, nitrate discharge by groundwater to by Yellow river was 100:2.4. This small contribution by fresh groundwater discharge (SFGD) may be due to denitrophication. However, the nitrate discharge by recirculated seawater discharge may cause the dissolution of nitrate from the sediments transported by the Yellow river.

6. Integration of the evaluation methods

Integration of the different methods have been made in this study to understand the interaction between river water, groundwater and sea water. Geophysical methods, such as GPS for regional groundwater survey, resistivity for saltwater-fresh water distribution, automated seepage meter to evaluate submarine groundwater discharge, groundwater potential measurement to identify the impact zone of the Yellow river, and geochemical methods, such as stable isotopes and chemical composition analyses, were used and compared each other.

The groundwater group made three field experiments with Bohai group. This is not only for sharing data for the model by Bohai group, but also for improving their model itself. The interdisciplinary study by groundwater hydrologists and coastal oceanographers has been made in the Yellow River delta.

7. Conclusions

The conclusions of the groundwater group are as follows;

(1) The usefulness of GSP measurements in the flat area such as Yellow river delta is shown,

(2) The deep information on saltwater/freshwater distribution can be found remotely by uses of resistivity without borehole data.

(3) The directions of water movement in the delta are evaluated to be from the Yellow river to the groundwater, and from the groundwater to the Bohai sea.

(4) The hydraulic impact zone of the Yellow river was estimated to be more than 40 km by use of correlation between river discharge and groundwater level,

(5) Comparisons of the results of groundwater discharge into the Bohai sea between different river discharge periods showed that the role of groundwater discharge increases during low flow (similar to the condition of the cut-off of the Yellow River).

(6) The distribution of the SGD shifted 2 km offshore during two years because of the offshore shift of the coastal line due to the sedimentation.

(7) The ratio of SFGD (fresh component of submarine groundwater discharge) was 5-8 % of the Yellow river discharge, which was smaller than global average, however, SGD (total submarine groundwater discharge including recirculated sea water) was 8 to 16 times of Yellow river discharge, which is much larger than the global average. This is attributed to the gentle slope of the coast in the Yellow River delta.

(8) Material transports by groundwater to by Yellow river were 100:60 for Phosphate and 100:50 for Silica, though fresh water discharge (SFGD) by groundwater to by Yellow river was 100:5.

(9) The nitrate discharge by recirculated seawater discharge may be caused by the dissolution of nitrate from the sediments transported by the Yellow river.

(10) The 60 percentages of the water loss between Huayuankou and Lijin was used by irrigation in the lower reach of the Yellow River basin.

(11) The interdisciplinary study by groundwater hydrologists and coastal oceanographers has been made in the Yellow River delta.

8. Remained subjects

(1) Some hypnoses have been raised to explain the increase of nitrogen in the Bohai sea, however, no single reason was identified.

(2) The process of the SGD and SFGD were clarified, however, the process of recirculated seawater, in particular the entry process of the recirculated water was remained to be unclear.

(3) Geophysical and geochemical methods were integrated, however, the effects on the ecology in the coastal zone should be evaluated in the future.

Observations in Laizhou Bay and tidal lands of Yellow River delta in summer of 2007

Guo X.[1] · Q. Wang[1] · H. Yamaguchi[1] · T. Yanagi[2] · L. Zou[3] · H. Gao[3] · T. Mi[3]

[1]Ehime University, [2]Kyushu University, [3]Ocean University of China

1. Introduction

In September 2004 and May 2005, we carried out two observations in Laizhou Bay and central area of Bohai, which allow us knowing general spatial distribution of water temperature, salinity and nutrients and their seasonal variations. A large difference was found between the nutrients concentration of sea water and those of Yellow River and ground water. This motivates us to know the nutrients above tidal lands and near shore area, where is between sea water and river water or ground water. Moreover, high nutrients concentration was observed far from Yellow River mouth in 2004 and 2005. This suggests the necessary to know nutrients loads from the small rivers around Laizhou Bay, which can be an important source for nutrients in the bay. On the other hand, an increasing trend in the past 30 years has been found in the nutrients concentration in Laizhou Bay, while the same trend cannot be found in nutrients loads from Yellow River. This inconsistence reminds us to examine the nutrients supply from culture ponds for shrimp and crab around Laizhou Bay since such fisheries have been greatly developed in the past 30 years.

For addressing the above problems, we carried out a survey in Laizhou Bay and tidal lands of Yellow River delta from July 3 to 9 2007. The survey is divided into three groups as shown in Fig.1: sea group for Laizhou Bay (Fig.1, upper panels), tidal land group for tidal lands and near shore area (Fig.1, middle panels), and land group for small rivers and ponds (Fig.1, lower panel). Since there is a large spatial gradient in nutrients concentration in these areas, we set stations as fine as possible. Our survey measured water temperature, salinity, nutrients, Chl-a、SPM, PAR, DO. The survey period is at the end of an artificial event for adjusting water and sand fluxes in Yellow River (Fig. 2).

2. Results

An apparent influence of Yellow River water on surface salinity distribution is presented in Fig. 3. In general, salinity in Laizhou Bay is lower than 30 psu, which in lower than the salinity observed in September 2004 and May 2005. Such low salinity is due to the large fresh water supply from Yellow River before the survey (Fig. 2). The most interesting finding in the salinity distribution is that the diluted water spread eastward, not southward. This suggests that with a large river discharge, inertial of Yellow River water contributes greatly to the behaviors of Yellow River plume. In addition, the southwest wind during the survey period also favors a northeastward movement of Yellow River plume (Wang et al., 2008).

Among nutrients (Figs. 4&5), high concentration areas of nitrate, TN, TP and silicate correspond to the diluted water: extending eastward. This feature indicates that the load of such nutrient components from Yellow River at this period mainly contributes to the central area of Bohai Sea, not inside of Laizhou Bay. On the other hand, high concentration areas of nitrite, ammonium and phosphate were found around tidal lands and near shore area, not corresponding to the river plume. Such feature suggests that biological activities at tidal lands, not the land loads, affect more on the distribution of ammonium. The phosphate distribution is due to its low concentration in Yellow River but high concentration in some small rivers around Laizhou Bay. This suggests that the small rivers around Laizhou Bay must be paid sufficient attention as we discuss the source of phosphate in sea water. Finally, since we did not observe high concentrations of nutrients in ponds for shrimp or crab, we can therefore remove the possibility for the culture ponds as an important source for nutrients in sea water.

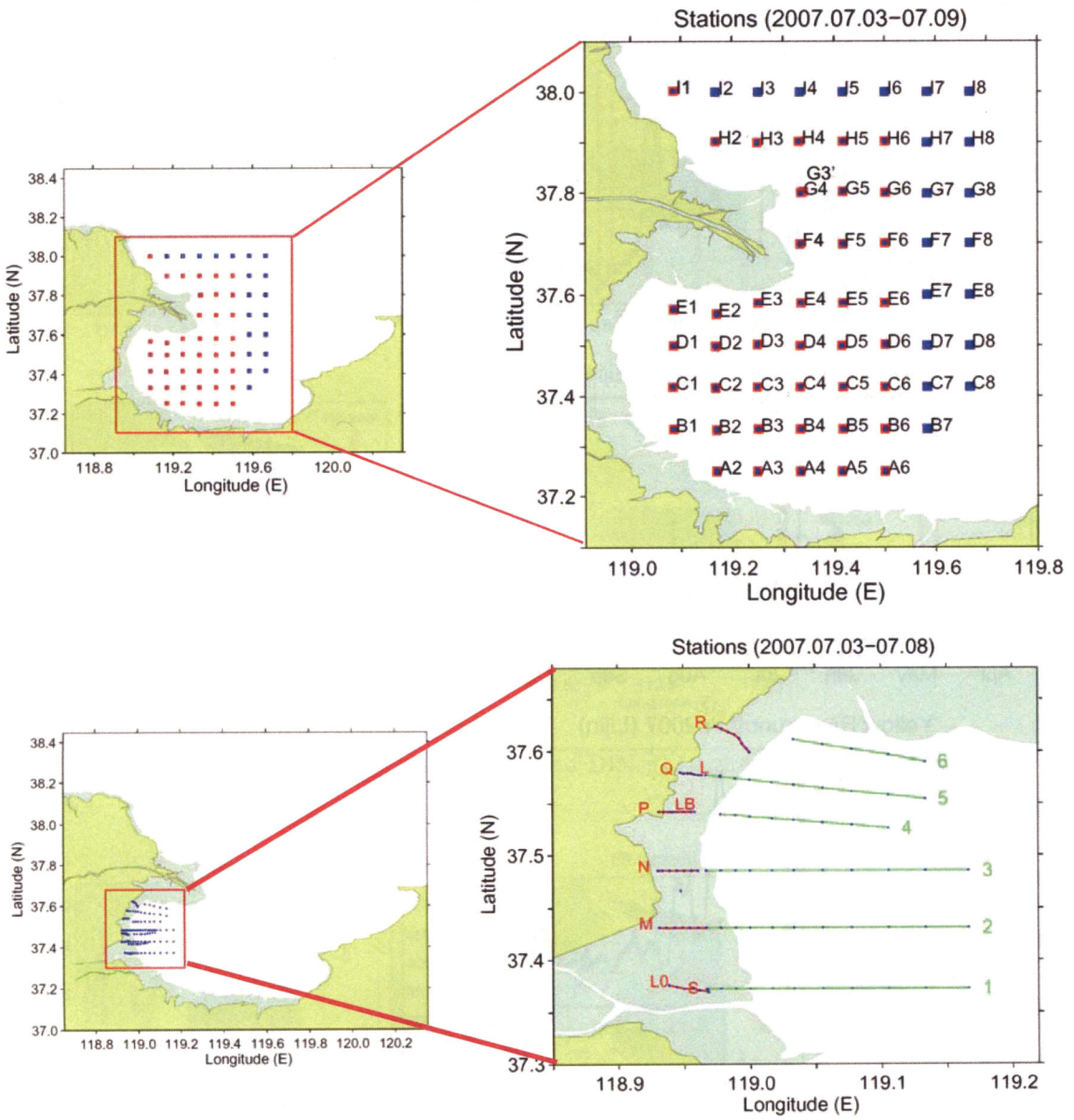

Fig.1. Stations in Laizhou Bay (upper panels), tidal lands (middle panels) and land (lower panel). In the upper panels, blue dots denote the stations of water temperature and salinity, while red dots denote the stations with biochemical parameters. In the milled panels, red lines were approached by foot while green lines by boats. In the lower panel, blue dots denote small rivers while red dots ponds for shrimp or crab.

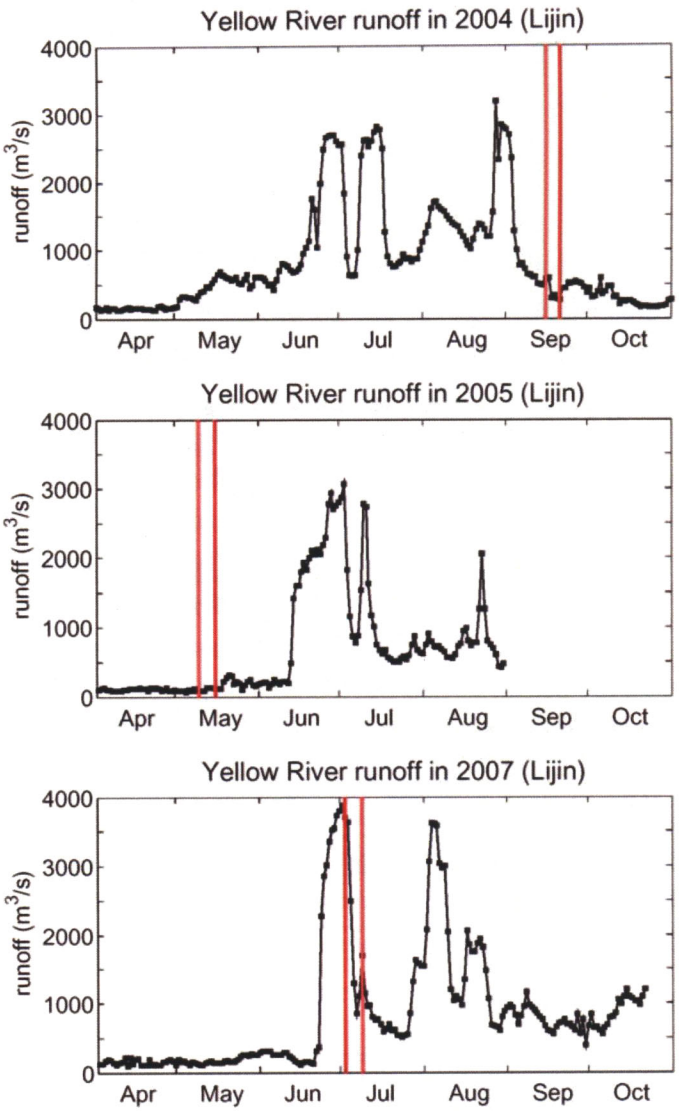

Fig.2. River discharge of Yellow River from April to October in 2004, 2005 and 2007. The time between two red lines denote the survey period in each year.

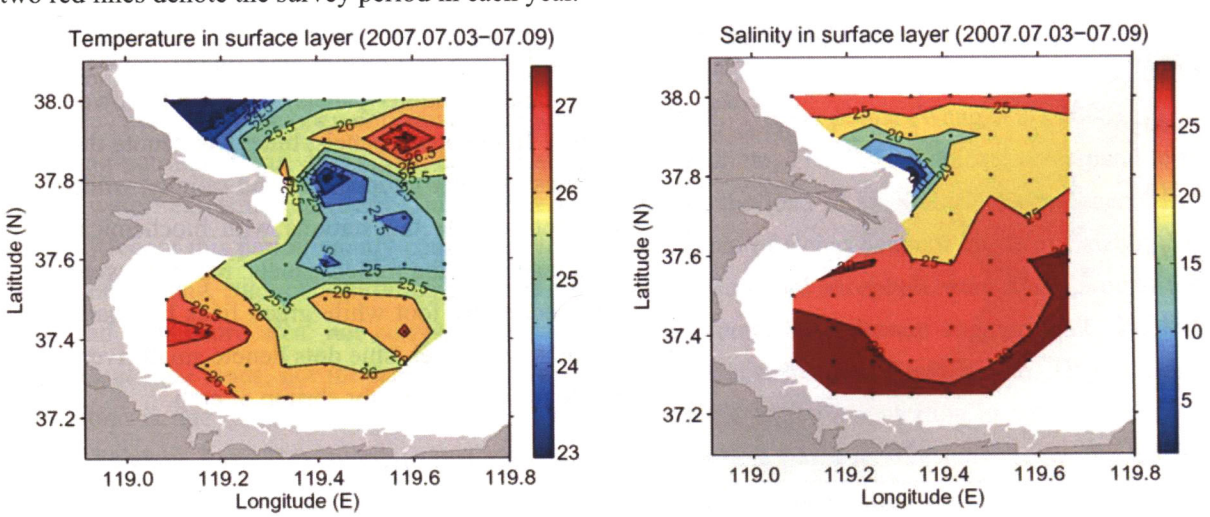

Fig.3. Surface water temperature (left) and salinity (right) in Laizhou Bay in July 2007.

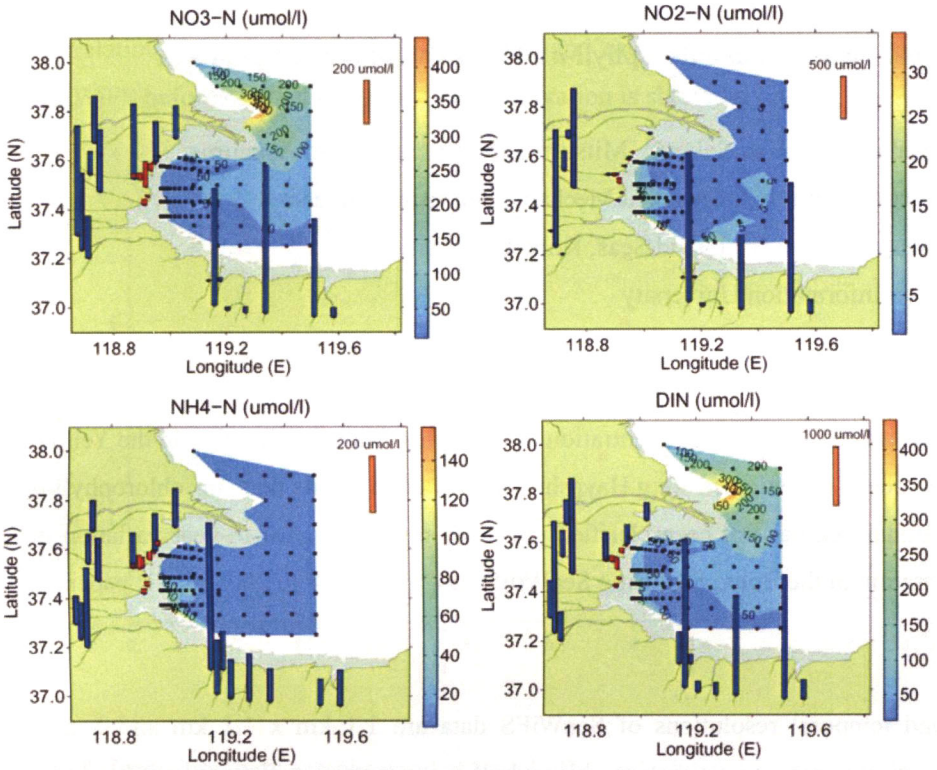

Fig.4. Distribution of nitrate, nitrite, ammonium and DIN in Laizhou Bay, tidal lands, small rivers and ponds.

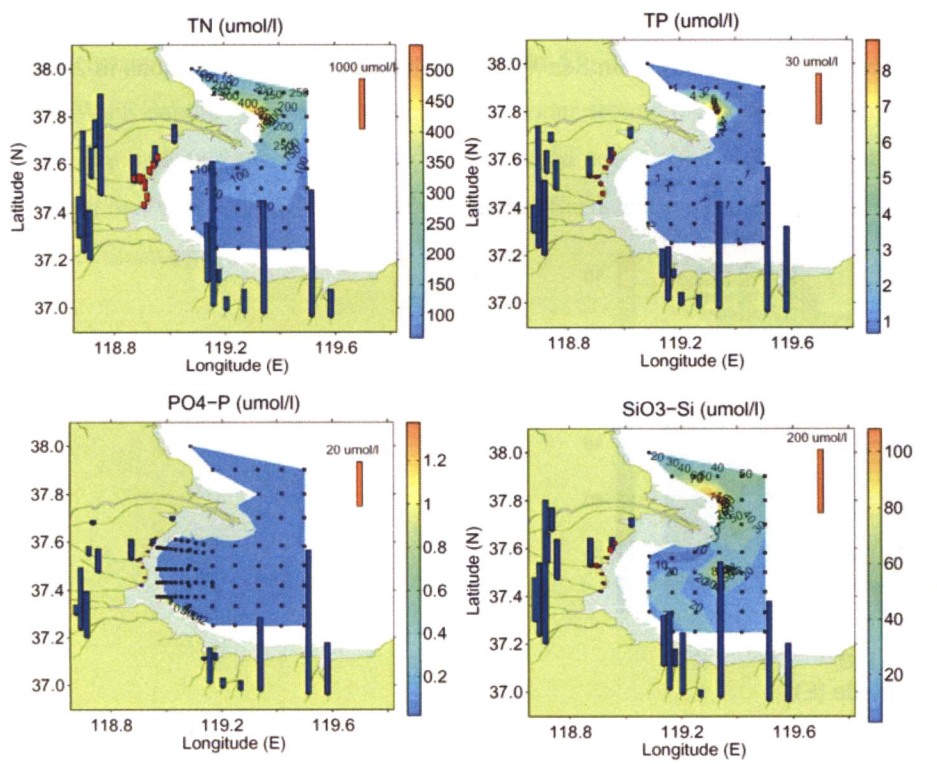

Fig.5. Distribution of TN, TP, phosphate and silicate in Laizhou Bay, tidal lands, small rivers and ponds.

Year-to-year variation in chlorophyll-*a* concentration in the Bohai Sea

Tetsuo Yanagi[1], Shouya Sakota[1], Mitsuru Hayashi[2] and Ichio Asanuma[3]

1. Research Institute for Applied Mechanics, Kyushu University
2. Research Center for Inland Seas, Kobe University
3. Tokyo Information University

1. Introduction

The year-to-year variation in nutrient concentration in the Bohai Sea related to that in the Yellow River discharge has been investigated (e.g.Hayashi et al., 2004) but that in chlorophyll-*a* concentration in the Bohai Sea has not been clarified yet. We reveal the year-to-year variation in chlorophyll-*a* concentration in the Bohai Sea using SeaWiFS data from 1998 to 2005 in this paper.

2. Satellite data

The horizontal and temporal resolutions of SeaWiFS data are 1.1 km x 1.1 km and 1 day, respectively. The usual algorism for estimation chlorophyll-*a* concentration from the visible band signals of SeaWiFS (for open sea water) is not available in the Bohai Sea because the water in the Bohai Sea is not Case I water (open sea water) but Case II water (turbid coastal water). Therefore we make the much-up data for obtaining the calibration curve to estimate the sea-surface chlorophyll-*a* concentration in the Bohai Sea from SeaWiFS data based on our observations in 2004 and 2005 and Gao et al. (2003) (Fig.1).

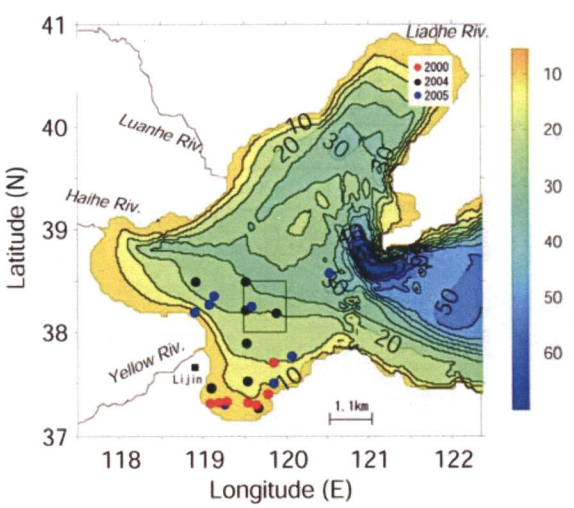

Fig.1 Observation points of sea surface chlrophyll-*a* in the Bohai Sea.

Correlation between observed chlorophyll-*a* and estimated chlorophyll-*a* by the usual algorism of SeaWiFS before or after 4 days of field observation is shown in Fig.2.

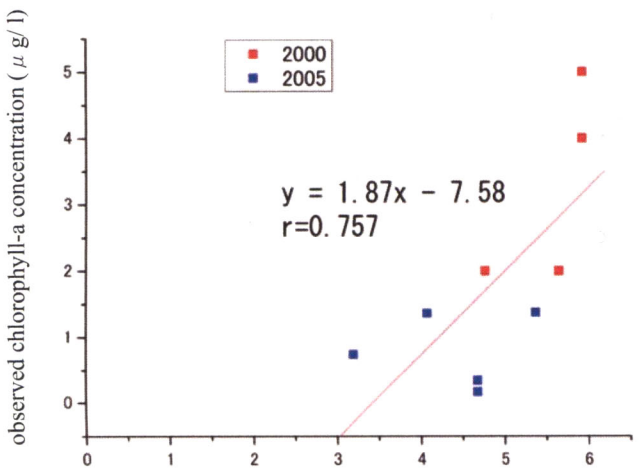

Fig.2 Correlation between observed chlorophyll-*a* and estimated chlorophyll-*a*.

3. Results

By using the calibration line shown in Fig.2, we estimate the sea surface chlorophyll-*a* concentration in the squared area shown in Fig.1 in the central part of the Bohai Sea from the SeaWiFS data in oder to avoid high turbid water around the Yellow River mouth.

The year-to-year variation in the estimated sea-surface chlorophyll-*a* in the central part of the Bohai Sea is shown in Fig.3 with that in Sea Surface Temperature (SST), solar radiation and Yellow River discharge.

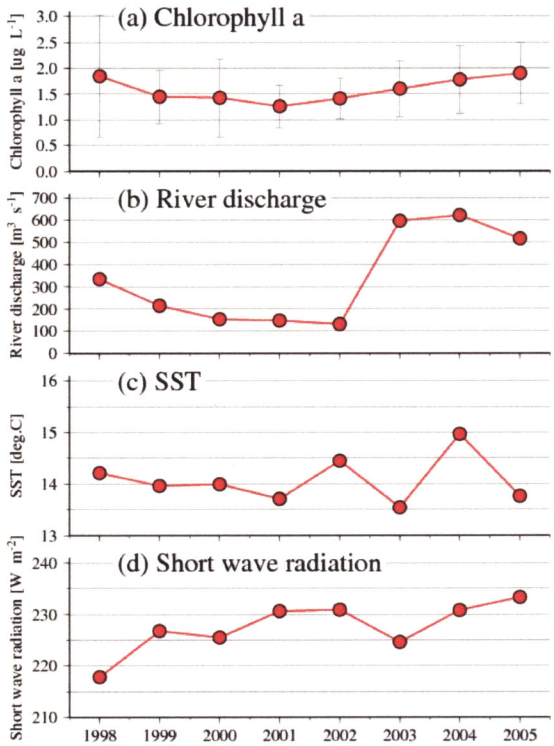

Fig.3 Year-to-year variations in sea-surface chlorophyll-*a* in the Bohai Sea, Yellow River discharge, SST and solar radiation in the Bohais Sea.

The year-to-year variation in the sea-surface chlorophyll-*a* does not have good correlation between those of SST and solar radiation but it has a good correlation to that of the yellow River discharge from Fig.3. This is due to that the Yellow River discharge controls the nutrient (Dissolved Inorganic Phosphorus; DIP) concentration in the Bohai Sea as shown in Fig.4 and DIP is the limiting factor of primary production in the Bohai Sea (Hayashi et al., 2006), that is, large (small) river discharge results in high (low) DIP and high (low) chlorophyll-*a* concentrations in the Bohai Sea.

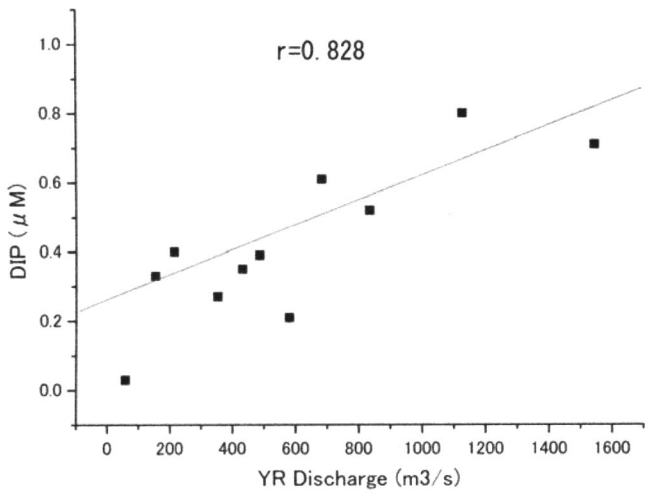

Fig.4 Correlation between DIP in the Bohai Sea and the Yellow River discharge.

3. Conclusion

When the Yellow River discharge is large (small), DIP concentration becomes high (low) in the Bohai Sea and it results in high (low) sea-surface chlorophyll-*a* concentration in the Bohai Sea.

References

Gao,H., D.Wu, J.Bai, J.Shi, Z.Li and W.Jiang (2003) Distributions of environment parameters in Laizhou Bay in summer 2000. J.Ocean University of Qingdao, 33, 185-191.

Hayashi,M., T.Yanagi and X.Guo (2004) Difference of nutrients budgets in the Bohai Sea between 1982 and 1992 related to the decrease of the Yellow River discharge. J.Korean Soc. Oceanogr., 39, 14-19.

Hayashi,M., T.Yanagi and R.Zeng (2006) Year-to-year variations in the Yellow River discharge and the environment of the Bohai Sea. Proceedings of Techno-Ocean 2006, paper No.162.

Some Thoughts on Development in the Yellow River Basin by Water Rights Transfers, and Possible Japanese Approaches to Help Address Key Concerns

Osamu HIGASHI (Nagoya University)

1. Introduction

China today is placing a high priority on national policies promoting further economic development through megaprojects like the country's south-to-north water diversion project, the west-to-east electricity transmission project, and the west-to-east natural gas transportation project. In this context, the Yellow River basin boasts a wealth of resources, including the natural gas of the Ordos basin, and the coal in Inner Mongolia, Shanxi Province, and Shaanxi Province, and widely expected to develop as an energy supply base. Meanwhile, it is undeniable that water shortages in the Yellow River basin have the potential to impede economic growth in the future.

A framework to stimulate energy production by using water rights transfers was launched on a trial basis in the Inner Mongolia Autonomous Region. The power generation sector invests in infrastructure for water-efficient irrigation and then obtains from the agricultural sector the surplus water thereby made available. If this water rights transfers system functions properly, it will facilitate development in the Yellow River basin even in the face of water supply constraints.

In that context, this paper outlines developments in the Yellow River basin in the context of water rights transfers and related issues, and then discusses possible ways for Japan to contribute to stable societal conditions in the river basin region. More specifically, this paper describes the role of the Yellow River basin in China's national development strategy and discusses the significance of water rights transfers in the basin. Next it takes a close look at the basin's stages of development in terms of Japanese and other overseas capital flows into China. Finally, this paper describes the correlation between increased energy production in the Yellow River basin facilitated by water rights transfers and China's overall development on one hand, and the expansion of environmental impacts and regional disparities on the other, discusses risk management approaches to address future droughts, and considers possible ways for Japan to contribute to the Yellow River basin.

2. Water rights transfers and the role of the Yellow River basin in China's national development strategy

(1) Three Chinese megaprojects (south-to-north water diversion, west-to-east electricity transmission, west-to-east natural gas transportation) and their relationship with the Yellow River basin

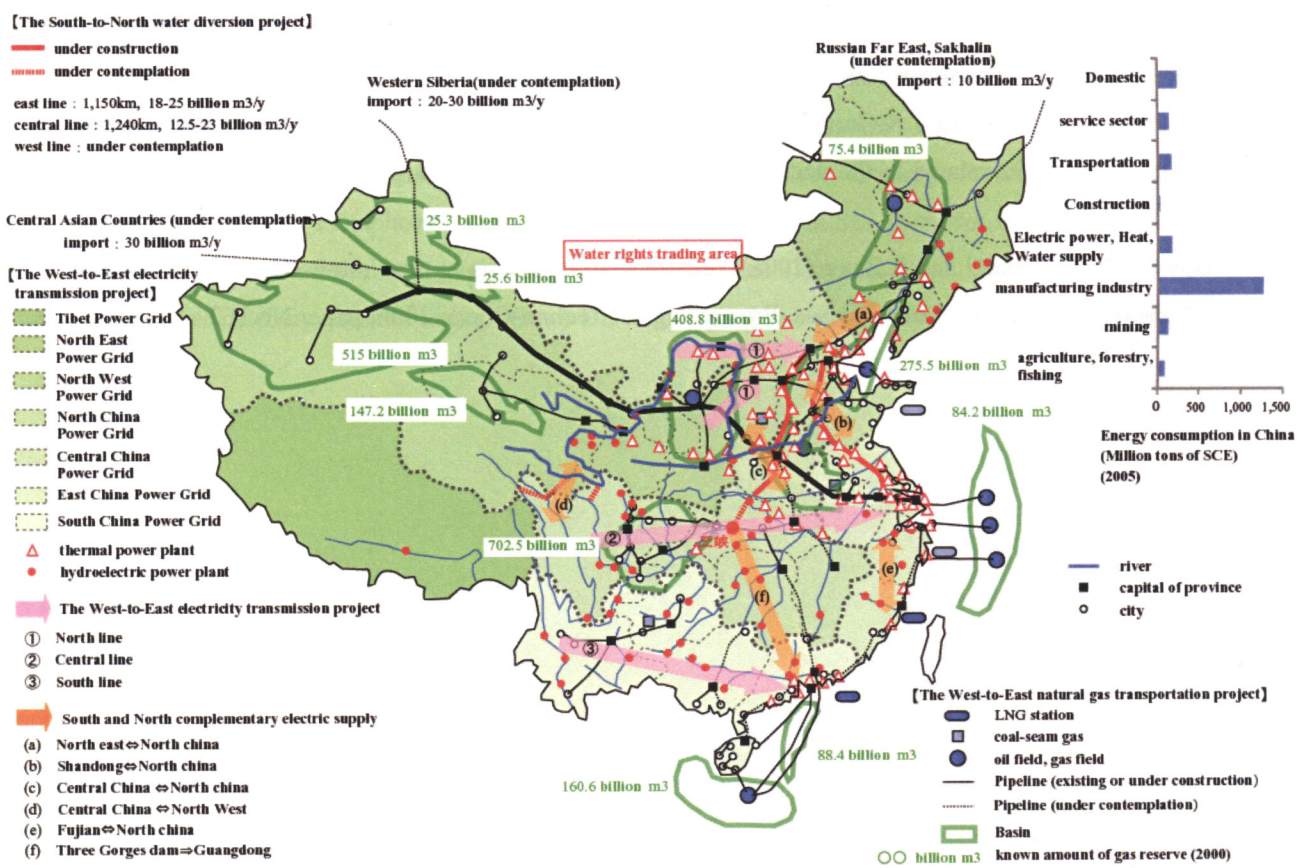

Figure 1. The Yellow River basin and China's national development strategy

Figure 1 shows the role of the Yellow River basin in China's national development strategy.

The west-to-east natural gas transportation project involves construction of a pipeline to link gas fields in the Tarim Basin and Qaidam Basin in the west and north with gas fields in the Ordos Basin (in the Yellow River basin), and then branch out from the Ordos Basin toward Beijing and Shanghai. The natural gas reserves in the Ordos basin hold 408.8 billion cubic meters (confirmed crude reserves, 2000), making this area an important supply base of natural gas for major cities.

The west-to-east electricity transmission project involves a northern route, a central route and a southern route, and the Yellow River basin is associated with the northern one. This project involves plans for the transmission of coal-generated electricity to Beijing, Tianjin, and Heibei Province using the abundant coal resources in the western part of Inner Mongolia and in Shanxi Province, and transmission of hydropower-generated electricity to northern China and Shandong Province from the Yellow River and coal-generated power electricity from the Ninxia Autonomous Region and northern Shaanxi Province. Thus, the upper and middle reaches of the Yellow River basin have an important role to play in expanding the supply of electricity for regional development in Beijing, Tianjin, and the lower reaches of the Yellow River basin.

As for the south-to-north water diversion project, the eastern and central routes are already under construction, and some relief for the water shortages facing Beijing and Tianjin is imminent as a result of water that will be diverted to these cities from the Yangtze River. The figure shows that many major coal-fired power plants are located along the eastern and central routes, making it possible to expand the electricity supplied further east. Meanwhile, the western route is the only one that can supply water directly to the Yellow River basin; it is now at the planning stage, but indications are that actual construction will be extremely difficult due to terrain and other challenges.

In conclusion, any development of the Yellow River basin as an energy supply base under current circumstances must be achieved in the context of constraints on the supply of water.

(2) The significance of water rights transfers in the Yellow River basin

In response to serious river flow of stoppages on the Yellow River in 1997, the Yellow River Conservancy Commission (YRCC) bolstered its management of the river water resources, and introduced controls on water withdrawals permitted in provinces and autonomous regions in the river basin. Inner Mongolia allocates 5.68 tons of water from the Yellow River for use per year (actual allocations in past drought years were 4.8 billion tons per year), and the actual amount of water currently being used in this autonomous region is already reaching that limit. It will be difficult to obtain new water resources from the Yellow River in the future for the purpose of increasing energy production. Meanwhile, the agricultural sector accounts for 94% of overall water use in Inner Mongolia, although the irrigation efficiency is low at about 40%.

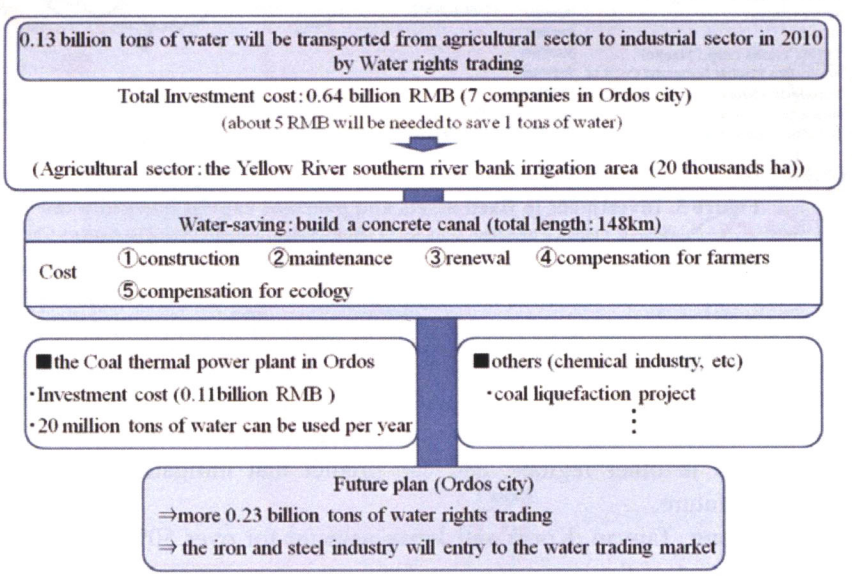

Figure 2. Status of water rights transfer projects in Inner Mongolia

Under these conditions, Inner Mongolia has obtained permission from the YRCC to implement a water-rights transfers system in which the power generation and industrial sectors invest into water-conserving irrigation infrastructure improvements in the agricultural sector, and the surplus water arising from increased water efficiency in the agricultural sector is made available to the power generation and industrial sectors. This system has revealed the potential for development in the Yellow River basin despite constraints on the water supply.

Figure 2 shows the current status of projects involving water rights transfers in Inner Mongolia. It indicates the need for a total investment of 640 million yuan, or about 5 yuan per ton of water saved, but this investment can probably be adequately recovered thanks to expanded electricity demand in Beijing and Tianjin.

3. Development and environmental impacts in the Yellow River basin and China overall

(1) Investment in fixed capital investment and overseas capital flows into the Yellow River basin and China overall

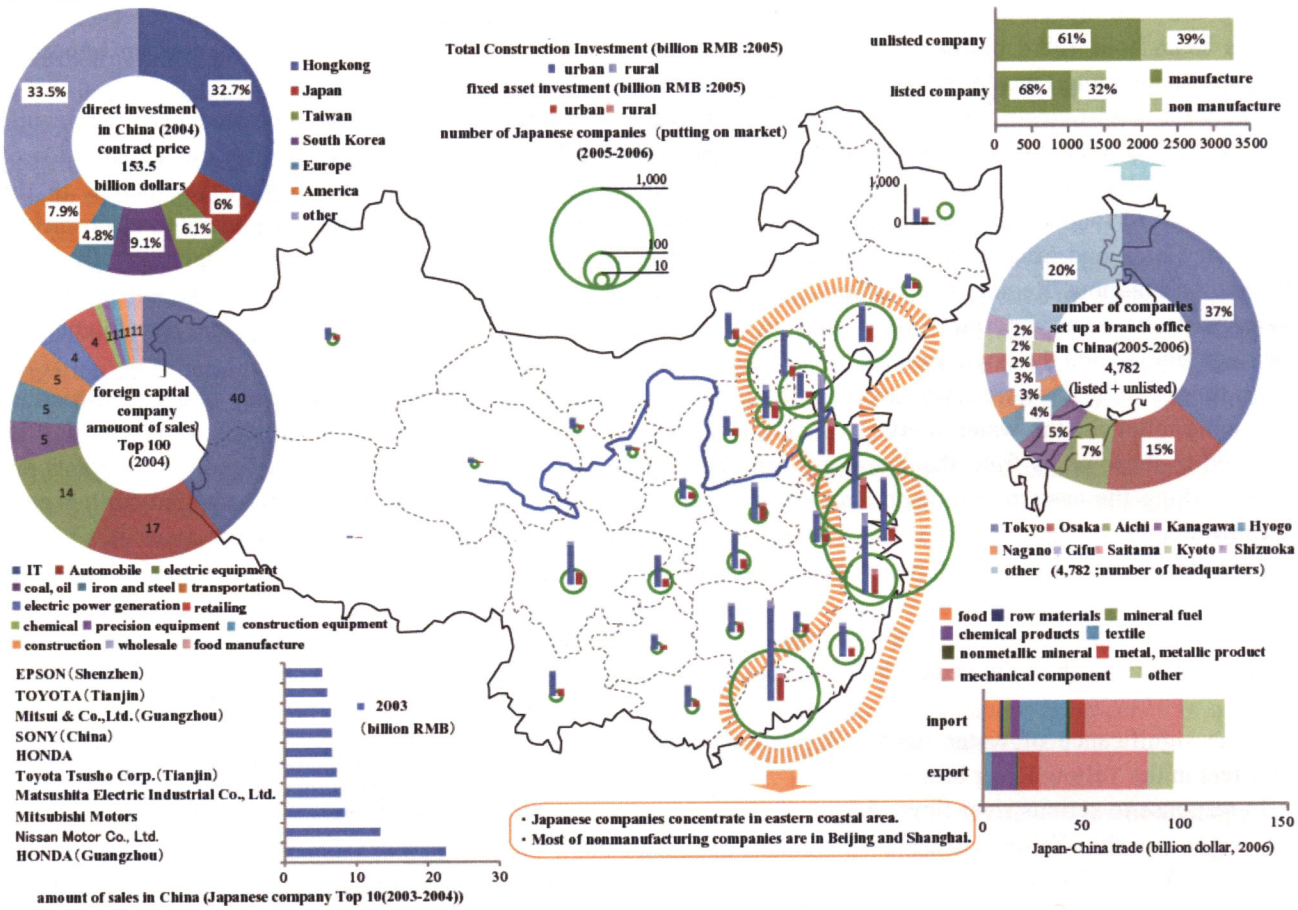

Figure 3. Investment in fixed assets and overseas capital flows into the Yellow River basin and China overall

Source: Prepared by author from list of foreign companies in China, 21st Century China Study (2005-2006), and China Statistical Yearbook (2006).

Figure 3 shows the status of fixed capital investment and overseas capital flows into the Yellow River basin and China overall. Over 60% of fixed capital investment in China in 2005 was focused in the eastern coastal region. An analysis of the state of implementation of the three megaprojects reinforces the observation that the focus of development in the coming years will continue to be in China's eastern coastal region. Looking at the Yellow River basin, we see that investment into the Bohai Sea area in the lower reaches of the Yellow River is much greater than in other regions, and can predict that mitigation of regional disparities will be difficult in the immediate future.

Hong Kong, Taiwan, Korea and Japan account for over 50% of total overseas direct investment into China in 2004, and most of the companies involved were concentrated in the eastern coastal region of the country. Thus, the scale East Asian economic region is very large—defined here as China's eastern coastal area plus Hong Kong, Taiwan, Korea and Japan. Overseas capital flows further inland in China are essentially focused on the creation of manufacturing centers, but the size of funds flowing here are considerably less than to the eastern coastal region. Thus, development of the central and upper reaches of the Yellow River basin as an energy supply base for the eastern coastal region will have an enormous impact on the further development of the East Asian economic zone, and also on China's securing of overseas capital in the coming years. Stated differently, overseas companies expanding into China stand to benefit further by the stabilization of the energy supply in the eastern coastal area as a result of China's national development strategy and water rights transfers in the Yellow River basin.

(2) Economic development in the Yellow River basin and increases in China's overall environmental impacts

Figure 4 shows conceptually the cause and effect relationships of economic development and the increase in environmental impacts in the Yellow River basin and China.

The figure shows that the promotion of water rights transfers is also likely to stimulate the industrial activity of companies from overseas, if the Yellow River basin development as an energy supply base under water supply constraints becomes fully operational through linkages with the three megaprojects, thereby further promoting

economic development in China's eastern coastal area. Coal-fired electrical power generation continues to account for a major percentage of the energy supply, however, and industrial development is likely to lead to the further spread of automobiles and household electrical products, thereby increasing greenhouse gas emissions and air and water pollution in China, as well as air and water pollution in the East Asian region through the transboundary movement of pollutants.

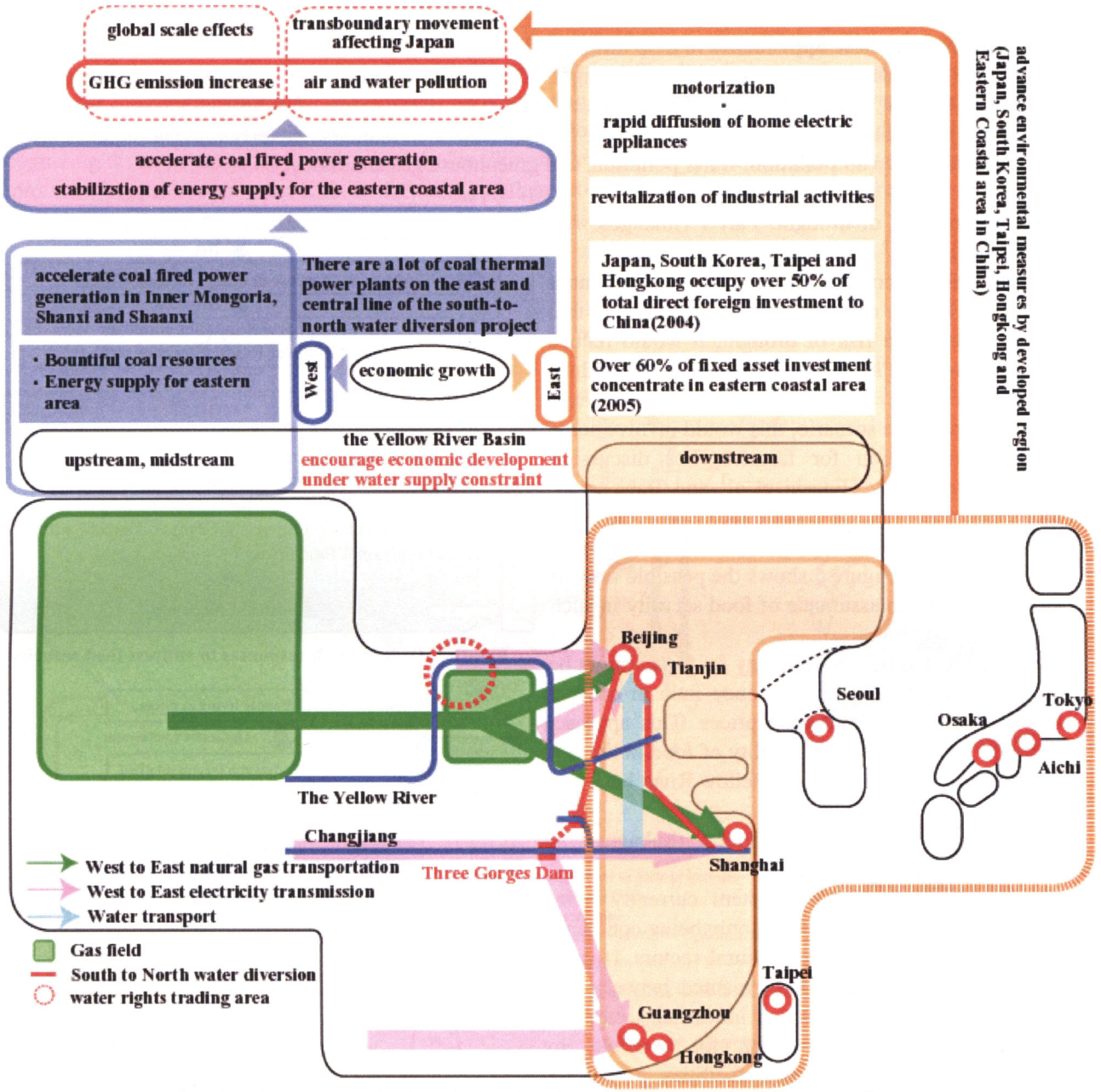

Figure 4. Cause and effect relationships between economic development and increased environmental impacts due to three megaprojects

China's greenhouse gas emissions are already among the highest in the world, and the transboundary movement of air pollution from China to the East Asian region is already significant. Meanwhile, major Japanese automakers and household electrical products makers are moving aggressively into China, creating production centers and aiming to promote their products particularly in the eastern coastal region. It is also worth noting that China accounts for the largest share of Japanese trade figures, so Japan clearly plays a significant role in environmental pollution and regional disparities arising from China's economic development.

Another point is that, as stated above, the energy supply to the eastern coastal region will be stabilized as a result water rights transfers in the Yellow River basin, but some attention must be given to address risks during periods of drought. A number of issues will arise if a serious drought occurs in the Yellow River basin. For example, will industrial activity be given the priority at the expense of agricultural production, and if agricultural production is restricted, how will China's food security be ensured?

The discussion above shows that Japan is intimately connected with China's economic development and an increase in environmental impacts, that a need exists to develop comprehensive approaches that will help to reduce environmental impacts and regional disparities, and that some consideration must be given to address risk in the event of periods of drought in the Yellow River basin. The next section outlines some thoughts on possible approaches by Japan that could help address these issues.

4. Thoughts on Japanese approaches to help address key issues

Below, we consider some approaches Japan might take to help address key issues raised above, including responses to the risk of drought in the Yellow River basin (i.e., stabilization of industrial activity, assurance of food security) and related to this, compensation for farmers (income assurance, poverty prevention, etc.), as well as strategies to reduce air pollution, water pollution, and greenhouse gas emissions.

(1) Addressing risk of drought: Part 1 (linkages with food security)

In interviews conducted for this study, Inner Mongolia's Ministry of Water Resources answered that as a response to the risk of drought, it would reduce agricultural water allocations (in other words, reduce food production), and give priority to energy production. In such a scenario, this would involve some kind of compensation for farmers. For discussion purposes, research by Higashi et al[1] and Baba et al[2] predicts that a drought on a scale likely to occur once every fifty years would mean a 10% to 20% reduction in food production. Figure 5 shows the possible flow of responses relating to assurance of food security in such cases.

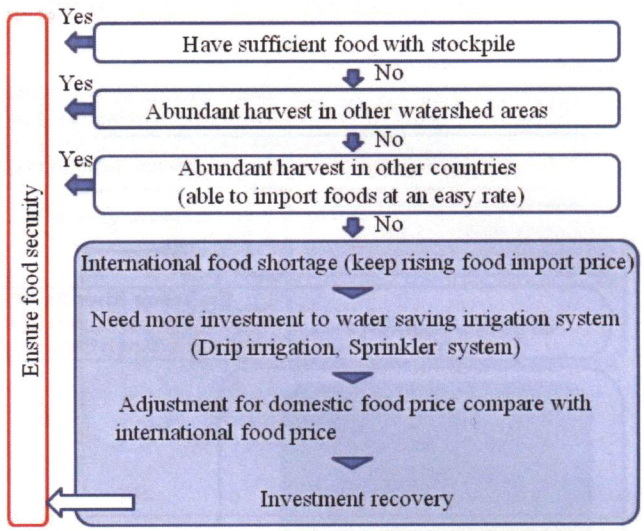

Figure 5. Drought risk responses to address food security

In this context, a possible strategy for Japan might be to boost its own food self-sufficiency ratio in order to help stabilize international food prices. This approach would also contribute to the stability of food policies in China in a time of drought in the Yellow River basin.

(2) Addressing risk of drought: Part 2 (linkages with water pollution countermeasures)

The water rights transfer system currently being tested in the Yellow River basin is only being conducted between the industrial and agricultural sectors. If water rights transfers were to be implemented between two industrial sectors, or between an industrial sector and the domestic (household) sector, for example, by investing in wastewater treatment facilities, in effect it would amount to water rights transfers by one sector obtaining treated water. This approach could facilitate not only water conservation but also water pollution countermeasures. Figure 6 shows an example of water rights transfers between the industrial and domestic sectors.

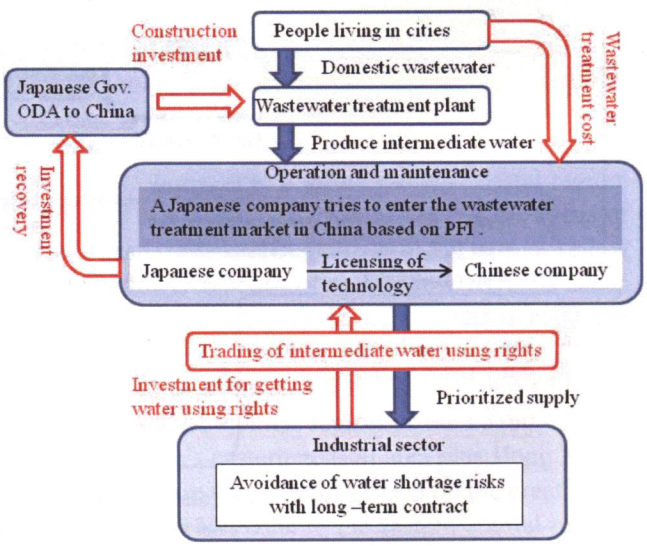

Figure 6. Example of water rights transfers between industrial and urban domestic sectors

The Japanese government already has a track record in the construction of water treatment facilities through official development assistance (ODA) to China, and French and other corporations have brought foreign capital into water treatment projects in places like Lanzhou City (Gansu Province).[3] Thus, the creation of schemes through private finance initiatives (PFI) as shown in the figure are also worth considering. Incidentally, the cost per ton of treated water has been estimated at about 5 yuan per ton, according to existing literature—based on initial investment, as well as maintenance and operating costs for wastewater treatments facilities in various provinces of China in 2004.[4] By way of comparison, municipal water in Beijing in 2004 was priced at 3.7 yuan per ton, and industrial water was 5.6 yuan per ton, and these prices are expected to continue rising.[5] Based on the above, if it were possible to provide recycled water at prices below the regular price of industrial water, water

rights transfers could occur between industrial and urban sectors. Thus, by providing not only technology but also effective water resource management systems, Japan could contribute to water conservation and the prevention of water pollution in the Yellow River basin.

(3) Assistance to farmers in order to address regional disparities

Under a system of water rights transfers between the industrial and agricultural sectors, the industrial sector would make investments to enable water-conserving irrigation in the agricultural sector. Here, benefit available to farmers would be the stabilization of food production, but this is difficult to link directly to increases in individual income. We must remember that, as indicated above, during a drought in the Yellow River basin, water rights transfers would probably result in priority being given to water resources for the industrial sector. Thus, recognizing the need to secure benefits directly for Chinese farmers, this paper now provides a logical justification to promote Japanese support for Chinese farmers, and then proposes concrete support measures.

a) Logical basis to promote Japanese support for Chinese farmers

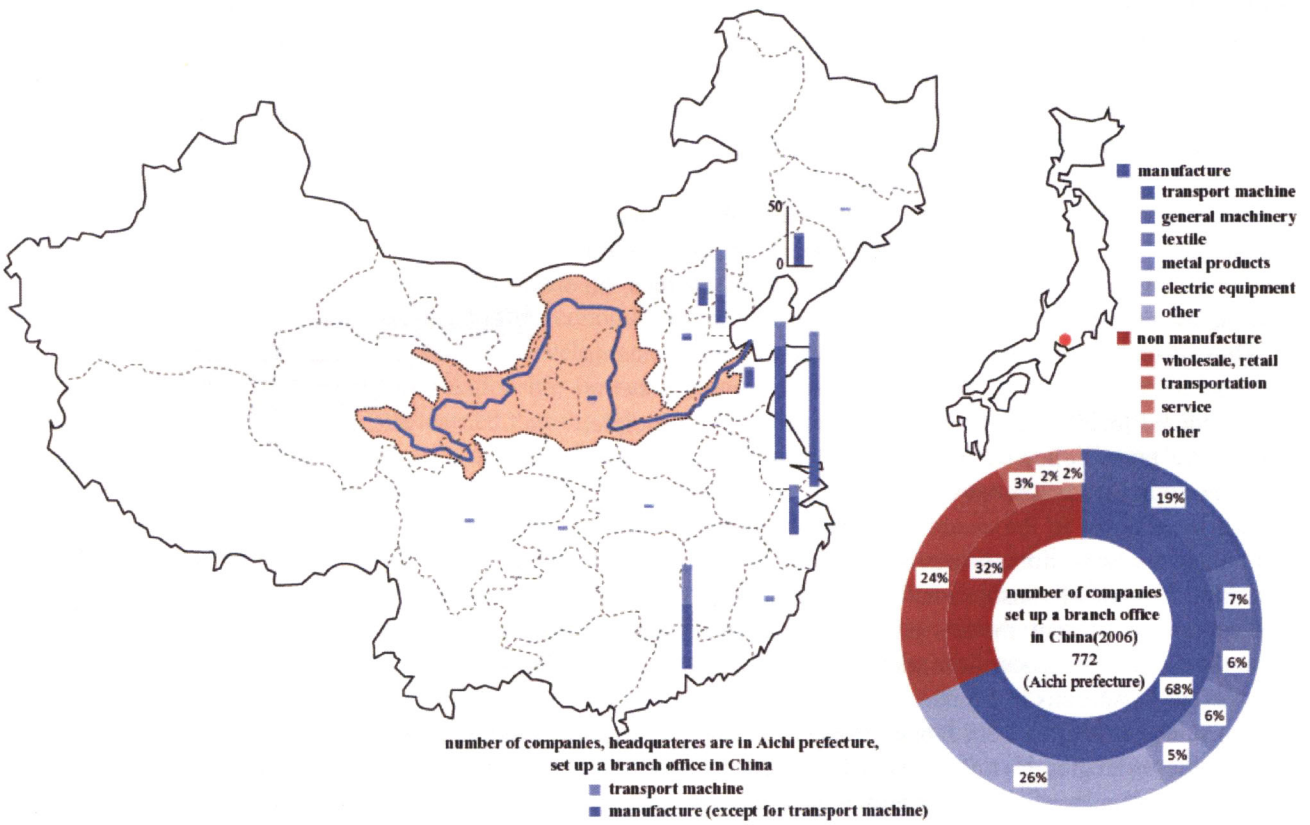

Figure 7. Activities of corporations from Aichi Prefecture (Japan) in operating China (2006)

Source: Prepared by author from "Overseas business activities of corporations based in Aichi Prefecture" (Aichi Prefecture, 2007, in Japanese).

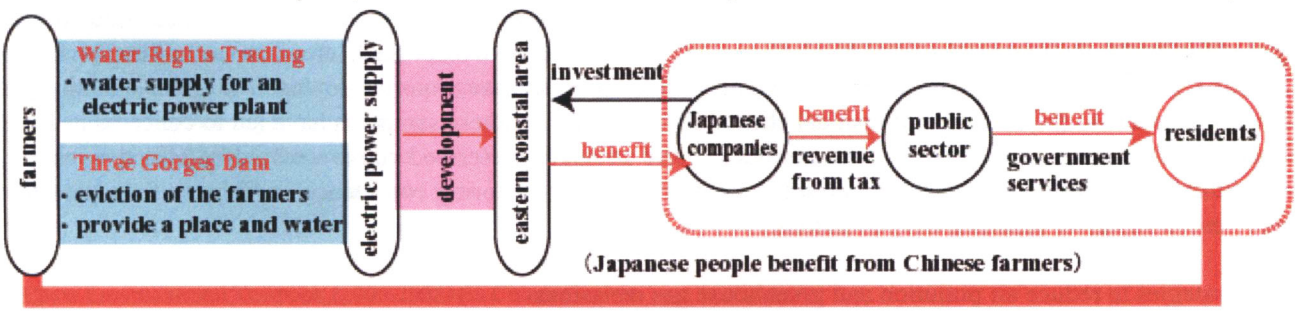

Figure 8. Benefits reaching Japanese citizens from Chinese farmers

Figure 7 shows the activities of corporations based in Aichi Prefecture operating in China. The activities of major automotive and related parts manufacturers from Aichi Prefecture operating in Tianjin and Guangzhou are significant, and they are receiving electricity supplied, respectively, through water rights transfers in Inner Mongolia, and from the Three Gorges Dam. Water rights transfers become possible thanks to water made available from farmers, and the resettlement of farmers makes water available in the case of the Three Gorges dam.

Economic development in the eastern coastal region of China is based on this water, so one could say that it is being facilitated by cooperation from farmers. The profits of Japanese corporations in this region are, in effect, a benefit for the local governments in Japan where the corporate head offices are located, and these benefits become a benefit for the local citizens who receive government services from their local governments (Figure 8). Based on these cause-and-effect relationships, one could say that local citizens in Japan are also—in a broad sense—beneficiaries of the Chinese farmers.

Consequently, the implementation of some kind of support or assistance for Chinese farmers from the local governments where many Japanese corporations are present—particularly where they are aggressively expanding in the eastern coastal region (see Figure 3)—or from citizens in those municipalities is in accordance with the "beneficiary pays" principle, and indeed one could say that there is a duty to promote this principle.

From the perspective of corporate logic, in the absence of any direct interests, assistance or support is difficult to implement so one could not expect much to be forthcoming. Thus, here we explore the idea of support or assistance strategies in terms of public policies from the perspective of both local and national governments.

b) Assistance strategies from Japan: Proposal 1 (microcredit)

At present, the Chinese state government is implementing rural financial market reforms and a variety of other initiatives toward the establishment of micro-credit institutions. Besides those efforts, cooperation is also coming from such bodies as the Grameen Bank, International Finance Corporation, and the German bank KfW.[6] Nevertheless, many challenges still exist for the establishment of microcredit markets in China, including a shortage of fund sources, an inadequate regulatory framework, and so on.

Thus, if local governments in Japan were to create systems similar to the forest environment taxes currently being implemented locally based on the beneficiary-pays principle, and if the taxes collected from citizens were to be used as funding sources for microcredit in China, this would likely give a huge boost to the establishment of similar systems in China. At the same time, however, it would also valuable for Japanese financial institutions and academic research institutions to present models of effective systems for the establishment of microcredit markets that are appropriate for the societal conditions in China.

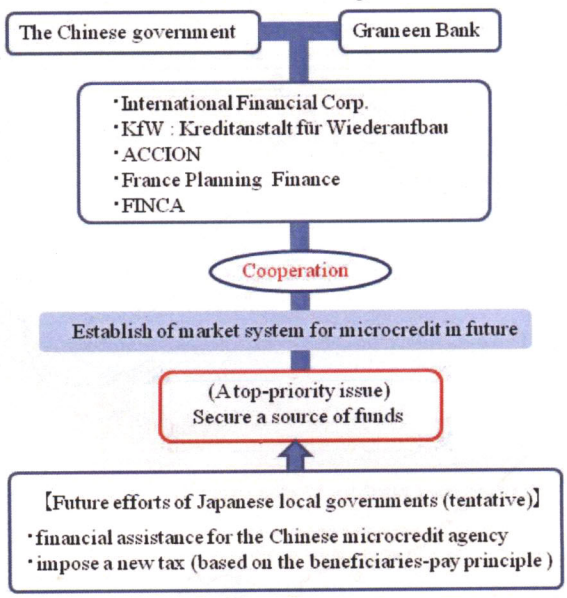

Figure 9. Issues for establishment of microcredit institutions in China, and possible support measures from japan

c) Assistance strategies from Japan: Proposal 2 (use of CDM as a measure to fight global warming)

Possible strategies to utilize the Clean Development Mechanism (CDM) in the agricultural sector include spreading agricultural methods that reduce the use of agricultural chemicals in rural China and promoting chemical-free organic farming methods in order to reduce the use of chemical fertilizers and reduce energy consumption in connection with agrochemical manufacturing; the resulting reductions in energy consumption would then be counted as reductions in Japan's CO_2 emissions. Because crops produced by chemical-free farming generally attract higher prices than conventional crops, one could expect such crops to contribute to higher incomes for farmers in China. Meanwhile, Chinese farm products are exported to Japan in great quantity, but import bans due to the detection of residual chemicals exceeding Japanese standards have led to concerns in Japan about food safety of those products. All considered, the strategies described above would be effective, as they would enhance food safety for both countries, benefit China by restoring confidence in Chinese farm products, and benefit Japan by reducing CO_2 emissions.

(4) Strategies to reduce air pollution and greenhouse gas emissions

Figure 4 suggests that the promotion of water rights transfers in the Yellow River basin will strengthen the foundations of the region as an energy supply base of coal-fired power generation, and that further development of the eastern coastal region by expansion of urban infrastructure will accelerate the spread of the automobile and household electrical products that require energy to operate. At the same time, there will be greater environmental impacts on the atmosphere, including air pollution and an increase in greenhouse gas emissions.

Meanwhile, an American and a German major automaker based in Shanghai and a total of five Japanese and Korean major automakers based in Guangzhou collectively passed the two million vehicle mark (annual production) in 2005, and are contributing to China's motorization and an increase in environmental impacts. There

is a need to create a framework to reduce air pollution and greenhouse gas emissions in developed countries, particularly in the East Asian region, when we consider that investment into China from Japan, Korea, Taiwan and Hong Kong accounts for half of global investment (Figure 3), that much of that investment is going into production bases, that the majority of China's energy production is used in the manufacturing sector, and that, conversely, Japan, Korea and Taiwan are also receiving air pollution due to the transboundary movement of air pollution from China.

The Bali Roadmap was adopted at COP13, and China has accepted some responsibility to reduce its greenhouse gas emissions. A new post-Kyoto Protocol regime is to be developed by 2009, but in the process of discussions, it is expected that some debate will deal with ways to address the issue of carbon "leakage" as indicated above. The Japanese, American and European share of the Chinese car market was 80% in 2002 and dropped to about 50% in 2005,[7] but the ratio is still relatively high. Because of this, in the absence of quantitative assessment methods for carbon leakage and clear strategies to address that topic, it will be difficult for developed countries to demand that China establish specific emission reduction targets.

Thus, Japan needs to propose systems to reduce air pollution and help cut greenhouse gas emissions—not only by providing technologies such as clean coal power generation to the Yellow River basin, but also through collaboration with developed countries in the Americas and Europe, collaboration with countries particularly in East Asia, and collaborative arrangements between local governments that are benefiting significantly from corporate activity in China.

5. Conclusion

This study proposed some strategies for Japan to contribute to China's efforts to address key issues. The discussion first addressed topics relating to the economic development of China overall, including an analysis of capital from overseas and the orientation of development in the Yellow River basin by promoting water rights transfers, as well as the cause-effect relationship between economic development and increased environmental impacts and regional disparities. We learned that the development of the Yellow River basin through water rights transfers has, in effect, major benefits for developed countries whose corporations are active in China. At the same time, development in the Yellow River basin also raises concerns about the transboundary movement of water pollution and air pollution, and about increases in greenhouse gas emissions.

The "beneficiary pays" principle is a key concept to guide Japan's contribution strategies. In short, it is not only the corporations involved who are enjoying benefits from corporate expansion into China an increase of industrial activity. In effect it is also the nations, local governments, and local citizens associated with those corporations who also feel the beneficial impacts of those profits. By expanding the definition of beneficiary, we can expect a large shift in the concept of contributions from developed to developing countries. In particular, it will be difficult to deal with the issue of carbon leakage without recognizing that developed countries are beneficiaries. As a first step, it is important to clarify this kind of understanding for developed countries and developing regions (such as the eastern coastal region of China) in order to protect the environment and limit the growth of regional disparities.

References

1. Osamu Higashi, Tetsuya Kusuda, Xiaochang Wang, Dawen Yang, Shimpei Ozaki, Keisuke Baba, Katsushi Shibata: Development of an water quantity and water quality integrated model and future projections of available water in the Wei River basin, Environmental Engineering Research Papers, vol. 42, pp. 111-118, 2005 (in Japanese).

2. Keisuke Baba, Tetsuya Kusuda, Xiaochang Wang, Dawen Yang, Osamu Higashi, Shimpei Ozaki, Katsushi Shibata: Crop production assessment and consideration of food security in the Wei River basin using EPIC, Environmental Engineering Research Papers, vol. 41, pp. 659-664, 2004 (in Japanese).

3. 21st Century Economy News (31 July 2007) (in Chinese).

4. China Environmental Yearbook (2000-2005) (in Chinese).

5. Xinhua Communication (31 July 2005) (in Chinese).

6. Chinanews website: http://view.chinawave.co.jp/detail/144.html

7. Development Bank of Japan, Status of automakers expansion in China and market forecasts, Ima no chumoku shihyo No. 099-1, 2006 (in Japanese).

Water Rights Transfers and Regional Development in China

Feng SHI[1] Hidefumi IMURA[1] Osamu HIGASHI[1] Xin CAO[1] and Akio ONISHI[2]
[1]Nagoya University, [2]Research Institute for Humanity and Nature

1. Introduction

Since its policies of reform and openness began in 1978, China has continued to enjoy rapid economic growth, although the country's coastal areas have been the main drivers of this growth. Meanwhile, the economic ripple effects reaching inland from coastal areas are minimal, and the regional disparities may become bigger in the future.[1] In recent years, along with rapid population growth and industrial concentration in urban centers, driven by economic growth, power shortages have become a problem particularly in coastal areas, and water shortages have occurred in northern China, particularly in the Yellow River basin. These factors are predicted to become important constraints upon future economic growth in China.[2]

In order to address such problems, in 1999 the central government of China announced that Western Development strategy would be a national strategy as a core part of its Tenth Five-Year Plan.[3] This strategy includes as key projects the West-to-East Natural Gas Transportation Project and the West-to-East electricity transmission project, to address power shortages in coastal areas, and South-to-North water diversion project to address water shortages in the north. The water diversion project aims to divert water northwards from the Yangtze (Changjiang) River, and work has already begun on the eastern and central routes that are intended to carry water to Beijing, Tianjin and other large cities. However, the western route—intended to relieve water shortages in the upper and middle reaches of the Yellow River—is still at the planning phase, as this is reportedly the most difficult one to build.[4]

The northern route of the West-to-East electricity transmission project is intended to carry electricity to Beijing and Tianjin from areas such as Inner Mongolia and Shanxi Province, in the upper and middle reaches of the Yellow River (the area targeted by the western route of the South-to-North water diversion project). Responding to this plan, the Inner Mongolia Autonomous Region considered establishing a new energy production base using its abundant coal resources. But because the maximum water allocations from the Yellow River based on the Yellow River Water Allocation Scheme (established as a result of flow stoppages on the Yellow River) were already being used, however, the Yellow River Conservancy Commission (YRCC) did not permit new water withdrawals needed for electrical power generation. This situation is a sign of the urgent need to secure water resources in the upper and middle reaches of the Yellow River if the West-to-East Electricity Transmission Project is to succeed.

For this purpose, there was a trial run of the Yellow River Water Rights Transfer Management Implementation Regulation in 2004, as a new measure to deal with the above situation. The term "water rights" here refers to the right to withdraw water from the Yellow River, and "water rights transfer" means the transfer of water withdrawal rights from the Yellow River.[5] The power generation sector in Inner Mongolia then sought to obtain water rights from the agricultural sector in an effort to develop the energy sector. The method of transferring water rights here was that the power generation sector invested to promote water conservation projects in the agricultural sector, and the resulting surplus agricultural water was used to generate electricity. This is seen as one effective approach for water resource allocation when there are constraints on the water supply.

Many studies have already examined water resource management for the Yellow River.[6] Higashi (2007) examined effective measures for water resource allocation under resource constraints, for each sector, in the Wei River basin (largest tributary of the Yellow River).[7] Zhang (2006), meanwhile, evaluated the

economic benefits that can be obtained by transferring water rights from the agricultural sector to the industrial sector, in Inner Mongolia and Ninxia Autonomous Region.[8] No research to date, however, appears to have comprehensively examined effective water and energy resource allocation based on water rights transfer systems. Furthermore, water rights transfers in China today are permitted only within a given province, and few studies have discussed any expanded scope or range of water rights transfers. Transfers of water and energy resources are tending to cover an increasingly vast area in China today (through projects such as the North Water Transfer Project and the West-to-East Electricity Transmission Project), so it would also be worthwhile to examine and consider the resulting regional impacts of scenarios that include water rights transfers *between* provinces.

In this context, the current study focuses on water rights transfers between the power generation sector and the agricultural sector in Inner Mongolia, and aims to assess the potential for regional development by utilizing water rights transfers. More specifically, we begin by estimating the transferable water volume from the agricultural sector in the target region. Next, we evaluate the effective allocation of water resources and energy to the power generation sector and the industrial sector, using two cases: (1) implementation only within Inner Mongolia, and (2) implementation in both Inner Mongolia and the city of Beijing based on existing policies.[9] In addition, comparing these two cases, we clarify the economic benefits that would arise if water rights transfers covered a broader region than current water rights transfer systems.

2. Regional development trends and water resource management in China

(1) Regional development strategy[9]

China's regional development strategy before 1978 was based on the "theory of balanced development," but after the beginning of reform and openness policies at the end of 1978, actual practice shifted toward "unbalanced development." Deng Xiaoping's "theory of allowing individuals to grow rich first" provides evidence of this change.

The regional development strategy in the Seventh Five-Year Plan, adopted in 1985, draws from the orientation toward the non-balanced development theory: "First, accelerate development in the eastern coastal region, and at the same time shift the centers of development for energy and raw materials to the central region. Work on infrastructure development for large-scale developments in the twenty-first century in the western region." Later, in 1988, when a "coastal region priority development strategy" calling for the promotion of manufactured goods exports, powered by coastal local enterprises, became the official national policy, the unbalanced development theory began to look even more unbalanced.

After the beginning of the 1990s, research into regional issues became a popular topic, amid growing regional disparities and growing dissatisfaction from inland regions. In this context, the "regionally coordinated development strategy" appeared, calling for "adequately exploiting regional comparative advantages while also giving priority to inefficiency and considering equity." This approach was based on the idea of maintaining rapid growth in the coastal regions while also promoting development inland. It was reinforced by the Western Development strategy that was hammered out as a new national strategy in 1999.

Western Development was a centerpiece of China's Tenth Five-Year Plan, which adopted four major projects: the West-to-East natural gas transportation project, the West-to-East electricity transmission project, the South-to-North water diversion project, and the Xizang railroad.

(2) Water resource management

As China promotes large-scale regional development strategies today, policies for securing water resources are becoming increasingly important. China's Ministry of Water Resources is using two strategies: large scale water resource developments such as the South-to-North water diversion project, and the promotion of water conservation. The Water Law, enacted in 1988, is a typical example of the promotion of water conservation. Article 7 promotes water conservation, and Article 32 law stipulates the establishment of water withdrawal permit systems for organizations that withdraw water directly from rivers. In recent years, there have been attempts to strengthen regulations for water conservation: for example, in 1999, implementation for the Yellow River Water Volume Integrated Regulation System began in order to strengthen water resources management on the Yellow River; and in 2002 the water law was amended to clarify in Article 8 the fact that water conservation is an obligation of industries and individuals. Below, we provide an overview of water withdrawal permit regulations and the Yellow River Water Volume Integrated Regulation system.

a) Water withdrawal permit regulations

In the Water Law of 1988, Paragraph 1 of Article 3 states that water resources belong to the state government; Paragraph 3 of the same article describes the separation of water resource rights of ownership and rights of use. Article 32 provides for water withdrawal permit regulations, targeting bodies that draw water directly from rivers. In addition, recognizing the State Council's 1993 enactment of the Water Withdrawal Permit Regulation Implementation Law, the Ministry of Water Resources issued the Notification of Authority of the YRCC for Water Withdrawal Permit Control as a notification relating to issuing bodies of water withdrawal permits for the Yellow River basin, stipulating that the Yellow River Conservancy Commission (YRCC) was to exercise its authority for implementation and supervision of the water withdrawal permit regulations for the Yellow River basin, on behalf of the said Ministry. In addition, in October of the same year, the YRCC enacted the Yellow River Water Withdrawal Permit Implementation Rules, which contain detailed provisions relating to application procedures for water withdrawal permits, decision-making authority for permits, water withdrawal permit registration, and so on. In this case, the basis for the water withdrawal permit regulations is the Yellow River Water Allocation Scheme. It establishes the maximum limits of water allocations for each province and autonomous region.

b) Yellow River Water Volume Integrated Regulation System

The Yellow River Water Volume Regulation coordinates the Yellow River's water resources temporally and spatially, using the function of dams to control water volume. Under this system, this Yellow River Water Volume Regulation is extremely important for the effective utilization of the Yellow River's water resources, because the water resource distribution of the Yellow River is non-uniform. The YRCC executes the Yellow River Water Volume Regulation by exercising integrated control of dams on the main course of the Yellow River.

3. Water rights transfer systems and their significance

In China, water conservation policies have already been promoted for some time, as in the amended Water Law (2002), which states that "Water conservation is the obligation of industries and individuals." Based on this system, the level of water conservation increased in the industrial sector, although in the agricultural sector no major improvement was observed, with irrigation efficiency holding steady at about 40 percent. This lack of improvement originated in a structural problem, as very few channels existed for investment in water conservation in the agricultural sector, so the introduction of water-efficient

irrigation depended on the scarce financial resources of governments (Figure 1).[10] Because agricultural water accounts for over 70 percent of water-use volumes in China overall, the promotion of water conservation in this sector is a critical issue to address if China is to deal with its water resource problems.

In this context, the trial run of the Yellow River Water Rights Transfer Management Implementation Regulation began in 2004. Water rights transfers mentioned here mean transferring the right to withdraw water from the Yellow River. Yellow River water rights transfers are only possible within a province or autonomous region.[5] At present, about 30 construction projects are underway in Inner Mongolia that involve water rights transfers by the power generation and agricultural sectors.[5]

Figure 2 shows the predicted results of the introduction of a water rights transfer system. The figure shows an example of water rights transfers between the industrial sector and the agricultural sector. Compared with Figure 1, in the case of utilizing water rights transfer system, Figure 2 suggests that a positive feedback cycle will emerge: corporations can obtain abundant water resources from the agricultural sector by investing in efficient irrigation, improved productivity in industry will boost government tax revenues and bolster its financial resources, and the respective governments will enhance water conservation investments in the domestic and agricultural sectors.

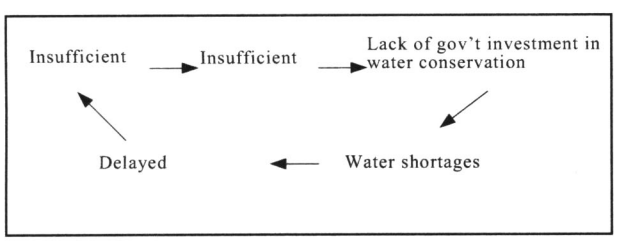

Figure 1. Example of typical issues of water resources management

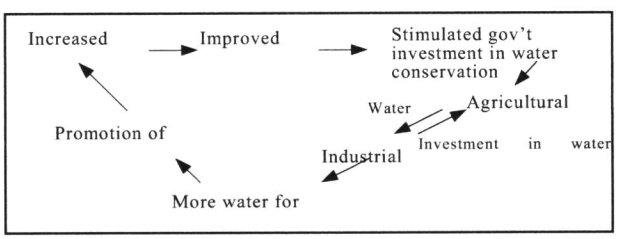

Figure 2. Potential for regional development through water rights transfers

4. Potential for regional development through water rights transfers

(1) Target region

Figure 3 shows the location of the Inner Mongolia Autonomous Region and the distribution of irrigation districts within the region.

Inner Mongolia has about 30 percent of China's entire coal reserves, giving this region great potential for coal-fired power generation.

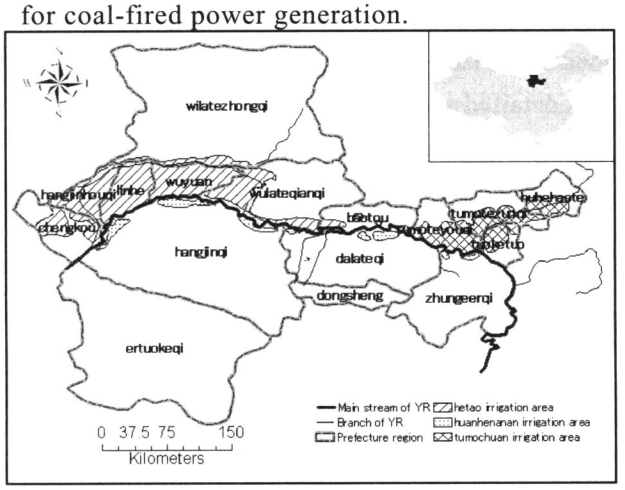

Figure 3. Location of major irrigation districts in Inner Mongolia
Source: Prepared by authors from Yellow River basin maps[11]

Table 1. Basic data on major irrigation districts in Inner Mongolia

Irrigation District	County	Cultivated area	Effective irrigation area	Cultivated area share of effective irrigation
		10,000 ha	10,000 ha	%
Hetao	Weikou County, Hangjin Back Banner, Linhe City, Wuyuan County, Wulate Front Banner, Wulate Middle Banner, Baotou City suburbs	51.6	57.64	100%
Yellow River South Bank	Hangjin Banner, Dalad Banner, Jungar Banner	3.3	4.62	100%
Tumochuan	Hohot City, Baotou City, Tumote Right Banner, Tumote Left Banner, Tuoketuo County	27.94	9.47	33.89%

Source: Prepared by authors from references[12]

About half of Inner Mongolia's coal deposits are in Erdos City.[13] Agricultural water accounts for about 90 percent of all water use in Inner Mongolia, so the water-saving potential in the agricultural sector is huge.[5] Thus, Inner Mongolia would appear to have good prospects for effective water rights transfers between the power generation sector and agricultural sector.

Table 1 shows an outline of the major irrigation districts in Inner Mongolia (Hetao Irrigation District, Yellow River South Bank Irrigation District, and Tumochuan Irrigation District). "Effective irrigation" area here refers to the area of level cultivated land with irrigation facilities and equipment installed, with adequate water resources, and with the potential to conduct normal irrigation during average years.[14]

(2) Calculation of transferable water volume

a) Annual transferable water volume in the agricultural sector

The current study follows the approach taken by Wang (2006)[15] to define the annual transferable water volume in the agricultural sector (TW) as difference between the original amount of allocated water (AW) and the annual volume of agricultural water after implementing water conservation measures (GIW) (Equation 1). Equation 2 can be deduced from Equation 1, because GIW can be derived from the relationship between the net amount of water required for irrigation (NIW), the irrigation water utilization efficiency ratio (η), and the irrigation shortfall coefficient (β). The ratio η is determined by the efficiency of facilities, and is the product of the canal irrigation water use efficiency ratio and field irrigation water use efficiency ratio. β is the irrigation shortfall coefficient. In areas with tight water supplies, farmers use less than the optimal water required for a given crop. In such cases, the irrigation shortfall coefficient is defined as the ratio of actual irrigation water volume and the optimal water demand volume.

Equations in this study use regular (non-italicized) letters to indicate variables that represent multiple meanings (volume) with multiple letters, and italics to indicate where one letter represents one thing (volume). All of the subscripts have been written without italics.

$$TW = AW - GIW \tag{1}$$

$$TW = AW - \beta\frac{NIW}{\eta} \tag{2}$$

TW: Total transferable water volume GIW: Gross irrigation demand volume NIW: Net irrigation demand volume

AW: Water allocated by water rights η: Irrigation water utilization coefficient β: Irrigation shortfall coefficient

b) Derivation of net amount of water required for irrigation (NIW)

NIW is derived from Equation 3, which was developed by Duan Ai Wang (2002),[16] Fu Guo Bin (2001),[17] and Liu Yu (2005),[18] but this methodology requires detailed soil data.

$$NIW = \sum_i (ET_i - PE - G_i - ASW_i)ISA_i \tag{3}$$

ISA_i : Irrigable area for crop i PE : Effective precipitation volume

ET_i : Water demand volume required for evapotranspiration for crop i G_i: Effective volume of groundwater supplement for crop i ASW_i: Change of effective water storage volume during growing period for crop i

Because we could not obtain adequate soil information for Inner Mongolia, we decided to express this value by the difference between the potential evapotranspiration amount of crops that have NIW and effective rainfall volume, based on the approach in CROPWAT by Smith (1992).[19] As an additional point, in Inner Mongolia it is common practice to irrigate pasture land, and to irrigate during the autumn season.[20] With this in mind, NIW can be derived as shown in Equation 4.

Autumn irrigation is conducted from the end of September through the end of October after crops have

been harvested. The moisture from irrigation freezes during the winter along with the soil, and is held there until it melts and is released in the spring during sowing season when water is scarce; this system could be considered to be an irrigation method unique to semi-arid regions.

$$NIW = \sum_i (ET_i - PE) ISA_i + \omega * IA \quad (4)$$

IA: Effective irrigated area ω: Units for autumn irrigation (m^3/day/ha)

Effective rainfall is the amount of precipitation that falls on cultivated land during the period of irrigation and can be used for crop growing.[21] Effective rainfall is calculated using Equation 5, as defined by the Food and Agriculture Organization (FAO).[19]

$$\begin{aligned} PE &= P(4.17-0.2P)/4.17 \quad && P < 8.3\text{mm/d} \\ PE &= 4.17+0.1P && P \geq 8.3\text{mm/d} \end{aligned} \quad (5)$$

***P*: Precipitation**

c) Allocated water are based on water rights (AW)

Table 2 shows volumes of YRCC-approved water withdrawals from the main course of the Yellow River for major irrigation districts in Inner Mongolia (Hetao Irrigation District, Yellow River South Bank Irrigation District, and Tumochuan Irrigation District).

Table 2. Approved water withdrawals from the main course of the Yellow River for major irrigation districts in Inner Mongolia

Associated irrigation district	Water withdrawal permit no.	Water withdrawal department name	Water withdrawal facility name	Name of water source	Approved water withdrawal (10,000 m3)
Yellow River South Bank Irrigation District	Withdrawal (State, Yellow) [2000] No. 14001	Inner Mongolia Yellow River Construction Administration Bureau	South Shore Main Canal Water Gate	Yellow River main course	41,000
Hetao Irrigation District	Withdrawal (State, Yellow) [2000] No. 14002	Inner Mongolia Yellow River Construction Administration Bureau	Shenwu Main Canal Water Gate	Yellow River main course	58,340
	Withdrawal (State, Yellow) [2000] No. 14003	Inner Mongolia Yellow River Construction Administration Bureau	Beizong Main Canal Water Gate	Yellow River main course	440,000
Tumochuan Irrigation District	Withdrawal (State, Yellow) [2000] No. 14007	Inner Mongolia Chengkou Irrigation Administration Bureau	Chenhkou Pump Site	Yellow River main course	28,000
	Withdrawal (State, Yellow) [2000] No. 14008	Tumete Right Banner Union	Union Canal Sub-Pump Site	Yellow River main course	8,000
	Withdrawal (State, Yellow) [2000] No. 14009	Tuoketuo Yellow River Irrigation Main Company	Madihao Pump Site	Yellow River main course	8,400

Source: Prepared by the authors from literature.[22]

For the Tumochuan Irrigation District, because actual water withdrawal data is available for sources other than the main course of the Yellow River, we calculate the volume of water withdrawals here from the main course of the Yellow River, following the approach taken by Wang (2006).[15] When calculating AW, we utilize the value of water withdrawal permits in 2000,[22] before the launch of the water rights transfer system. This calculation results in the following withdrawal volumes from initial (2000) water rights for the three irrigation districts: 4,983 million m^3 (Hetao), 410 million m^3 (Yellow River South Bank), and 690 million m^3 (Tumochuan).

1. Irrigable cultivation area, by zone and by crop

The land use classifications for major irrigation districts in Inner Mongolia are shown in Figure 4. Using provincial boundaries we classify the irrigation districts into 15 zones. The cultivated land of Baotou City is separated into the Hetao and the Tumochuan irrigation districts. Next, the irrigated areas are calculated by zone and by crop, as shown in Equation 6.

$$ISA_{mij} = \left(\frac{SA_{ij}}{SA_j}\right) * \left(\frac{ICA_m}{CA_m}\right) * \left(\frac{CA_{mj}}{CA_j}\right) * SA_j \qquad (6)$$

ISA_{mij}: Irrigable area, by zone and by crop **SAij: Seeded area of crop i in province j**

ICAm: Effective irrigation area of cultivated land in irrigation district m

CAm: Cultivated area in irrigation district m **CAmj: Cultivated area in each zone**

CAj: Cultivated area in province j **SAj: Total seeded area in province j**

The methodology is explained below in more detail.

- Step 1: Calculate cultivated area in each county using the land-use classification map for the year 2000 (Table 3). CAj in the table is the cultivated area in the entire county, and CAmj is the cultivated area associated with each major irrigation district within the cultivated area in each county, in other words, the cultivated area for each zone.
- Step 2: Using the results of Step 1 and the total crop area in each county SAj, calculate crop area in each zone (CAmj / CAj) * SAj.
- Step 3: To calculate the irrigable area in each zone, multiply the crop area in each zone as calculated in Step 2 by the ratio of effective irrigated area of cultivated land in each irrigation district (ICAm / CAm).
- Step 4: Calculate the irrigable area for each zone and each crop ISAmij, from the ratio of crop area for each crop (SAij/ SAj) and the irrigable area in each zone as calculated in Step 2 (Table 4).

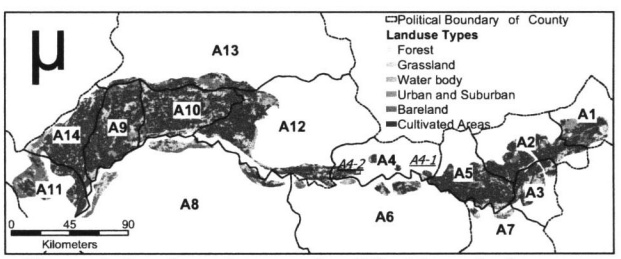

Figure 4. Land use types and political boundaries or counties of major irrigation districts in Inner Mongolia (2000)

Table 3. Basic data on zones of major irrigation districts in Inner Mongolia

Irrigation District	County	Zone	CAj (ha)	CAmj (ha)	CAmj / CAj (%)
Tumochuan	Hohot City	A1	53,391.9	41,462.2	77.66
	Tumote Left Banner	A2	103,846.5	88,690.9	85.41
	Tuoketuo County	A3	66,261.7	36,959.6	55.78
	Baotou City B	A4-1	59,152.4	8,437.2	14.26
	Tumote Right Banner	A5	101,628.1	101,611.2	99.98
Yellow River South Bank	Dalad Banner	A6	103,342.9	10,360.4	10.03
	Jungar Banner	A7	46,618.6	2,958.7	6.35
	Hangjin Banner	A8	78,009.7	17,067.8	21.88
Hetao	Linhe City	A9	118,821.8	118,821.8	100
	Wuyuan County	A10	117,517.8	117,517.8	100
	Weikou County	A11	60,743.3	45,439.4	74.81
	Wulate Front Banner	A12	160,515.0	114,375.8	71.26
	Wulate Middle Banner	A13	90,951.8	39,674.2	43.62
	Hangjin Back Banner	A14	137,107.9	137,107.9	100
	Baotou City A	A4-2	59,152.4	8,502.6	14.37

Table 4. Irrigable area by zone and by crop in Inner Mongolia (2000)

County	Zone	Wheat (ha)	Mais (ha)	Cotton (ha)	Beans (ha)	Rice (ha)	Yams (ha)	Oily vegetables (ha)	Hemp (ha)	Vegetables/sugar (ha)	Fruit (ha)	Pasture (ha)
Hohot City	A1	3254.53	2889.54	0.00	958.11	0.00	1134.52	1256.19	0.00	1572.52	907.32	3292.85
Tumote Left Banner	A2	5052.07	7744.05	0.00	516.27	0.00	1880.70	3503.26	36.88	1106.29	291.32	1594.67
Tuoketuo County	A3	940.96	3277.78	0.00	509.47	0.00	0.00	1614.19	0.00	579.65	221.46	5809.31
Baotou City B	A4-1	176.79	146.02	0.00	31.05	3.64	0.00	73.85	0.00	219.87	37.62	0.10
Tumote Right Banner	A5	7849.26	8898.13	0.00	289.82	0.00	1635.41	7497.34	0.00	3053.45	443.35	6638.11
Dalad Banner	A6	1905.17	3439.89	0.00	203.07	0.00	717.52	1767.33	16.00	770.44	100.06	2635.83
Jungar Banner	A7	153.48	742.93	0.00	332.25	0.00	618.97	692.34	0.00	121.43	527.81	1400.02
Hangjin Banner	A8	1770.69	3556.31	0.00	268.96	0.00	1191.66	2286.20	0.00	556.61	580.52	796.58
Linhe City	A9	40787.41	14409.61	0.00	280.50	0.00	550.62	11718.85	0.00	10586.44	8960.56	7477.45
Wuyuan County	A10	44820.95	12272.54	0.00	325.72	0.00	639.80	16390.53	0.00	8189.45	4681.01	2134.31
Weikou County	A11	6574.77	3477.71	0.00	51.91	0.00	25.95	2655.86	0.00	2993.25	1576.21	519.32
Wulate Front Banner	A12	32992.26	11399.26	0.00	478.66	230.47	1870.33	9458.02	177.28	6266.93	889.07	10497.14
Wulate Middle Banner	A13	8966.53	2050.79	0.00	39.88	0.00	1145.03	2831.23	0.00	472.82	34.18	1582.59
Hangjin Back Banner	A14	29868.40	12205.08	0.00	0.00	0.00	157.15	8014.49	0.00	6945.90	6859.99	3176.70
Baotou City A	A4-2	529.80	437.59	0.00	93.05	10.90	179.39	221.31	0.00	658.89	112.75	159.49

e) Determination of other parameters

- For precipitation, we use the average values from seven weather monitoring stations in Inner Mongolia for the years 1971 through 2000.
- For water demand by each crop ET_i, because insufficient data was available from weather monitoring stations, we utilize values for each crop in Inner Mongolia, calculated using the Penman-Monteith

equation, based on existing literature.[24, 25]

- We assume no changes in crop-specific ET and precipitation for future planning years.
- The irrigation shortfall coefficient is set as 0.8 based on Fu Guo Bin (2003).[26]
- The irrigation water utilization ratio for the year 2000 is set as 0.336 for the Hetao Irrigation District,[24] and 0.24 for the Yellow River South Bank Irrigation District,[5] based on existing literature. Because no information was available for the Tumochuan Irrigation District, here we assume the value 0.336, the same as in the Hetao Irrigation District.
- For the field irrigation water use efficiency after implementation of water conservation measures, we use the value 0.9, based on Chinese water conservation technology standards.[27]
- Based on testing in the South Bank Irrigation District in Inner Mongolia, we use 0.7 as the canal irrigation water use efficiency ratio after water conservation measures were implemented.[5]
- We assume that future crop patterns will be the same as in the year 2000.

f) Results of estimates of annual transferable water volume in the agricultural sector

Figure 5 shows the calculation results of the annual transferable water volume of the agricultural sector. The table shows that water conservation measures, if implemented, would results in a transferable water volume of 2,571 million m^3 per year in the target region.

Table 5. Transferable water volume (100 million m3)

Irrigation district	Water rights (volume)	Water demand (2000)	Future planned annual water demand	Transferable water volume
Tumochuan	6.90	7.76	4.51	2.39
Yellow River South Bank	4.10	4.07	1.94	2.16
Hetao	49.83	49.26	28.67	21.16
Total	60.83	61.08	35.12	25.71

(3) Case study of regional development using water rights transfers

Below we compare the economic impacts of two cases for water rights transfers: transfers conducted within one single province (Case 1), as is the present case; and transfers conducted between provinces (Case 2), with a view to the future expansion of the scope of water resource and energy transfers in China. Case 1 focuses on Inner Mongolia alone, while Case 2 considers a water rights transfer system covering Inner Mongolia and the city of Beijing. Figures 5 and 6 show the general concepts of water resource and energy allocation.

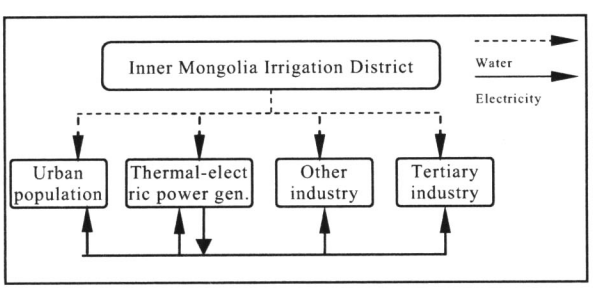

Figure 5. Allocation system within one region

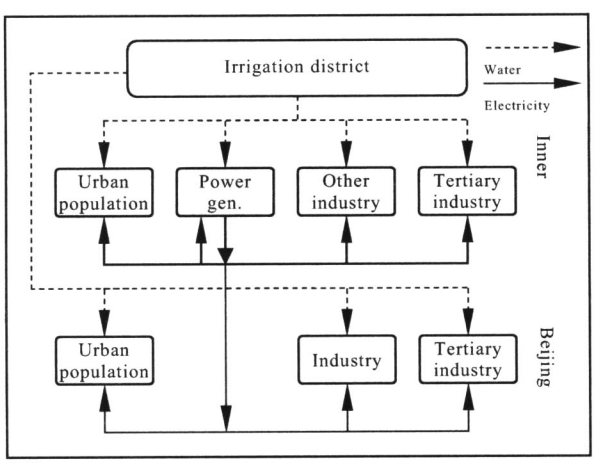

Figure 6. Allocation system between two regions

(4) Analytical methods

We apply the Leontief production function to represent the relationships among industry k (excludes electricity generation industry), electricity generation industry e, and service industry s, and increased value added ΔV for each industry, as well as labor ΔL, water resources ΔW, and electricity inputs ΔE. We

use the upper limits of increases of labor, water resources, and electricity generation as constraining factors (Equations 7 to 12). The increase in electricity generation is determined endogenously from the relationship with water resource allocation to the electricity generation industry, as shown in Equation 13.

$$\Delta V_{\mathrm{k}} = \min\left\{\frac{\Delta L_{\mathrm{k}}}{l_{\mathrm{k}}}, \frac{\Delta W_{\mathrm{k}}}{w_{\mathrm{k}}}, \frac{\Delta E_{\mathrm{k}}}{e_{\mathrm{k}}}\right\} \quad (7)$$

$$\Delta V_{\mathrm{e}} = \min\left\{\frac{\Delta L_{\mathrm{e}}}{l_{\mathrm{e}}}, \frac{\Delta W_{\mathrm{e}}}{w_{\mathrm{e}}}, \frac{\Delta E_{\mathrm{e}}}{e_{\mathrm{e}}}\right\} \quad (8)$$

$$\Delta V_{\mathrm{s}} = \min\left\{\frac{\Delta L_{\mathrm{s}}}{l_{\mathrm{s}}}, \frac{\Delta W_{\mathrm{s}}}{w_{\mathrm{s}}}, \frac{\Delta E_{\mathrm{s}}}{e_{\mathrm{s}}}\right\} \quad (9)$$

Constraining factors

$$\Delta L_{\mathrm{k}} + \Delta L_{\mathrm{e}} + \Delta L_{\mathrm{s}} = \Delta L_{\mathrm{total}} \quad (10)$$

$$\Delta W_{\mathrm{k}} + \Delta W_{\mathrm{e}} + \Delta W_{\mathrm{s}} + \Delta L * p = \Delta W_{\mathrm{total}} \quad (11)$$

$$\Delta E_{\mathrm{k}} + \Delta E_{\mathrm{e}} + \Delta E_{\mathrm{s}} + \Delta L * q = \Delta E_{\mathrm{total}} \quad (12)$$

$$\Delta E_{\mathrm{total}} = \frac{\Delta W_{\mathrm{e}}}{\alpha}(1-\delta) \quad (13)$$

ΔV: Increased value added ΔL: Increased labor inputs ΔW: Increased water inputs Δ: electricity inputs $\Delta W_{\mathrm{total}}$: Potential increase in water resources $\Delta E_{\mathrm{total}}$: Potential increase in electricity $\Delta L_{\mathrm{total}}$: Potential increase in labor l: Labor input per unit of value added w: Water input per unit of value added e: Electricity input per unit of value added p: Water use per capita q: Electricity use per capita α: Water demand per unit of electricity generation δ: Power transmission loss ratio k: Industry (excluding electricity generation) e: Electricity generation industry s: Service industry

The increase in labor is determined endogenously based on the existing urban plans of each region.[28, 29] The upper limits of future population increases for Inner Mongolia and Beijing are calculated (at 13.6 million, and 18.0 million persons, respectively) from the differences between the respective urban populations in the year 2000 and the upper limits for Inner Mongolia and Beijing according to their urban plans. The increase in water resources (in other words, the transferable water volume), is, as previously calculated, 2,571 m^3 million for Inner Mongolia. It is assumed that Beijing's increased water demand for industrial development and domestic uses will be met by Inner Mongolia.

Data for the year 2000 are used for resource inputs per unit of value added, and for average resource consumption per capita (Table 6).[30, 31, 32, 33, 34, 35]

Table 6. Basic units for analysis (2000)

		Beijing	Inner Mongolia
Annual domestic electricity use per capita (urban)	kWh/person	549.90	155.20
Annual domestic water consumption per capita (urban)	m^3/person	127.44	37.08
Industrial water demand (excluding power gen. industry) per unit of value added	m^3/10,000 yuan	114.43	153.58
Industrial electricity use (excluding power gen. industry) per unit of value added	kWh/10,000 yuan	1813.96	3672.58
Industrial workers (excluding power gen. industry) per unit of value added	persons/10,000 yuan	0.13	0.17
Service industry water demand per unit of value added	m^3/10,000 yuan	10.15	2.06
Service industry electricity use per unit of value added	kWh/10,000 yuan	790.30	445.00
Service industry workers per unit of value added	persons/10,000 yuan	0.24	0.65
Electricity generation industry water demand per unit of value added	m^3/10,000 yuan	77.63	139.36
Electricity generation electricity use per unit of value added	kWh/10,000 yuan	2002.28	3538.70
Electricity generation workers per unit of value added	persons/10,000 yuan	0.03	0.07
Water demand per unit of value added	m^3/10,000 kWh	28.80	28.80
Power transmission loss ratio	%	6.18	5.56

Source: Prepared by authors from literature.[30, 31, 32, 33, 34, 35]

(5) Results and discussion

The economic impacts of water rights transfers for each case are shown in Figures 7, 8, and 9. The figures show that multiple provinces can have more economic development when multiple provinces participate in a water rights transfer system than when water rights transfers are conducted within one province alone. Thus, in the context of megaprojects such as China's South-to-North water diversion project, and the West-to-East electricity transmission project, an effort to expand the scope of water rights transfers is likely to benefit the economic development of the country overall.

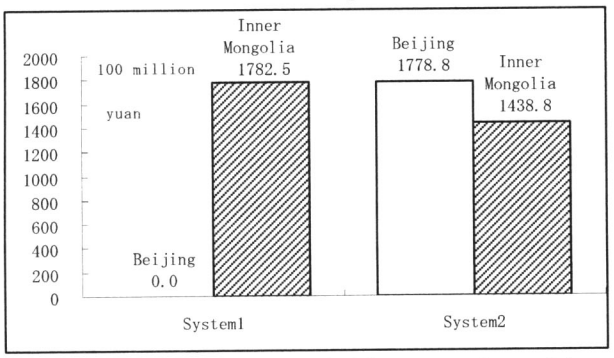

Figure 7. Comparison of extra value added for one-region and two-region systems

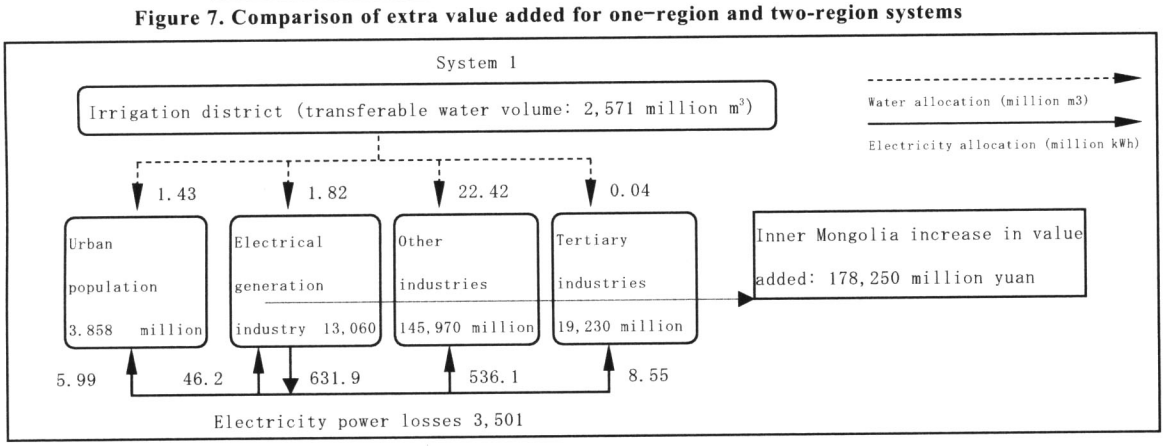

Figure 8. Resulting allocation with one region

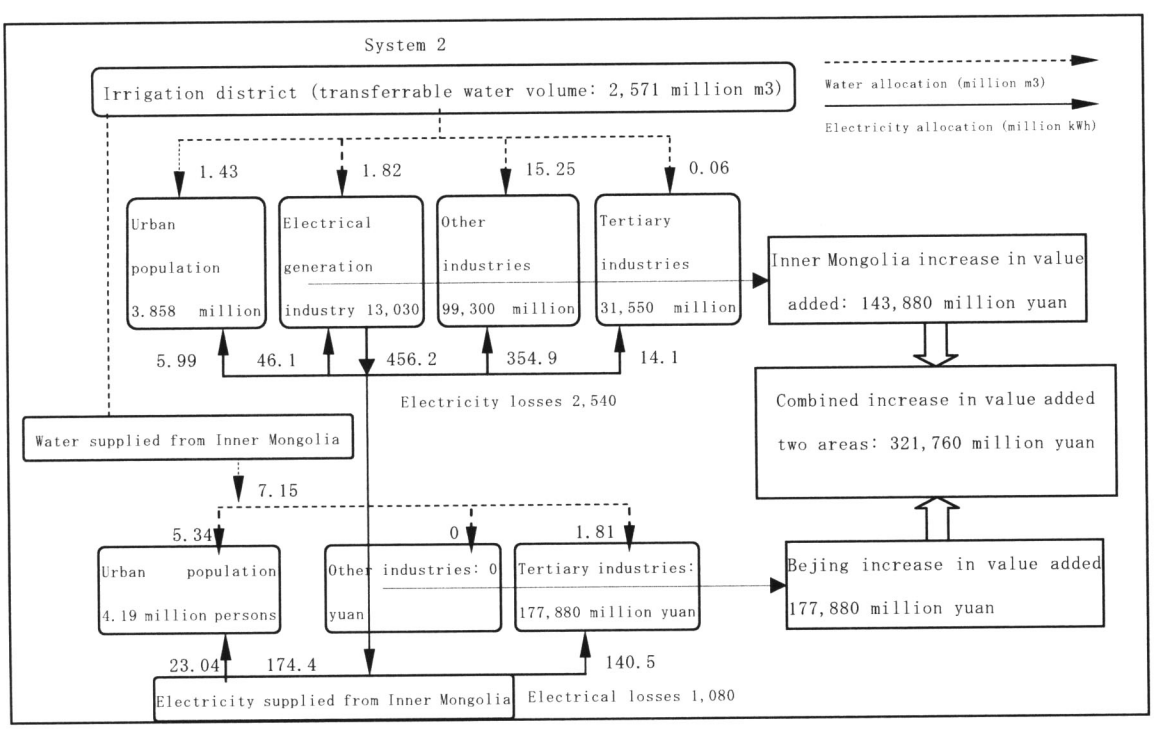

Figure 9. Resulting allocation with two regions

5. Conclusion

The current study focuses on water rights transfers between the power generation sector and the agricultural sector in the Inner Mongolia Autonomous Region, and uses two separate cases to assess the potential for regional development by utilizing water rights transfers. Case 1 is based on water rights transfers conducted only within Inner Mongolia, while Case 2 is based on a water rights transfer system between two provinces, using Beijing and Inner Mongolia as an example. This analysis produces an increased economic value-added of 178,250 million yuan per year for Case 1, compared to the remarkable total of 321,760 million yuan for both provinces in Case 2. The findings suggest that when promoting water rights transfer systems in the future, it would be beneficial for the economic development of the entire country if China were to encourage interprovincial transfers.

For future topics, it would be worth developing a detailed water rights transfer system that articulates the rules and other aspects between the various stakeholders involved in the transfers. For example, in the case of water rights transfers between cities, the development of City A, which has obtained water rights, may inhibit the development of City B, which has sold water rights. This could also be a problem between industries and companies. It is also conceivable that the agricultural sector might expand its irrigated area as a result of water rights transfers, but this should be done only after careful consideration of the state of soil salt damage. Meanwhile, in cases in which the industrial sector obtains water rights from the agricultural sector, simply investing in water-conserving irrigation is not the only option; there is also the potential to help create a more stable society, such as by bolstering the safeguard systems in the context of water rights transfers, for example, by preferential hiring of surplus labor from the affected villages. In the future, we also intend to investigate safeguard systems such as these.

References

1) Shiro Hioki: Regional disparities and the trickle-down effect from coastal to inland areas in China—An examination from the perspective of regional industrial input-output analysis, Bulletin of the Japan Association for Comparative Economic Studies: 41:1, pp. 27-38, Jan. 2004 (in Japanese).
2) Japan Bank for International Cooperation, JBIC Institute: Current water resource conditions and challenges in northern China—analysis of water supply and demand in the Yellow River Basin, JBICI research paper No. 28, 2004 (in Japanese).
3) Osamu Tanaka: China's Tenth Five-Year Plan, Sososha Ltd., 2001 (in Japanese).
4) Reiitsu Kojima: "Factors that constrain economic development, in structural change," in "Structural changes in contemporary China," ed. Kazuko Mori, Chapter 4, Perspectives toward a superpower China, Volume 1, University of Tokyo Press, 2000 (in Japanese).
5) Water Resource Department : Summarize of water right transfer sysetem (1), China Water Power Press, 2006.
6) Hidefumi Imura, Akio Onishi, Mina Okamura, and weihua Fang: Research into spatial structure of water resources supply and demand based on county and city data in the Yellow River basin, Environmental Systems Research, Vol. 33, pp. 477-487, 2005 (in Japanese).
7) Osamu Higashi: Research on development of water volume and water quality integrated model of China's Wei River Basin, Nagoya University Graduate School, Environmental Studies Research Thesis, 2007 (in Japanese).
8) Huimin zhang,fang xing, huiti cao:Evaluaton of experimental value of water right transfer in Ning-Meng section of Yellow River Basin, China Water Resources 2006,No.15,pp34-36, 2006.
9) Lin Jiabin: Inland development and infrastructure improvements in China, Twentieth Transportation Policy Seminar, 2001 (in Japanese).
10) Juqin Shen, ming chen, xiaokun chen : Method of Input-Output Analysis for Agricultural water saving, Irrigation and

Drainage, Vol.20, No.4, pp51-55, 2001.

11) YRCC : Yellow River Basin Atlas, SinoMaps Press, 1989.

12) YRCC : Recent key of renovation and development planning in YR, YRCP, 2002.

13) Inner Mongolia : Inner Mongolia autonomy district energy industry five year plan2005-2010, 2006.

14) Reiitsu Kojima, Commentary on Chinese economic statistics and economic law (in Japanese), Institute of Developing Economies, 1988.

15) Lanming Wang,Yan Li : Argue for water right transfer plan in Inner Mongolia Yellow River Basin, Inner Mongolia Water Resource, 2006, No.1, pp55-56, 2006.

16) Aiwang Duan,Nanquan Xin,Lixian Wang : The Definition and Calculation of Agriculatural Water Saving Potential, Irrigation and Drainage, Vol.21, No.2, pp25-28, 2002.

17) Guobin Fu, Jingjie Yu, Changming Liu, Huian Li, Fugui Hang : Method and Application of Water Saving Potential in Irrigation District, Irrigation and Drainage, Vol.20, No.2, pp24-28, 2001.

18) Yu Liu, Jiabing Cai, Lingen Can, L.S.Pereira : Irrigation System and Water balance Analysis for YR downstream Irrigation District, Journal of Hydraulic Engineering, Vol.36,No.6, pp1-10, 2005.

19) FAO (1992) : CROPWAT－A Computer Program for Irrigation Planning and Management. FAO Irrigation and Drainage Paper 46, Rome.

20) Suhong Qin, Yuzhe Li, JInfeng Li, Jianguo Zhang : Measure of water saving for Irrigation and water resource shortage in the Hetao Irrigation District, Inner Mongolia Water Resource, 2005, No.2, pp37-39, 2005.

21) Japanese Society of Irrigation, Drainage and Rural Engineering: Handbook of Irrigation, Drainage and Rural Engineering, 1989 (in Japanese).

22) Guangsheng Sun, Xixian Qiao, Shousong Sun : Water Resource Management of YR, YRCP, 2001.

23) Japan Supermap: Data provided by United Research Center for Water Problems, Chinese Academy of Sciences

24) Irrigation and Drainage Development center of China : Study on Strategy of water saving in Large-scale Irrigation District of YRB, YRCP, pp65-67, 2002.

25) Di Xu, Lingen Cai, Zhi Yan : Study on water saving in YR Water drawing Irrigation District, China Agriculatural Press, pp142-143, 2004.

26) Guobin Fu, Lijuan Li, Jingjie Yu, Changming Liu : Estimation of water-saving potential in the Hetao Irrigation District, Transactions of the CSAE, Vol.19, No.1, pp54-58, 2003.

27) Agriculatural Water Resource Department : Standard of Water Saving Irrigation Technology –China Nation Standard SL207-98, 1998.

28) Beijing Development Committee : Beijing economy and Social Development five years program 2006-2010, 2006.

29) Inner Mongolia Development Committee : Inner Mongolia economy and Social Development five years program 2006-2010,, 2006.

30) Inner Mongolia Autonomous Region Bureau of Statistics : Inner Mongolia Statistics Yearbook 2001, China Statistics Press.

31) Beijing Bureau of Statistics : Beijing Economy Statistics Yearbook 2001, China Statistics Press.

32) National Bureau of Statistics of China : China Industry Economy Statistics Yearbook 2001, China Statistics Press.

33) National Bureau of Statistics of China : China Energy Statistics Yearbook 2000～2003, China Statistics Press.

34) National Bureau of Statistics of China : China Electric Statistics Yearbook 2001, China Statistics Press.

35) The Ministry of Water Resources of China :Water Resource Report 2000, The Ministry of Water Resources of China.

Sustainable agriculture production and agricultural water use in the Yellow River basin, China

-Evaluation by index of agricultural WUE (Water Use Efficiency) -

AKIO ONISHI*, YOSHINOBU SATO*, XIN CAO**, MASAYUKI MATSUOKA***, HIDEFUMI IMURA**, FENG SHI**, YOSHIHIRO FUKUSHIMA*

*Research Institute for Humanity and Nature, **Graduate School of Environmental Studies, Nagoya University, ***Faculty of Agriculture, Kochi University, ****Faculty of urban science, Meijo University

1. Introduction

Food demand in China is increasing due to rapid population growth, changes in society and economic development. Food production has therefore become an important state policy issue. Amid this background, in the Yellow River basin, grain production has expanded dramatically through increases of agricultural yields per hectare. However, as a region suffering from severe water shortages, there were concerns that excessive water use will deplete the water resources in the Yellow River basin. Such shortages were caused by increased agricultural water use (Otsubo *et al.*, 2000) and its inefficient use. Thus, it is essential to consider how to manage agricultural water use while continuing increasing agriculture production.

The area of the Yellow River basin is vast (about twice the area of Japan) (JBIC, 2004), and the conditions of agricultural production vary greatly within it. In the river source region (upper than Lanzou) precipitation supplies about 60% of the water resource to the Yellow River. In the upstream there are extensive irrigated areas, including for example the Qingtongxia irrigation district in the Ningxia, and the Hetao irrigation district in Inner Mongolia (Watanabe and Hoshikawa, 2006). These irrigation districts are mostly located in the arid and semi-arid areas, and the level of precipitation is low. Therefore, the large quantity of water for grain production is drawn from Yellow River. The midstream region is located in the Loess Plateau region which covers the arid and semi-arid areas. Grain production is high here, but in the basins of the Fen River and Wei River (tributaries of the Yellow River), groundwater levels are dropping due to urbanization and industrialization. The downstream region is located in the North China Plain, where modern agricultural technology has been widely introduced —including mechanization

and the use of chemical fertilizers — and the region grows wheat and maize with high yields per hectare. Although the characteristics of each area are different, it is clear that advances in modern agricultural technology has raised grain production by producing higher yields per hectare (Onishi *et al.*, 2005), and the increases in grain production have come at the cost of excessive use of agricultural water —a situation that exacerbated the dry up phenomenon. Thus, when considering the effective and proper use of agricultural water, it is important to consider approaches that limit to the lowest possible level the amount of water used while obtaining a certain amount of production.

This study evaluates the agricultural water use efficiency (WUE) of year 2000 by using the statistic data, land use data and hydrological model.

2. Background

Grain production in the Yellow River basin has been increasing steadily (Figure 1).

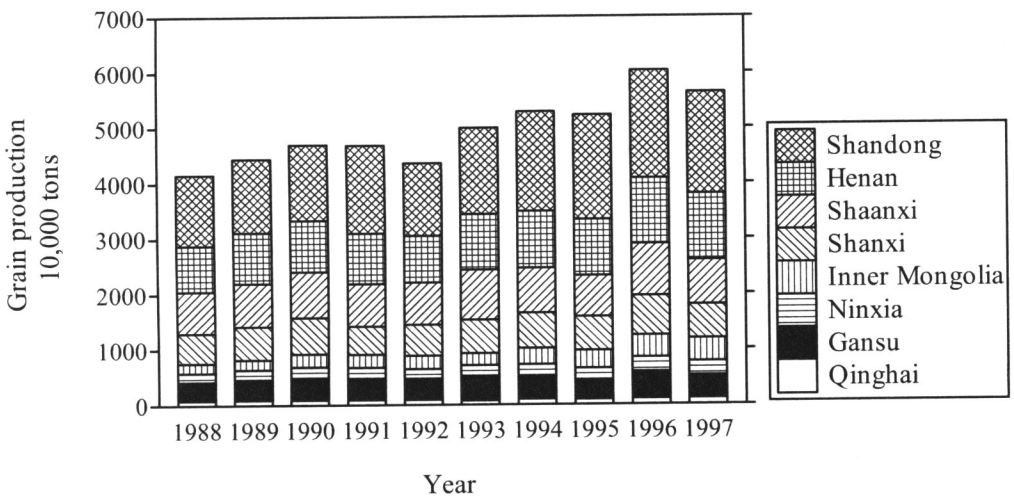

Figure 1. Grain production trends.

Source: Prepared by authors from National Bureau of Statistics of China (1989-1991), National Bureau of Statistics of China, and the Institute of Geographic Sciences and Natural Resources Research (Chinese Academy of Sciences)[1].

Note: Grain Production includes production of rice, wheat, maze, beans and tubers.

Grain production is accomplished through the use of irrigation, which accounts for about 84% (calculated by authors from data on the amount of water use for 1988 through 2002) [2] of all usable water (Sun *et al.*, 2001; Yellow River Conservancy Committee, 1997-2002). In particular, Shandong Province and Inner Mongolia have some of the largest irrigation districts in the river basin and use enormous amounts of water for

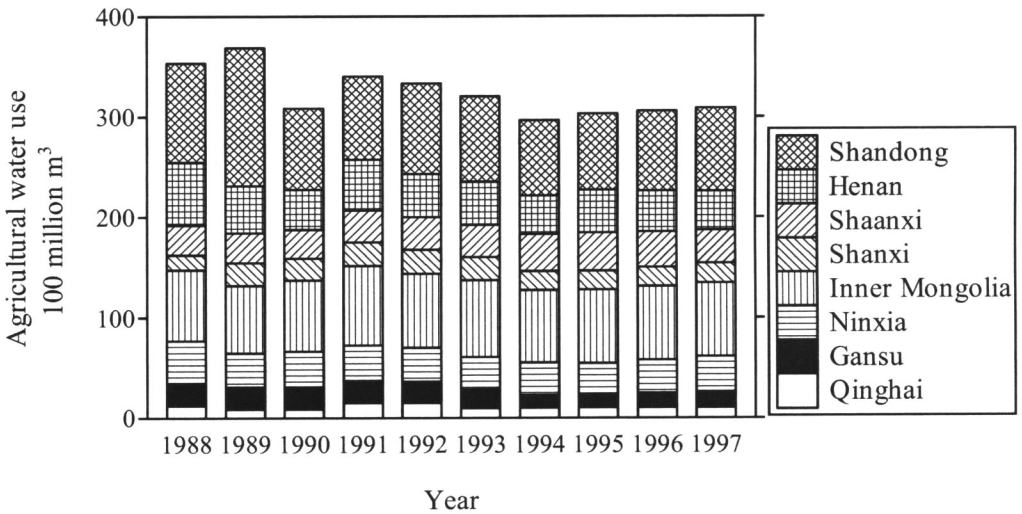

Figure 2. Agricultural water use trends.
Source: Prepared by authors from Sun *et al.* 2001.
Note: Figures for 1996 and 1997 are estimates.

agriculture, accounting for about 50% of use in the entire river basin (Figure 2).

Meanwhile, food production per cubic meter of agricultural water used has been increasing in recent years. And its average amount of the river basin rose from about 15 to 20 tons/ten thousand cubic meter during 1990's (Figure 3).

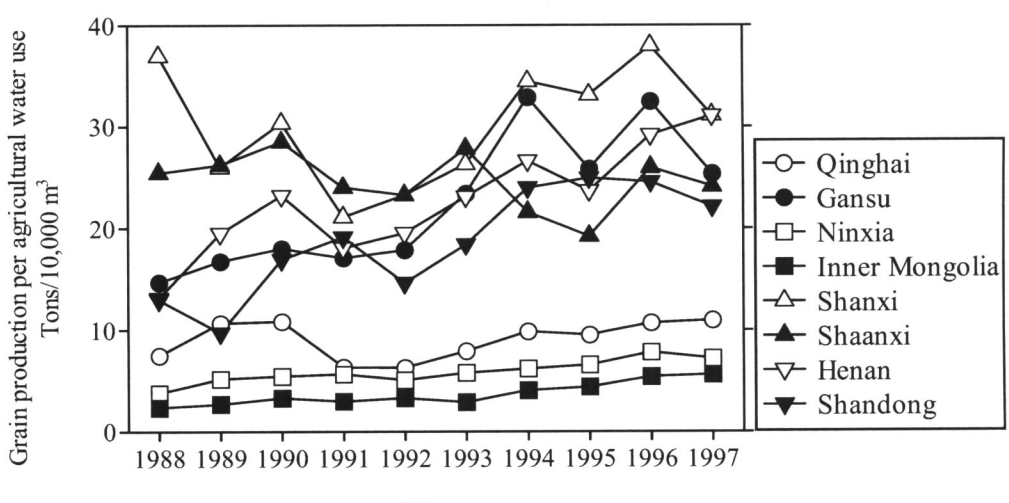

Figure 3. Grain production per agricultural water use.
Source: Prepared by authors by using Figure 1. and 2.

The dry up phenomenon were first happened in 1972, but worsened dramatically in the 1990s, with the most extreme event occurring in 1997 (Figure 4). During this period, the amount of water used for agriculture has been on a declining trend, but in the Yellow River basin which has unstable water resource amounts, so excessive water use leads easily to depletion of water resources. For this reason, it is important that water be used efficiently and rationally. Furthermore, the amount of water for industrial and urban household has been increasing in recent years, along with industrialization and urbanization. Thus, it is likely that the agricultural use of water will be increasingly constrained (Chinese Academy of Engineering, 2001).

In order to achieve sustainable development in the Yellow River basin under water resource constraints, it is essential to have information about how water can be allocated in the most physically and economically efficient ways, and about the extent to which water use can be reduced in what regions. Thus, it is important to estimate the efficiency of agricultural water use.

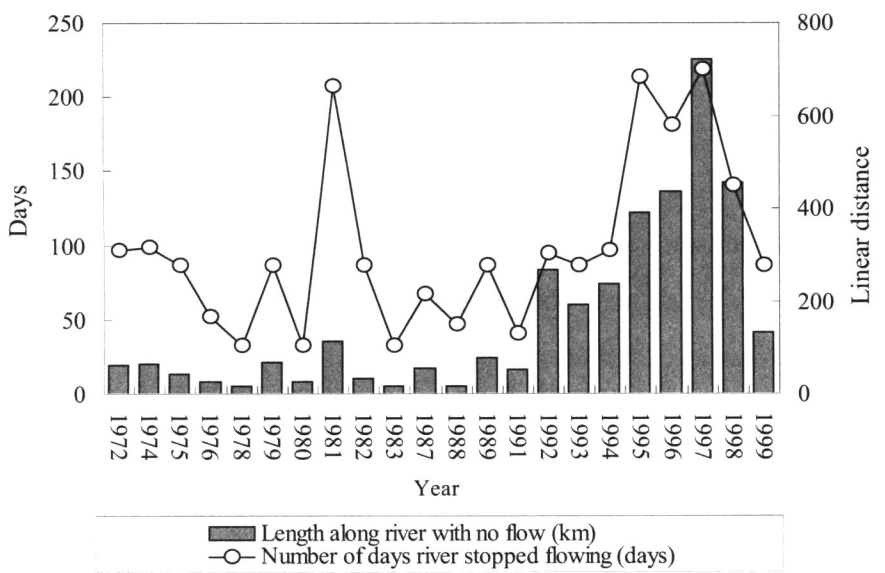

Figure 4. Dry up phenomenon: duration and linear distance.
Source: Prepared by authors from Sun *et al.* 2001.

3. Methods

In this study, we estimated agricultural Water Use Efficiency (WUE = grain yield/ actual evapotranspiration) of year 2000 by the SVAT-HYCY model (Sato *et al.*, 2007) combining with the agricultural filed data and grain yield statistic data. The actual

evapotranspiration and grain yield were calculated by the 0.1°×0.1°grid. To estimate the actual evapotranspiration by the grid, the following procedures were applied. Firstly, we estimated the potential evaporation by the heat balance equation by following Kondo and Xu (1997) method. Secondly, the evapotanspiration from the agricultural filed without soil water deficit was estimated by using a function of LAI (Leaf Area Index) (Kondo, 1998). Finally, the actual evapotranspiration was estimated by the soil water content. To estimate the grain yields, grain production statistic data in each county and city was interpolated into the grid scale, based on the agricultural filed distribution data acquired by the remote sensing (Matsuoka *et al.*, 2007). Also, in order to evaluate the agricultural WUE in different irrigation districts, irrigation maps (Yellow River Conservancy Committee, 1989) were used.

4. Results

The results are shown in Figure 5. Here, we show the result of each mesh WUE from upper reach to middle reach. From this result, the WUE in upper reach is lower than middle reach; especially worsen in the large irrigation districts of upper reach. This result shows the same spatial trend of Figure 3. In order to summarize the above obtained result more precisely, we calculated agricultural WUE in different regions and irrigation districts (Figure 6). Here, the result of agricultural WUE in irrigation district of lower reach is included. From this result, the irrigation districts in Ningxia and Inner Mongolia recorded much lower scores compare with other regions and irrigation districts. Especially, the irrigation district in upper reach is approximately 3 times lower than irrigation districts in lower reach. However, we have not acquired some references to check accuracy of our results in detail. So, we have to carefully evaluate our obtained results in future.

This study suggests that further improvement in agricultural WUE in the arid and semiarid areas, especially upstream, is necessary toward sustainable agricultural production and toward prevention from water shortages.

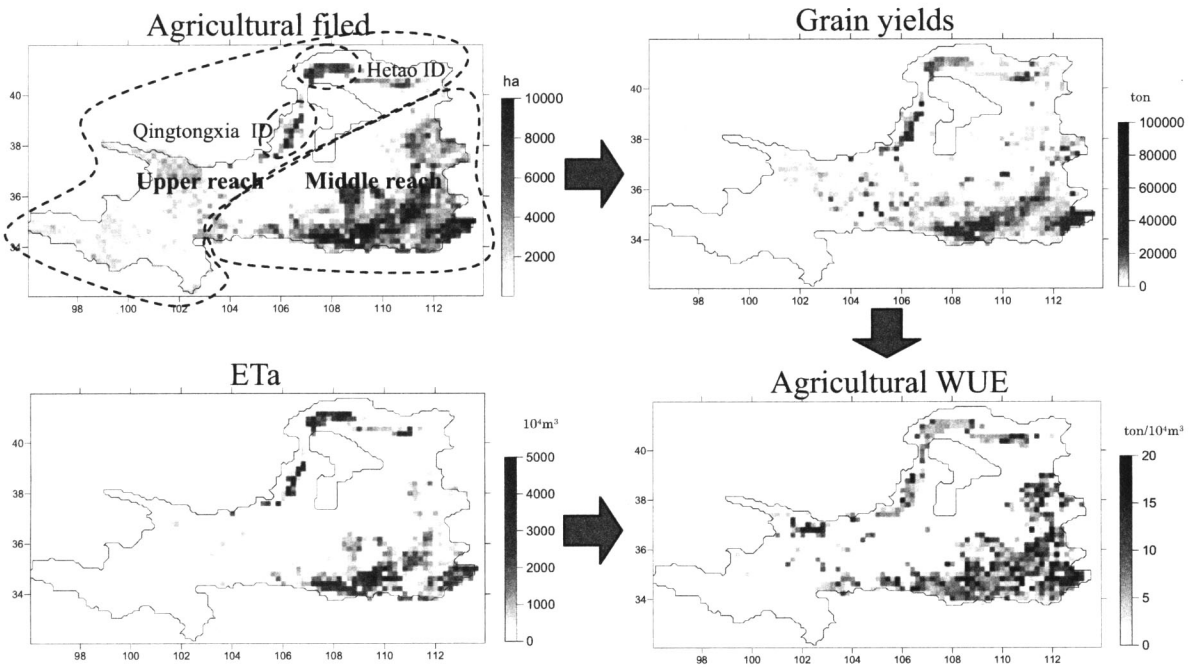

Figure 5. Results for agricultural WUE of year 2000

ID: Irrigation District, Eta: actual evapotranspiration

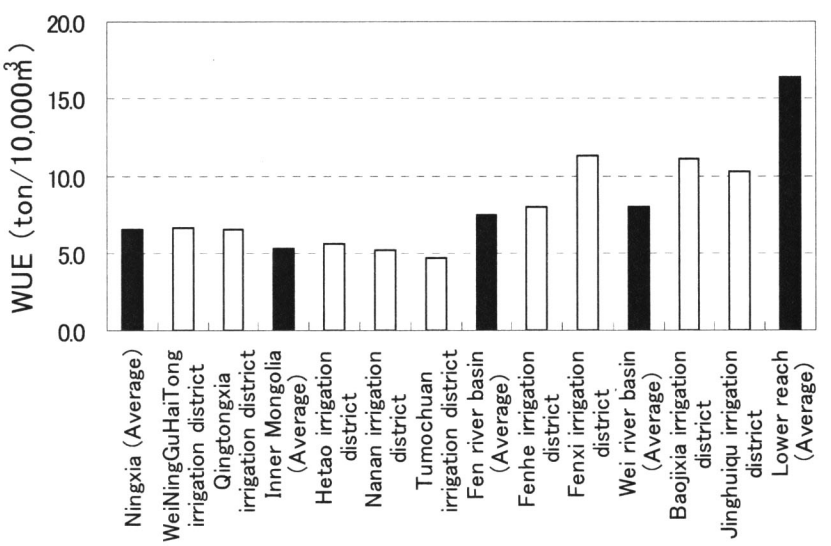

Figure 6. Results for agricultural WUE of year 2000 in different

5. Conclusions

This study evaluated the agricultural WUE of year 2000 by using the statistic data, land use data and hydrological model. As a whole result, the agricultural WUE is lower in upper reach. However, we have not analyzed what influences cause the differences of WUE. By showing this concrete improvement plan, we can suggest more about what

sorts of preventions and policies are necessary.

Notes

1) China Natural Resources Database is from the Institute of Geographic Sciences and Natural Resources Research (Chinese Academy of Sciences), accessed 1 Oct. 2006: http://www.naturalresources.csdb.cn/index.asp

2) In this study, we use the data of agriculture water use as water loss. The amount of water loss is the portion of water that evaporates or is absorbed by soil during transport and use, the portion contained in products, and the portion ingested by the human population and livestock—portions that are not restored to surface water bodies or groundwater layers (Xi, 1996; Ministry of Water Resources, 2000).In other words, this is the amount of water lost in the course of being used and not returned to the river or groundwater. Agriculture water loss is calculated from the difference between the amount of water used (including losses) and the amount of water recovered in surface water and groundwater (Ministry of Water Resources, 2000).This study defines agriculture water use to be the amount of water loss, calculated as the amount of water drawn for irrigation purposes and consumed completely within the region.

References

Chinese Academy of Engineering (2001): A Series of Reports on Water Resource Strategies for China's Sustainable Development Vol. 1-9. Water Publication Company of China (in Chinese).

Japan Bank for International Cooperation (JBIC) (2004): Facts and issues regarding water resource issues in northern China -- analysis of water supply and demand in the yellow River basin. *JBIC Research Paper No. 28* (in Japanese).

Kondo J. (1998): Dependence of evapotranspiration on the precipitation amount and leaf area index for various vegetated surfaces, *Journal of the Japan Society of Hydrology and Water Resources* 11: p.679-693.

Kondo J. and Xu J. (1997): Potential evaporation and climatological wetness index. *Tenki*: *Journal of the Meteorological Society of Japan* 44: p.875-883.

Matsuoka M., Hayasaka T., Fukushima Y. and Honda Y. (2007): Land cover in East Asia

classified using Terrra MODIS and DMSP OLS products, *International Journal of Remote Sensing*, Vol.28, Nos. 1-2, p.221-248.

Ministry of Water Resources (2000): China Water Resources Gazette, Ministry of Water Resources.

National Bureau of Statistics of China (1989-1991): China County Agricultural Economics Statistics Summary. China Statistics Press (in Chinese).

Onishi A., Imura H., Han J. and Fang W. (2005): A Study on Grain Productivity changes in 5 different basins in Yellow River basin. *Environmental Systems Research*, Vol.33, p.79-88 (in Japanese).

Otsubo K., Wang Q. and Liu C. (2000): River Cut-off and Salinization Problems at the Lower Yellow River Basin, *LU/GEC Project Report VI*— Study On The Processes and Impact of Land-use Change in China, p. 242-248 (in Japanese).

Sato Y., Ma X., Matsuoka M., Xu J. and Fukushima Y. (2007): Hydrological impacts of the land-use change in the middle reaches of the Yellow River basin, *3nd International Workshop on Yellow River Studies*, p.97-102.

Sun G.., Qiao X. and Sun S. (2001): Yellow River Water Resources Management. Yellow River Water Conservancy Press (in Chinese).

Watanabe T. and Hoshikawa K. (2006): Water Management in Large Irrigation Districts of Yellow River Bain. *Journal of Arid Land Studies*, 16-2: p.97-101 (in Japanese).

Xi J. (1996): Yellow River Water Resources. Yellow River Water Conservancy Press (in Chinese).

Yellow River Conservancy Committee (1989): Yellow Rover Basin Map. Sinomaps.

Yellow River Conservancy Committee (1997-2002): Yellow River Water Resources Gazette. Yellow River Conservancy Committee (in Chinese).

Water balances in large scale irrigation districts in the Yellow River basin

Keisuke Hoshikawa(Kyoto University), Tsugihiro Watanabe(RIHN)
Takashi Kume(Tottori University)

1. Introduction

This report will present water balances in large scale irrigation districts in the Yellow River basin briefly based on some existing reports and studies by management organizations, institutes and universities in China. In addition, details of water balance and directions for more adequate water management in Hetao Irrigation District that is the largest irrigation district in the basin will be discussed through analysis of simulation results by IMPAM (Irrigation Management Performance Assessment Model) (Hoshikawa et al., 2007).

2. Water balances in primary large-scale irrigation districts

Outline of water balance structures, monthly water withdrawals and long-term trends of them in Qingtongxia Irrigation District (Qingtongxia ID) (Ningxia Autonomous Region; upper basin), Hetao Irrgation District (Hetao ID) (Inner-Mongolia Autonomous Region; upper basin) and Weishan Irrigation District (Weishang ID) (Shandong Province; lower basin) will be presented in this section. Qingtongxia and Hetao IDs which withdraw $6\times10^9 m^3$ and $5\times10^9 m^3$ annually from the Yellow River respectively strongly affect runoff of the Yellow River especially. Weishan ID is the largest irrigation district in the lower basin. Such information is important to discuss future changes in water resource reallocation in this basin.

Qingtongxia Irrigation District

Annual precipitation around Ningxia ID is about 200mm. Agriculture in this area almost completely depends on irrigation. This autonomous region has four major irrigation districts (Qingtongxia, Weining, Taole Pumping, Guyuang Pumping Irrigation Districts), group of which are called Ningxia Yellow River Irrigation District. Qingtongxia and Weining Irrigation Districts which are gravity irrigation districts return about a half of water withdrawn from the Yellow River as drainage to the Yellow River. Drainage water mostly consists of tail-water. Because of a terrain, this region is ill-drained. North of Yinchuan City is troubled by salt accumulation.

Monthly water withdrawal and drainage is shown in Fig.1. Irrigation is applied also during the late autumn to the early winter after harvest. Drainage quickly follows water withdrawal. This indicates that drainage water mostly consists of tail-water.

No drastic change in amount of annual water withdrawal can be seen in the last 20 years. Institute for Hydraulic Power Survey, Ningxia Autonomous Reion (1999) presented a plan for reducing annual water withdrawal from the Yellow River to $4.0\times10^9 m^3$. According to it, lining and rearrangement (making shortcut routes) of main canals enables to reduce delivery losses 63% to 50%. In addition, exploitation of groundwater will be promoted. However, *net* water requirement of the districts will rather increase slightly. This plan also aims to increase irrigated area by 251,000 ha at the same time. Measures for water saving presented in the plan are not for reducing water consumption in the area but for increasing agricultural production within the area. Amount of water consumption will not be changed substantially. A reason why this district is not required to reduce water use different from Hetao ID is that agriculture in this region is one of the important

components of the Great Development of the Western (*xibu dakaifa*).

Hetao Irrigation District

Hetao ID locates in a dry-area with annual 100–200mm of annual precipitation. Agriculture of this region completely depends on irrigation. At Sanshenggong Headworks, $5.3\times10^9 m^3$ and $0.6x10^9 m^3$ of river water is diverted to Conveyance Canal (*Zongganqu*) and the First Main Canal (*Yiganqu*) of Hetao ID. In addition, Yimeng Irrigation District, which is out of Hetao ID, on the right bank takes about $0.3\times10^9 m^3$ annually. Conveyance Canal releases $0.7–1.0\times10^9 m^3$ annually as tail-water. Difference of total amount of water withdrawal at Sanshenggong and tail-water from Conveyance Canal is reported as amount of water withdrawal of Hetao ID (about $5\times10^9 m^3$/year). About 0.2 – 0.3×10^9 m^3/year of water is drained through drainage canal network. It is much less than that of Qingtongxia ID. Analysis on quality of drainage water indicates that drainage water is mostly from irrigation canals directly (Wang et al., 1993).

Fig.2 shows monthly pattern of water withdrawal by Hetao Irrigation District. It is almost stable every year. Irrigation after harvest for cultivation in next spring is also applied in autumn. Much more water is allocated for autumn irrigation than in Qingtongxia ID. It accounts 30% of annual total water withdrawal.

Water withdrawal by Hetao ID was increasing year to year by 1980s because of enlargement of irrigated area, and it leveled out in 1990s. Hetao ID is now requested to decrease water annual water withdrawal to $4.0\times10^9 m^3$. Lining of main canals has been conducted to decrease seepage loss that accounts for 60% of total withdrawn water. In addition, irrigation after harvest was decreased from $2.0\times10^9 m^3$ to $1.6\times10^9 m^3$.

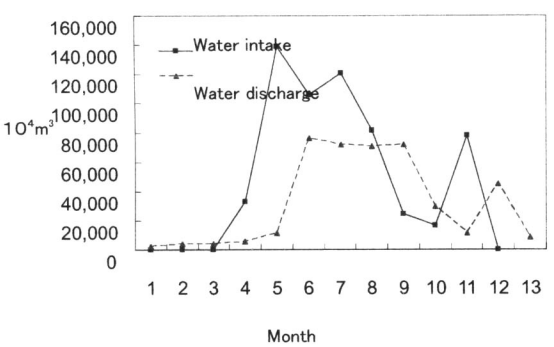

Fig.1 Monthly water withdrawal and drainage from/to the Yellow River (2000)
X-axis: Julian month; Y-axis: 10,000 m^3

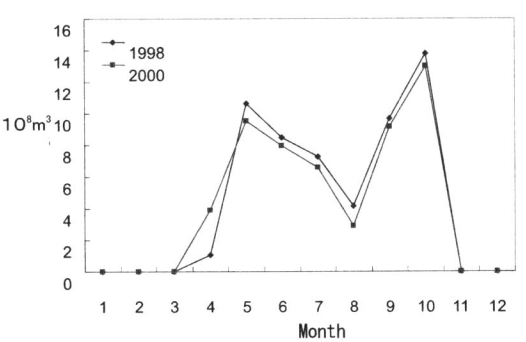

Fig.2 Monthly water withdrawal from the Yellow River (1998 and 2000)
X-axis: Julian month; Y-axis: 0.1 billion m^3

Weishan Irrigation District

Area around Weishan ID has precipitation mostly in summer. Irrigation is applied for winter wheat in spring and autumn. Crops other than wheat are maize as second crop of winter wheat, vegetables, cotton, and beans etc. All of them are cultivated in summer. Annual precipitation is around 600mm. It is barely enough to cultivate crops without irrigation. Irrigation is irregularly applied to supply deficit when droughts. Although area of irrigated wheat is almost stable, water withdrawal for

irrigation varies much year to year because of annual variation of amount of precipitation.

There is no drainage system. In the lower part of the irrigation district where elevation is relatively low, depth to groundwater becomes shallow (less than 1m) in summer. Significant part of the irrigation district was salt affected in 1960s to 70s. It is said that salt affection was reduced by digging riverbed of two natural streams for drainage.

Weishan ID is located in the lower part of Yellow River basin where water shortage is severe. Secure of water for irrigation is important subject for the ID. In addition to various measures of water saving, exploitation of groundwater is being tried. Significant part of irrigation canal system is lined to prevent soil contained in irrigation water from depositing in canals. This lining helps water saving. Reduce of water withdrawal may not be important subject for Weishan ID.

One of the important topics about water management in Weishan ID is the "From the Yellow River to Wei River (*Yinhuangruwei*)" Project. This project aims to send water of the Yellow River to Tianjin City using the irrigation canal system of Weishan ID and Wei River. Although Weishan ID withdraws water from the Yellow River for this project, Tianjin City is responsible for the water withdrawal. Water for this project is not included in amount of water withdrawal by Weishan ID and Shandong Province. Water withdrawal for Tianjin City is conducted in winter not to disturb irrigation. Fig.3 shows amount of water withdrawal from November to February. This strongly indicates that withdrawal for Tianjin is rapidly increasing,

3. Water balance and possibility for water saving in Hetao ID

Of the above mentioned three irrigation districts, only Hetao ID is required to reduce water consumption. Water saving in Hetao ID will substantially affect runoff of the Yellow River. It is not easy for Hetao ID where agriculture completely depends on irrigation to reduce water consumption without reducing agricultural production. This section will provide results of assessment of impact of water saving measures progressing in Hetao ID on its water balance and agricultural production with the simulation model IMPAM.

Materials and method

In addition to ten-year simulation period, five-year spinning up was done for establishing initial conditions of soil moisture and groundwater level. Parameters for soil physics, groundwater flow, and irrigation management were adjusted through calibrations for groundwater level, water delivery patterns of irrigation canal network, and amount of drainage. Simulation period was from 1988 to 1997 for which calibration data was available.

Simulations were done under four cases: management before modifications after 2000s (base case), and three modified cases. Main canals were lined and seepage was reduced (case1), irrigation after harvest was reduced (case2), both seepage and irrigation after harvest were reduced (case 3) were assumed as the modified cases.

Model was applied to command areas of Yongji and Beibian Main Canals (83,562 ha and 4,156 ha respectively).

Results

Fig.4 shows details of annual water outflow from the simulation area. Soil evaporation accounted for about 60% of total outflow of the HID in the base case. Nearly 80% of the inflow to the HID is

water from the Yellow River. These facts mean that at least about 50% of water diverted for irrigation was wasted due to soil evaporation from the area. Such predominance of soil evaporation in the outflow was attributed to the dry climate, vast seepage rate, bare areas scattered among irrigated farm plots and a rather large groundwater transmissivity that enabled quick water transfer from irrigated farm plots to bare areas. Under such a climate condition with a large saturation deficit, soil moisture was much more quickly evaporated than discharged to drainage channels.

Soil evaporation was decreased in every modified case. It is notable that transpiration that is deeply concerned with crop production merely decreased. Although irrigation after harvest is applied for crop growth in the next spring, it can be decreased without significant effect on agricultural production.

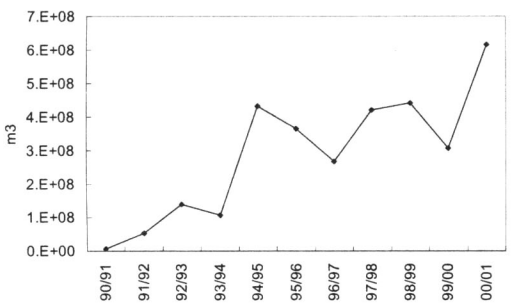

Fig.3 Water withdrawal during November to February (1999–2001)

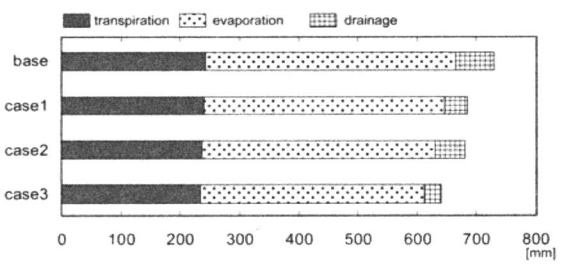

Fig.4 Details of annual water outflow from the simulation area for the four cases (10-year mean).
Base: management before modifications; Case 1: seepage was reduced; Case2: irrigation after harvest was reduced; Case3: both seepage and irrigation after harvest were reduced

4. Conclusions

Water saving in Hetao ID strongly affects reallocation of water resource in the Yellow River basin. It is technically possible for Hetao ID to reduce water consumption and water withdrawal without significant decrease of agricultural production. Possibility of water saving strongly depends on how investment will be done for Hetao ID. In other words it depends on economy and food demand and supply in China.

References

Hoshikawa K., Watanabe T., Nagano T., and Kume T., 2007, Developing a hydrological model with spatial information on irrigation management, *J. the Japanese Society of Irrigation, Drainage and Rural Engineering*, **75**(11): 11-14 (in Japanese)

Institute for Hydraulic Power Survey, Ningxia Autonomous Reion, 1999, Study report on modification of Qingtongxia Irrigation district for water saving. (in Chinese)

Wang, L., Chen, Y., Ceng, G., 1993. Irrigation drainage and salinization control in Neimenggu Hetao Irrigation Area, Water Resource and Hydropower Pres. (in Chinese)

Cognitive Background to Flood Control Work

Tetsuya Kinoshita
Research Institute for Humanity and Nature

This paper describes the ideas behind the promotion of flood control work in the history of flood control on the Yellow River. Broadly, the conclusion is that the conflict between the ideas of civil government and considerations of national sovereignty and national defence are visible here.

Yellow River flood control, and in particular, flood control as major construction overseen by the central government, is mainly performed downstream of the Yellow River, on the so-called "North China Plain". This is a map of the North China Plain (Fig. 1). This is a geologic map of the North China Plain (Fig. 2). The Yellow River forms a type of fan while flowing both north and south on the North China Plain. With regard to this branch in the flow of the Yellow River, however, when its continuous history is regarded, the most basic framework can be said to be the sinking of the land of the North China Plain due to geotectonic movement, which is called neotectonic movement that happened in the middle and later periods of the Himalayan orogeny. This is a distribution diagram of the rise and fall of the Earth's crust between approximately 3.4 million years ago and today due to this neotectonic movement (Fig. 3). Looking at this, the sinking is great in the northern North China Plain, at more than -500m. The sinking around the flow of the Huaihe River, which is in the saddle of modern central Henan Province, is considerable, at greater than -200m. Seen from this elevation diagram, the most natural flow of the Yellow River, which emerges in upper Zhengzhou today, is to flow north from there along the Taiheng Shan mountain range until it reaches the same latitude as Tianjin, and then to flow east through eastern Tianjin into the sea. Further, the flow can also be said to branch en route to emerge in the upper part of the modern estuary delta and further north. In reality, the flow of the Yellow River as understood from various historical data ever since the Holocene epoch has always broadly been along these two branches.

After the last glacial period ended, during the warm period, there was a cold period called the Younger Dryas that lasted for 1,300 years approximately 10 thousand years BCE, followed by a period of rapid warming, which is deemed to be the start of the Holocene epoch. From around 6,500 BCE to 2,000 BCE, this period of considerably stable warming continued, and there are clusters of archaeological remains to indicate the start of agriculture independently in the three regions of the eastern foothills of the Taiheng-Shan mountain range (modern-day western Handan), north of the Shandong mountain mass adjacent to the alluvial plain, and in the eastern foothills of southern Zhengzhou. Ever since, agricultural cultures based on these have continued to spread, but none have made any real inroads into the central region of the North China Plain.

The most stable warm period continued from 5,000 to 4,000BCE, but looking at the distribution of remains from the Yangshao culture, which appeared at this time (red dots in Fig. 4), it stopped spectacularly at the modern Jing-Guang railway line as can be seen, and east from there made no inroads into the central North China Plain. From about 2,000BCE, Longshan culture arose, but its remains are also distributed centred on the hills around the Shandong Mountain mass and the Jing-Guang railway line. There are remains in the exact centre of the North China Plain in this area, however, but this is presumed to have probably been sited on a diluvial bed.

Changes can be seen after the start of the Holocene epoch of the Yellow River waterways leading to the present day, which are shown in the diagram (Fig. 5). In the ancient times from the Yangshao to the Longshan culture, of which I am currently speaking, the main waterways of the Yellow River were this yellow line, the southern flow, and the upper tip of the modern estuary delta. This has been made evident by examinations of the ancient delta region of the Yellow River in this area.

Although not perfectly understood, it is estimated that these tributaries from the waterways arose within several hundred years after 2,000BCE, and a waterway appeared that travelled north from the Taiheng Shan mountain range, near Tianjin, and into the sea.

The more northerly of these two waterways is called the "Yugonghe" according to the "Yogong", an ancient document that records the path of the watery, and the other, older waterway to the southeast is called the "Hanzhi-he" according to the "Han shu" and "Gou-xu zhi", ancient documents which, naturally enough, record the path of this waterway (Fig. 6). In both cases, the lowest point of flow is unknown, with both waterways spreading out by dividing into so may flows that which is the main flow cannot be stated with any certainty.

These conditions continued, but in the middle Zhanguo period, the Qi from the east of the Hanzhi-he River, and the Zhao and Wei from the west, built embankments on both sides of the river to fix it as the boundaries between their nations. The Yugong River was dammed by the embankments built on the west bank by the Zhao and Wei, and the river's flow was cut off.

From the middle Zhanguo period, the development of arable land spread in the central region of the North China Plain. The construction of levees also progressed as a consequence. The flow of silt downstream of the Yellow River increased due to the development of the Weihe and Funhe river basins in the middle basin, and the river flows converged at the Hanzhi-he River, raising the Hanzhi-he riverbed, so the embankments failed when the water levels in creased, thus causing flooding. In the end, the embankments failed in the east around Puyang, and a comparatively stable waterway consequently emerged. During the reign of the Emperor Ming, the second emperor of the Hou Han dynasty, in 69 to 70CE, major reconstruction and repair of the waterway was implemented by Wang Jing, basically to use embankments to augment the stable waterway that had appeared naturally.

This is a diagram of the waterway determined by Wang Jing's river administration (Fig. 7). The

important thing in Wang Jing's river governance was planning and implementation from the viewpoint of a civil government. The core of Wang Jing's river administration was not the building of embankments, but the creation of an artificial canal system called "Canal Bian", which is written here. This was the provision of an infrastructure for the stability and development of an agricultural economy in the region, coupled with irrigation routes and waterways for ships on the plains of what is today Henan Province in the North China Plain, and had been required by the people of the region for a long time. The creation of the embankments was one link in the provision of this canal system.

The waterway determined by Wang Jing remained stable for approximately 800 years thereafter, and then from the latter half of the Tang Dynasty entered a period of instability, but continued to function as a main waterway until the North Song Dynasty.

With the beginning of the North Song Dynasty in 1048, the Yellow River finally collapsed fatally in Chanzhou in the north, and a waterway arose that led to Tianjin and flowed into the sea. This was called the "Northern Flow". Further, in 1060, the river collapsed to the east in Damingfu, and a waterway arose southeast of there. This was called the "Eastern Flow" (Fig. 8).

Ever since, the central government has argued policy over whether to leave the "Northern Flow" as is, or so dam it up and divert to the "Eastern Flow". The main policy has tended towards damming up the "Northern Flow", and making the "Eastern Flow" into the main waterway. This policy has been tried three times, and succeeded twice, but 12 years after the first attempt and five years after the second attempt, the Yellow River collapsed to the north and the "Northern Flow" was restored. In other words, it is presumed that the "Northern Flow" was indeed the most natural and stable waterway at the time. The central government of the Northern Song, however, implemented construction to change to the "Eastern Flow" by force from the most natural and stable route, and so compounded failure with failure, ending with a massive waste of personnel and material. Consequently, the agricultural economy of the northern half of the North China Plain fell into unrecoverable decline.

The biggest reason for the Northern Song central government's intransigence over the "Eastern Flow" was the military and national defence advantages. At the time, the country of Khitai, which is beyond modern Beijing and called Liao in Chinese, was pressing for attack, so the Northern Song decided to broaden the ring of lakes and marshes that originally spread west from Tianjin to create a buffer zone against the southern advance of the Khitai army. If here we consider the Yellow River only as the "Northern Flow", the waterlogged areas become covered with silt, and it would be difficult to halt the southern advance by the cavalry. This can be cited as a major reason for the policy of eliminating this "Northern Flow". Further, even if the cavalry boarded boats to come by sea, they would land further north due to the more south-easterly flow of the Yellow River, and this would enable the "Eastern Flow" waterway to be used as a national line of defence.

In other words, the forced construction of embankments by the North Song central government against the natural trend of the waterway was done from the viewpoint of a national defence strategy, not from

the viewpoint of civil government, which aimed to stabilize and improve the local agricultural economy of the region along the shores of the Yellow River.

After the start of the South Song Dynasty, the path of the Yellow River was massively diverted from its flow across the northern half of the North China Plain, thus starting the era of the "Southern Flow", where it flowed into the Huaihe River system to converge with the Huaihe River before flowing into the Yellow Sea. This "Southern Flow" waterway, however, was unnatural and unstable from the start, even in light of the "rise and fall" of the Earth's crust, which was shown before (Fig. 3). By diverting to the south past the sunken saddle that runs almost perfectly east-west in the southern part of Zhengzhou, the river flow travels diagonally southward. As this saddle is positioned considerably to the south of the exit of the flow into the North China Plain, however, it was probably more natural for the river itself to flow north around Zhengzhou. Heading south was truly unstable in this region. Diverting to the "Southern Flow" was, from the start, for artificial reasons rather than according to natural trends.

After the Jin Dynasty army invaded the city of Dongjing (modern-day Kaifeng City), besieging it and bringing about the destruction of the North Song, they returned north in 1127, but the following year, the Jin Dynasty army once again marched south. At the time, Du Chong, who was taking charge of Dongjing in their absence, destroyed the Yellow River to the east to thwart the southwards march of the Jin Dynasty army. This led to the emergence of a waterway when the overflow headed south from the east to converge with the Huaihe River, before discharging into the Yellow Sea. Later, this "Southern Flow" waterway became the border between the Jin and South Song. In other words, the "Southern Flow" waterway itself was created and maintained from the start for reasons of national security.

From the beginning of the Yuan Dynasty, despite the further damming of the eastern and northern overflow of the "Southern Flow" from the viewpoint of a new national sovereignty, the fact was that the overflow to the south was left as it was, uncorrected. The reason being, to create the Jing-Hang Canal.

The Jing-Hang Canal used this "Southern Flow" waterway from Xuzhou southwards. Further, the addition of lock gates to the eastern side of the Shandong Mountain mass gradually raised the water level, so that when it receded, ships could travel on it. The volume of water was also low, and became clogged up in here. When the north of the "Southern Flow" waterway was destroyed, the waterway overflowed to the east, and this part was attacked directly as shown, leading to the damming of the Jing-Hang Canal (Fig. 9 and Fig. 10). During the Ming and Qing Dynasties, four million bushels of rice were transported via the Jing-Hang Canal to the then-capital (modern-day Beijing), so the main objective of quelling the Yellow River water was to protect the Jing-Hang Canal from the destruction and flooding of the Yellow River. In any case, construction and repairs such as embankments were made with the primary objective of maintaining the Jing-Hang Canal, which was the main route for

the food supplies that sustained the capital, Beijing, which had been set for geopolitical reasons, and not from policies for the Yellow River performed from a civil government viewpoint of stabilizing and improving the local people.

In the twilight of the Ming Dynasty, during the Wanli era, Pan Jixun implemented construction to systematically maintain and repair the Jing-Hang Canal, Hongze Hu Lake, Huaihe River, and the waterways downstream of the Yellow River, and to create a high-level system of embankments (Fig. 11). Further, at the beginning of the Qing Dynasty, under the rule of the Emperor Kangxi, Jin Fu and Chen Huang implemented construction to further refine the water-controlling ideas of Pan Jixun. These water-controlling ideas, based on systematic observations, are imbued with the spirit of Neo-Confucianism, which is the essence of civilian governmental thought in China. On this point, civilian governmental ideas, which are the backbone to the water-controlling notions of Wang Jing of the How Han Dynasty, can be said to govern the character of the water-control construction work even here, but it cannot be denied that the framework to the greatest policy was the enacting of these water-controlling ideas with the basic objectives of protecting and maintaining the Jing-Hang Canal as the main artery for the food supplies that sustained Beijing, and the basic objective of water control by the central government. This is because the ultimate objective was the fortification of the southern-flowing waterway.

This ends my attempts to elucidate the opposition between the ideas of civil government and the sovereign and national defence considerations that were behind these historical water-controlling works. Policies vis-à-vis the Yellow River that focused on considerations of national sovereignty and defence rather than the people in the region along the banks of the Yellow River downstream were adopted as the main platform from the North Song through the Qing Dynasties, so the North China Plain ended up becoming a wasteland. There is great interest in what shape water-control operations will take in modern China.

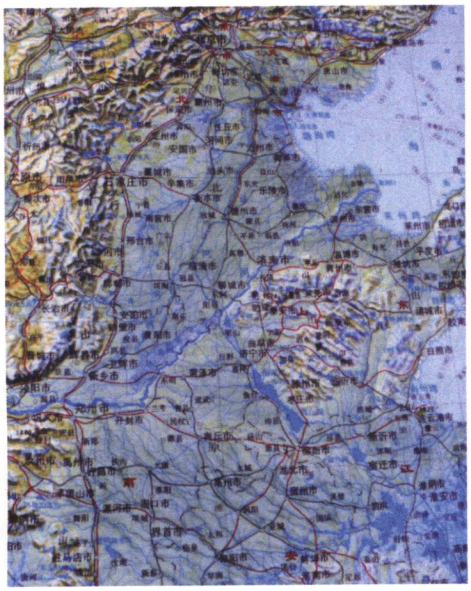

Fig 1 .Map of North China Plain

* Standard Atlas of China (1995) ,P42

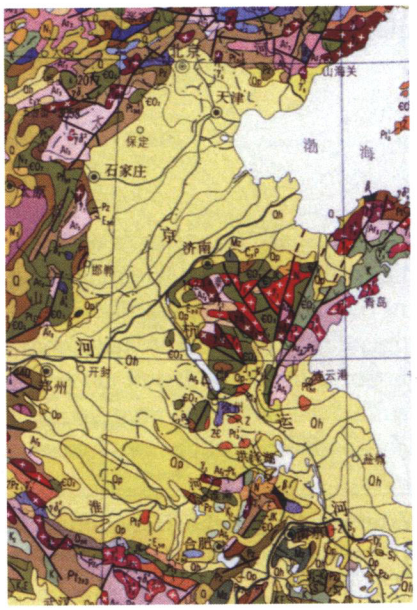

Fig 2 . Geologic Map of North China Plain

* Geological Atlas of China (2002), P11

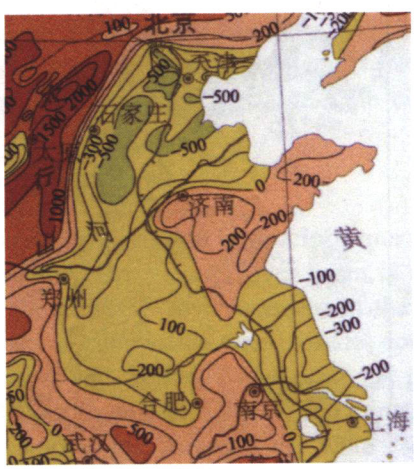

Fig 3 . Map of neotectonic movement

* Geological Atlas of China (2002), P52

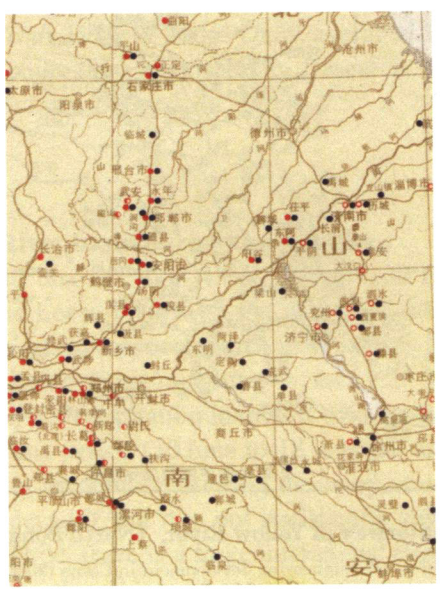

Fig 4 .Map of Yangshao culture remains in North China Plain BC5000 ● red dots

* The Historical Atlas of China V1.P7-8

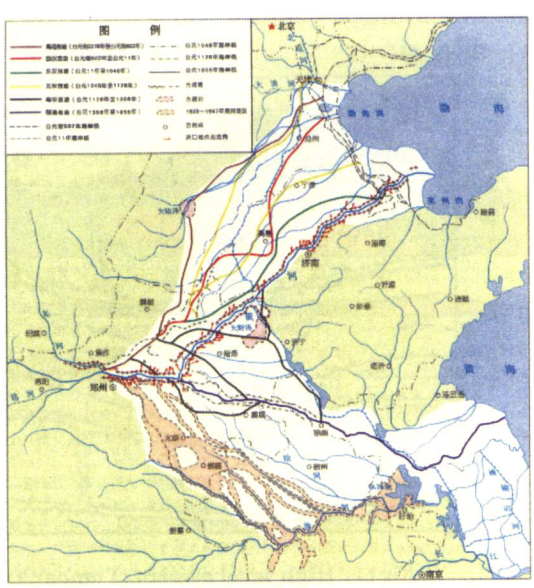

黄河下游河道历史变迁图

Fig 5 .Changes of waterway (Hollocene epoch～)

* 人民治理黄河六十年(2006), P84

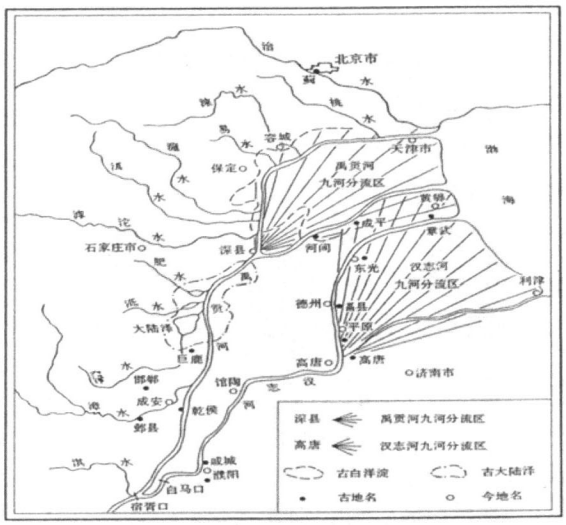

Fig 6 . Waterway (Yugonghe, Hanzhi-he) Changes

* Studies on Historical Geomorphology and Ancient Maps of China , (2006) , P 369

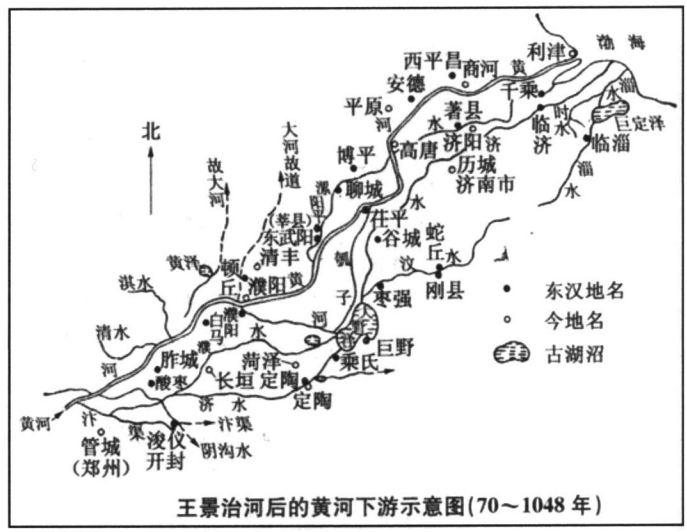

Fig 7 . Waterway determined by Wang Jing

* History of water engineering development in China (2005), P68

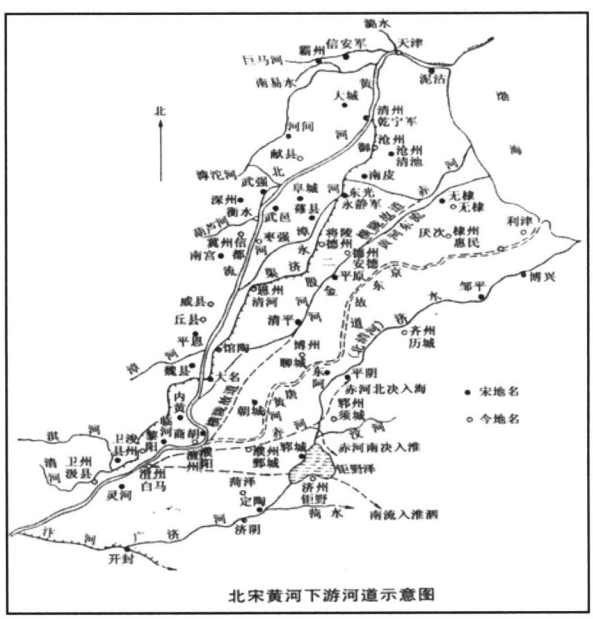

Fig 8 .Waterway in Yellow River, (North Song dynasty)

* History of water engineering development in China (2005), P189

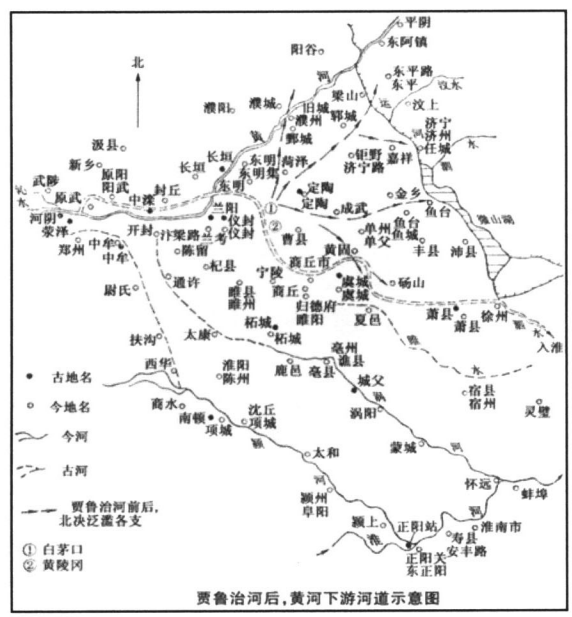

Fig 9. Waterway in Yellow River,(Qing dynasty)

* History of water engineering development in China (2005), P189

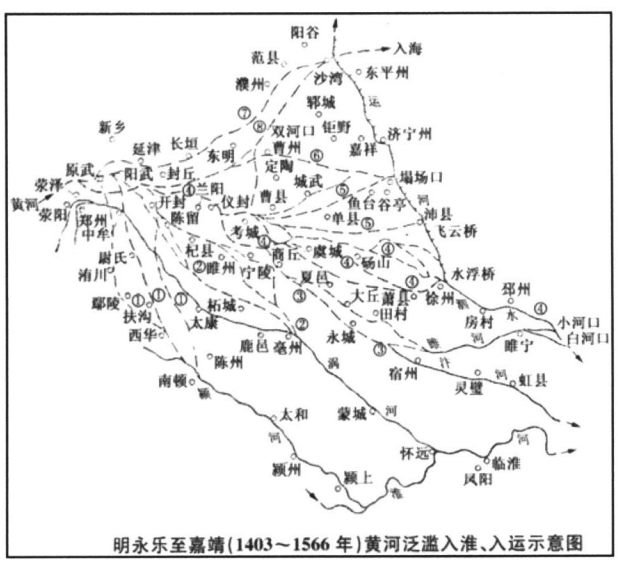

Fig10. Waterway in Yellow River (Ming dynasty)

* History of water engineering development in China (2005), P189

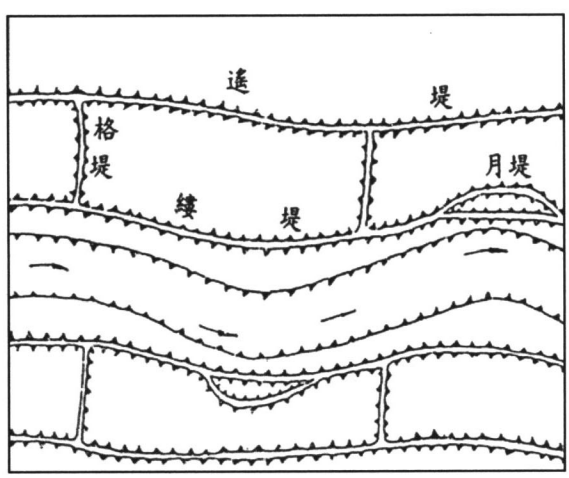

Fig11. High-level system of embankments (Ming dynasty) * 晚明黄河水患与潘季馴之治河(1998),P327

Synoptic-scale intraseasonal variation and its effect on interannual variation in precipitation over the middle-lower reaches of the Yellow River basin.

Hatsuki Fujinami (HyARC, Nagoya University)

1. Introduction.

The Yellow River is an important water source for people who live in the basin. Recently, The decrease in the water source becomes a serious problem in the area. The interannual variation in precipitation over the Yellow River basin is a main factor for inducing the flow fluctuation of the Yellow River. In the basin, the summertime (June – September) precipitation account for more than 60% of annual precipitation (e.g. Yatagai and Yasunari 1995). Therefore, the interannual variation in summertime precipitation and a factor for inducing the variation are important issues. In this study, the long-term trend and interannual variation in summertime precipitation over the Yellow River basin is examined. In addition, intraseasonal variation and its effect on the interannual variation are also discussed.

2. Data

Daily gridded (0.5° latitude–longitude grid) precipitation data made by Xie et al (2007) is used in this study. This data was made using many gauge observations over China, including the daily gauge data from the Chinese Yellow River Conservation Commission over the Yellow River basin. The data is available for the period from 1978 to 2002. GPCP (Global Precipitation Climatology Project; Huffman et al., 1997) data is also used to investigate precipitation variability in broader area for longer period. The data has global coverage on 2.5° latitude–longitude grid. The data is used from 1979 to 2006. Daily averaged National Center for Environmental Prediction (NCEP)/National Center for Atmospheric Research (NCAR) reanalysis data represent the large-scale circulation. The data are defined on global 2.5° x 2.5° grids (Kalnay et al. 1996).

3. Results

3.1 Interannual variation in precipitation over the Yellow River basin during the summer

In this study, the Yellow River basin is defined as the grid box of 34° – 43°N, 105° – 120°E, which contains the middle – lower reaches of the Yellow River (the Loess Plateau to the mouth of the Yellow River). Figure 1 shows the time-latitude section in the climatological seasonal march of precipitation in the longitudes of the Yellow River basin. A precipitation maximum from mid-June to mid-July over the Yangtze River basin (30° – 34°N) is a rainy season called Meiyu. Precipitation increases from early July to mid-August over the Yellow River basin. Hereafter, we treat this period (30 June to 18 August) as a rainy season. Figure 2 indicates the interannual variation in the total precipitation during the rainy season. The long-term trend shows a weak decrease (−0.17mm/day per decade), but it is not statistically significant. This result is consistent with that of Endo et al.(2005). Meanwhile, there is a large interannual variation of ~100mm in amplitude. This is a significant variation because the climatological annual total precipitation is ~450mm. The interannual time series in the rainy season has significant correlation with that in the annual

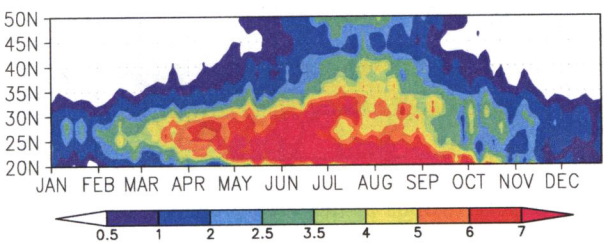

Fig.1: Time-latitude section in 25-year averaged precipitation (Xie et al. 2007) between 105° to 120°E. A unit is mm/day.

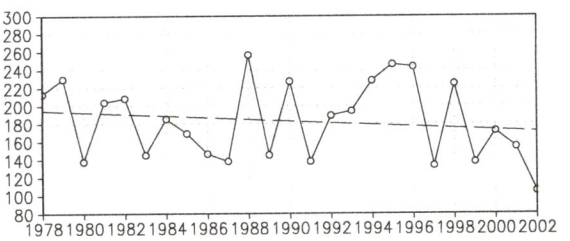

Fig. 2: Time series in the total precipitation (Xie et al., 2007) in the rainy season over the Yellow River basin (solid line with open square) and its linear trend (dashed line). A unit for the vertical axis is mm/50day.

total precipitation (about 0.7), suggesting that precipitation variation in the rainy season strongly affects the interannual variation in the annual total precipitation.

Next, precipitation variability in a lager area, associated with the interannual variation in rainy-season total precipitation over the Yellow River basin, is examined using GPCP data (Correlation between the interannual time series of the gauge-based precipitation and GPCP is 0.96 during 1979 – 2002).

Figure 3 shows the spatial distribution in the correlation coefficient between the interannual precipitation variation over the Yellow River basin and that in every grid point. Statistical significant positive correlations (shown as red shadings) extend from the Yellow River basin to western arid regions along 40°N, whereas significant negative correlations appear from the Yangtze River basin to the Korean Peninsula. Positive correlation is also observed over the western India. Figure 4 shows composites of precipitation distribution in wet years (1979, 1988, 1990, 1995 and 1998) and dry years (1980, 1991, 1997, 1999 and 2002), based on the time series in the Yellow River basin (Fig. 2). In the wet years, high precipitation area is observed centered around the Yellow River basin, while there is less precipitation areas from central China to the East China Sea (Fig4-left). In the dry years, high precipitation areas extend from southern China to the Korean Peninsula (Fig. 4-right).

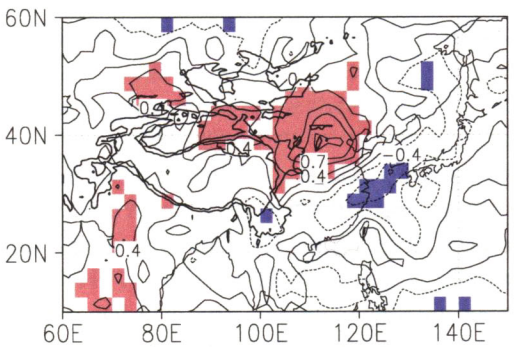

Fig.3: Correlation coefficients between the interannual variation in the rainy-season total precipitation over the Yellow River basin and that in every grid. Red (blue) shadings denote areas of positive (negative) correlation > 95 % confidence level. The 1,500 m and 3,000 m topographic contours are shown as thick solid lines.

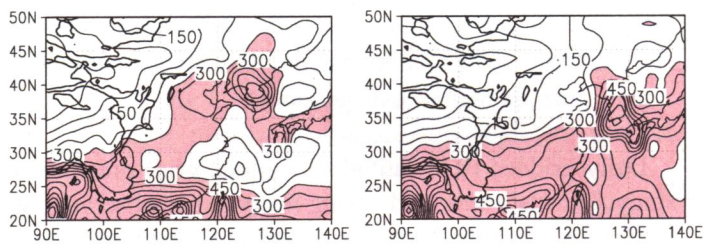

Fig. 4: Composites of precipitation distribution in wet years (left; 1979, 1988, 1990, 1995 and 1998) and dry years (right; 1980, 1991, 1997, 1999 and 2002). The contour interval is 50mm. Shading denotes areas with precipitation > 250mm.

Using the time series in precipitation shown in Fig.2, atmospheric factors causing the interannual variation around the Yellow River basin are investigated by calculating regression patterns of meteorological fields in the rainy season. In the upper troposphere (200hPa; ~12000m), a wavetrain pattern (alternative distribution of cyclonic and anti-cyclonic anomalies) is remarkable to the east of 40°E along 40°N (Fig. 5-upper). Associated with the wavetrain, there are an anticyclonic anomaly centered on 40°N, 120°E and a cyclonic anomaly to its west. In middle to lower troposphere (500hPa; ~5500m and 850hPa; ~1500m), there is an anticyclonic circulation near

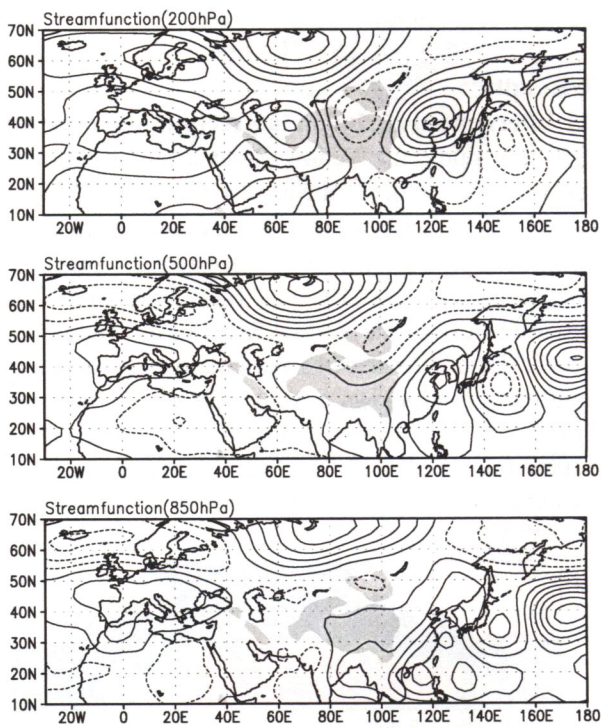

Fig. 5: Regressions of the streamfunction at (upper) 200 hPa, (middle) 500hPa and (bottom) 850 hPa in the rainy season for 1979 – 2006 to the timeseries in rainy-season precipitation over the Yellow River basin (Fig. 2). A positive (negative) value indicates anti-cyclonic (cyclonic) anomalies. Shading denotes areas > 1500m above sea level.

40°N, 120°E, similar to the location at 200 hPa. Therefore, the waves are nearly barotropic. The wavetrain is interpreted as a quasi-stationary Rossby wave propagating eastward along the Asian subtropical jet (Iwao and Sato 2006, Ding and Wang 2005). Pacific-Japan pattern (so-called PJ pattern), which is induced by convection anomalies over the western Pacific, is a major agent for forming large-scale circulation anomalies around East Asia (Nitta 1987). The PJ pattern is important for the interannual variation of summertime precipitation over the Yangtze River basin. However, the PJ-like pattern can not be observed in Figure 5, indicating that the interannual variation over the Yellow River basin is strongly affected by the eastward propagating stationary waves, rather than the PJ pattern.

The barotropic circulation structure around the Yellow River basin plays an important role in a moisture transport toward the basin. Figure 6 indicates regressions of moisture flux vector and its divergence. The anticyclonic circulation anomaly over the lower reaches of the basin induces the increase of southerly moisture flux into the basin at its southern boundary. The cyclonic anomaly, located to the east of the anticyclonic anomaly, also increase moisture flux crossing into the western boundary of the basin. Both the enhanced southerly and westerly fluxes results in the increase of precipitation over the Yellow River basin.

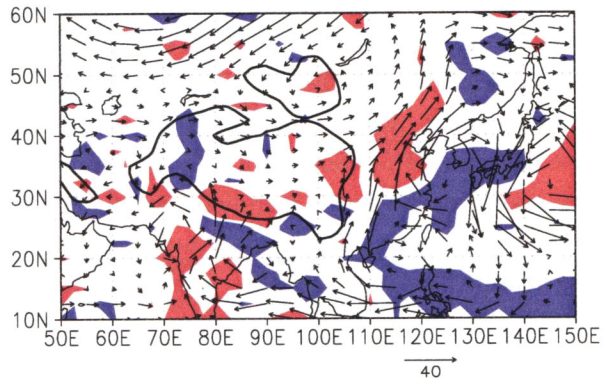

Fig.6: Regressions of moisture flux (vectors) and its divergence (shading) in the rainy season for 1979 – 2006 to the time series in rainy-season precipitation over the Yellow River basin (Fig. 2). Red (blue) shading denotes areas of convergence (divergence) anomaly.

3.2. Intraseasonal variation in precipitation over the Yellow River basin during the summer

In the rainy season, the precipitation time series shows alternatively active phase and inactive phase on 10 – 60 day timescales. The phenomenon is referred to as an intraseasonal variation. Figure 7 shows the timeseries in a wet-year (1988) summer precipitation over the Yellow River basin and its wavelet power spectrum. Precipitation increases in early July and then intraseasonal variation on ~14-day period becomes prominent (Fig.7-upper). ~3-day variation is also observed, probably associated with eastward migratory disturbances. Precipitation decreases again after mid-August. Interestingly, the amplitude of ~3-day variation is modulated on ~14-day period. In a dry year of 1997, ~14-day period was also dominant during the summer. This suggests that the period of intraseasonal variation is not necessarily associated with the interannual variation of rainy-season total precipitation.

The intraseasonal variation in precipitation over the Yellow River basin is induced by that in quasi-stationary waves along the Asian subtropical jet. Rainy-season mean circulation fields are provided by the modulation of the activity of the intraseasonal variation. Figure 8 shows the time-longitude section in a 200-hPa meridional wind component along 40° N in 1988 summer. An active (inactive) phase in precipitation over the Yellow River basin (105° –

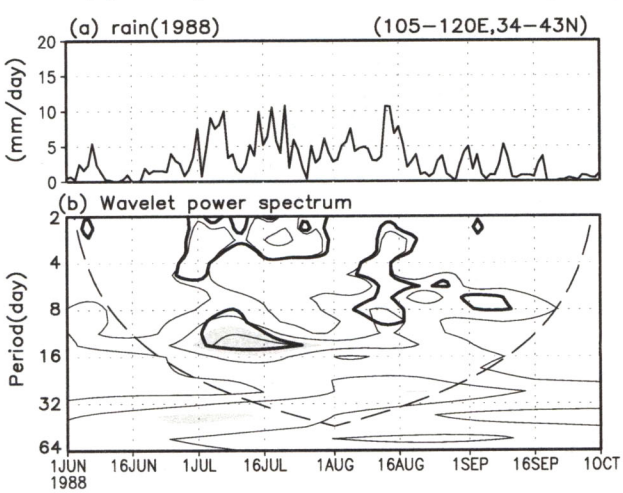

Fig. 7 : Timeseries in summertime precipitation of 1988 (upper) and its wavelet power spectrum (bottom). The thick solid (dotted) contour line encloses regions of > 95% confidence for a red-noise process with a lag-1 coefficient.

120° E) corresponds to a southerly (northerly) phase at the upper troposphere. The alternation between southerly and northerly winds over the Yellow River basin causes the large amplitude precipitation fluctuation. A large circulation fields causing the meridional wind variation has a barotropic structure as well as the interannual variation as shown in Fig. 5. Thus, southerly (northerly) winds import moist (dry) air masses over the Yangtze River basin and cause the increase of convective activity there. The rainy-season mean value in meridional wind of 1988 shows positive (i.e. southerly wind) over the Yellow River basin. This is consistent with wind fields induced by circulation anomalies shown in Fig.5-upper. In 1997, intraseasonal variation in a meridional wind was also remarkable over the Yellow River basin as well (not shown). However, 1997 summer had a longer spell of dry phase than 1998 summer did because northerly wind last for a longer time. The rainy-season mean meridional wind showed negative value (i.e. northerly wind) over the Yellow River basin in 1997. In short, the interannual variation in the rainy-season total precipitation over the Yellow River basin depends on the meridional wind variation induced by intraseasonal variation of waves in the upper troposphere. Whether the upper-level waves induce northerly or southerly over the Yellow River basin depend on the location of wave generation, wave length, periodicity of intraseasonal variation and so on. Further studies will be needed to understand what process determines them.

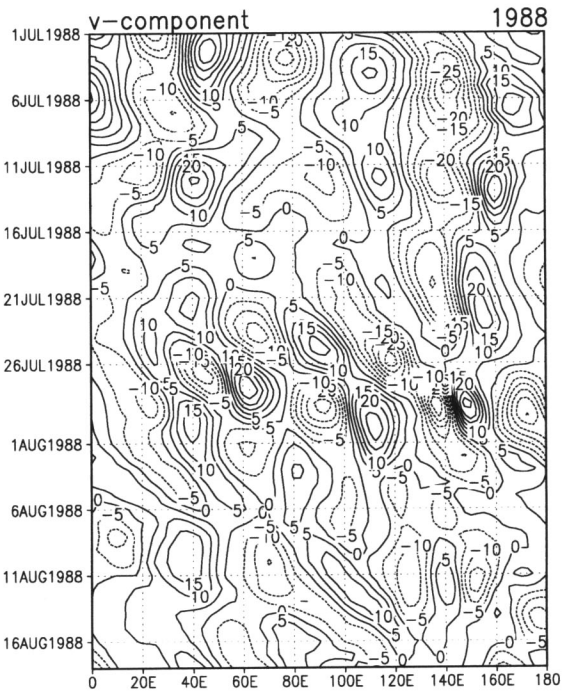

Fig. 8: Time-longitude section in 200-hPa meridional wind in 1988 along 40°N. Positive (negative) value indicates a southerly (northerly) wind.

References

Ding, Q. and B. Wang, 2005: Circumglobal Teleconnection in the Northern Hemisphere Summer, *J. Climate*, **18**, 3483-3505.

Endo, N, Ailikun, B. and T. Yasunari, 2005: Trends in precipitation amounts and the number of rainy days and heavy rainfall events during summer in China from 1961 to 2000, *J. Meteor. Soc. Japan*, **83**, 621-631.

Huffman, G. J. and Coauthors, 1997: The global precipitation climatology project (GPCP) combined precipitation dataset, *Bull. Amer. Meteor. Soc.*, **78**, 5-20.

Iwao, K., and M. Takahashi, 2006: Interannual change in summertime precipitation over northeast Asia, *Geophys. Res.Lett.*, **33,** L16703, doi:10.1029/2006GL 027119.

Kalnay. E, and Coauthors, 1996: The NCEP/NCAR 40-Year reanalysis project, *Bull. Amer. Meteor. Soc.*, **77**, 437-471.

Nitta, T. 1987: Convective activities in the tropical western Pacific and their impact on the northern hemisphere summer circulation, *J. Meteor. Soc. Japan*, **65**, 373-390.

Xie, P. and Coauthors, 2007: A Gauge-Based Analysis of Daily Precipitation over East Asia, *J. Hydrometeor.*, **8**, 607-626.

Yatagai, A and T. Yasunari, 1995: Interannual variations of summer precipitation in the arid/semi-arid regions in China and Mongolia: their regionality and relation to the Asian summer monsoon, *J. Meteor. Soc. Japan*, **73**, 909-923.

Vertical transport of water vapor and the atmospheric water budget over the Loess Plateau in China – Comparison of the cases in 2005 and 2006 –

Atsuhiro Takahashi[1] · Tetsuya Hiyama[2] · Masanori Nishikawa[3] · Atsushi Higuchi[4] · Yoshihiro Fukushima[1]

1 : Research Institute for Humanity and Nature (RIHN)

2 : Hydrospheric Atmospheric Research Center (HyARC), Nagoya University

3 : Graduate School of Environmental Studies, Nagoya University

4 : Center for Environmental Remote Sensing (CEReS), Chiba University

1. Introduction

The Loess Plateau is located in middle part of the Yellow River basin. The land-atmosphere interaction is considered to have a critical role in precipitation and the water circulation in the Yellow River basin.

The Loess Plateau consists of a characteristic complex terrain including flat tableland and steep gullies. The surfaces of the tableland are covered by various types of crop fields such as wheat, maize, and apples. The long-term continuous observations of the atmospheric boundary layer (ABL) were conducted from June 2004 till September 2007, in order to clarify diurnal, seasonal, and annual variations of the water budget and transport of water vapor over such complex and heterogeneous surface of the Loess Plateau. The observation has revealed that development of strong vertical wind in ABL (Nishikawa et al., 2005) and cumulus convection enhanced the vertical transport of water vapor, which is likely to cause clear diurnal variations of water vapor content in the upper and lower atmospheric layer in the troposphere (Takahashi et al., 2007).

This study reports seasonal variation of the water budget as well as characteristic diurnal variation of summer precipitation with considering vertical transport of water vapor in 2005 and 2006.

2. Observation site and methods

Observation site is located at the wheat field of the Changwu Agro-Ecological Experimental Station (35.24 °N, 107.68 °E, 1224 m a.s.l.) in the southern part of the Loess Plateau in China. Fields of apple trees and maize are also distributed around the observation area, and residential buildings stand in some parts of the area. In the experimental field, winter wheat is seeded in September and harvested in June in every year. We installed the 30 m-high tower in May 2004, for measuring turbulent fluxes of momentum, sensible heat, latent heat, and carbon dioxide. Three-dimensional wind velocity and air temperature have been measured using the ultra-sonic anemometers (1210R3, Gill Instruments Ltd., UK), and densities of water vapor and gaseous carbon dioxide have been measured using the open-path type H_2O/CO_2 gas analyzers (LI-7500, Li-Cor Co., USA). These instruments have been equipped to heights of three levels, i.e. 32 m, 12 m, and 2 m. Sensible heat and latent heat fluxes were calculated using the eddy correlation method (EC). For compensation of the fluxes during the periods when EC method could not be applied due to some troubles in the instruments, Bowen ratio method was applied using data of air temperature and humidity, which have been measured at heights of 32 m and 12 m and averaged in 30 minutes. If either of the average data at heights of 32 m and 12 m were missed, the average data at height of 2 m was used for compensation.

The vertical profiles of water vapor from the ground up to a height of 10 km were measured with time resolution of 1minute using a microwave radiometer (MR) (TP/WVP-3000, Radiometrics Co, USA), which was installed at the observation site in May 2005.

3. Results and discussion

Figure 1 shows seasonal variation of monthly precipitation and evapotranspiration and monthly mean of daily averaged sensible heat flux in 2005 and 2006. Annual precipitations were 515 mm and 452 mm in 2005

and 2006, respectively. Annual evapotranspirations were 440 mm and 350 mm in 2005 and 2006, respectively. About 80 % of annual precipitation was returned to the atmosphere by evapotranspiration. Infiltrations into the soil were 80 mm and 100 mm in 2005 and 2006, respectively. These correspond to 15 % (2005) and 22 % (2006) of annual precipitation.

Figure 2 shows seasonal variation of the monthly mean of water vapor contents (WVC) in the atmosphere from the ground to 2 km and to 10 km in 2005 and 2006. Seasonal variation of annual precipitation and evapotranspiration are also shown in Fig. 2. WVC increased abruptly in the period from June to July in both of years. The data of WVC was missed during period from July in 2005 to April in 2006, due to the trouble of the electric power board of MR. The monthly mean WVC had its maximum in July and decreased monotonically till December in 2006. Seasonal variation of evapotranspiration was similar to that of WVC in 2006. On the other hand, precipitation had its maximum in August in 2006. Precipitation concentrated to three months from July to September in accordance with the result in past literature (Owada et al., 2005). Figure 3 shows hourly precipitations accumulated during four months from June to September in 2004, 2005 and 2007, respectively. The data of hourly precipitation was missed in 2006 due to troubles in the instruments. In 2004 and 2007, hourly precipitations show apparent decreases in daytime and had maximum peaks in the early morning and the evening. On the other hand, in 2005, hourly precipitations had a maximum peak in daytime and had a strong peak in the evening. Although shapes of diurnal variation of hourly precipitation are different among years, strong peaks in the evening were commonly observed. Such strong peaks in the evening were likely to be caused by active cloud convection due to development of the ABL in daytime.

Strong convective activities could be observed when strong vertical winds were observed in the ABL and these were likely to link to cumulus convection developed in the afternoon. Active cumulus, which is defined in this study as that especially developed cumulus with its cloud top reaching to high altitudes, were frequently observed in our site in late of June, when WVC increased, in both of 2005 and 2006 (Takahashi et al., 2007). During the period, active cumulus tended to be observed in the afternoon in daytime. Figure 4 shows diurnal variation of WVC measured by MR, latent heat fluxes that were calculated by Bowen ratio method, and the ABL heights that were estimated using the data of wind velocity measured by a wind profiler radar on 15, 16, and 17 June of 2006. As for ABL heights, we depicted only its variation in daytime. We excluded data in the periods when stratiform clouds influenced estimation of ABL heights or too high echoes measured in nighttime. As shown in Fig. 4, WVC decreased rapidly in the lower atmospheric layer and increased in the upper atmospheric layer in the afternoon when active cumulus developed. This suggests that the vertical mixing of water vapor was enhanced between the upper and lower atmosphere due to strong cumulus convection of active cumulus. On the other hand, decrease of WVC started earlier in the layer at a height of 700 m than that in the layer near the ground surface, where WVC started to increase before noon. This suggests presence of a local circulation influencing diurnal variation of WVC over the area. That is, WVC near the ground surface increased due to supply of water vapor by evapotranspiration, while WVC in the layer at a height of 700m decreased around dawn that was likely to be caused by downward penetration of dry air from the upper atmosphere caused by development of a local circulation. Such influence of a local circulation to diurnal variation of WVC has been reported in Tibetan Plateau (Takagi et al., 2000), Sumatra island (Wu et al., 2003), and coastal area of Thailand (Fujita et al., 2006). A small-scale local circulation is probable to be generated by a thermal convection around edge of the tableland (Zängle and Chico, 2006), although a large scale local circulation is considered to be difficult to be generated in the Loess Plateau.

4. Conclusions

About 80 % of precipitation has been evapotranspirated to the atmosphere. In the period from July to September, precipitation was larger than evapotranspiration. The surface soil layer had been moistened during

this period. On the other hand, in the period from October to next April, evapotranspiration was larger than precipitation. The surface soil layer had been dried during this period. A part of water that was supplied by summer precipitation had been stored within surface soil layer and had been returned gradually to the atmosphere, especially in spring when plant grew actively. Consequently, plants could use water even if precipitation was not enough in the growing season. Water content in the surface soil layer was consumed rapidly by plants. This is effective to the growth of winter wheat.

Development of the ABL accompanied with strong vertical wind and transported water vapor to the cloud layer. When active cumulus developed, clear diurnal variations of WVC were observed. From the early morning after dawn, WVC decreased in the lower atmosphere except the layer close to the ground surface. In contrast to this, WVC increased in the upper atmosphere. Development of the ABL and cumulus convection in the afternoon might have significant influences to the diurnal variation of the WVC. Such strong mixing due to links of strong vertical wind in the ABL and cumulus convection enhanced mixing of water vapor between the atmospheric boundary layer and free atmosphere. These diurnal variations of the WVC might be also related with a small-scale local circulation, which was likely to be generated around the edge of the tableland of the plateau (Zängle and Chico, 2006).

It is necessary to study further on the relationship between such transport of the atmospheric water vapor and synoptic weather conditions in order to clarify the water circulation in the Yellow River basin.

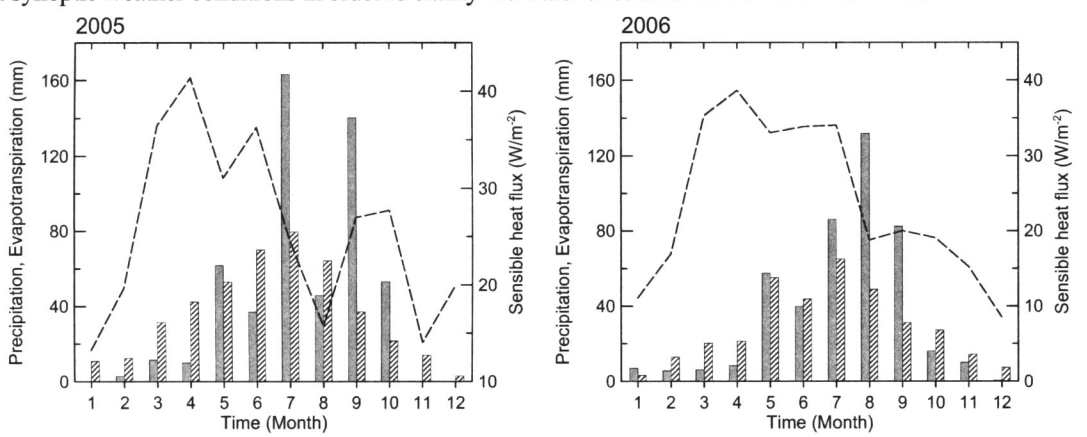

Fig. 1. Seasonal variation of monthly precipitation (grey bars), monthly evapotranspiration (bars with oblique), and monthly averaged sensible heat flux (dashed line) in 2005 and 2006.

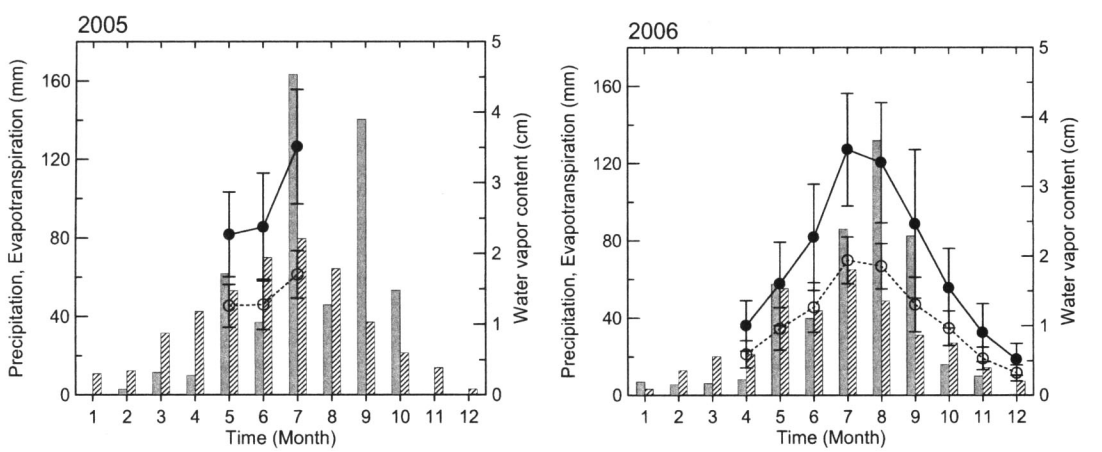

Fig. 2. Seasonal variation of monthly precipitation (grey bars), monthly evapotranspiration (bars with oblique), and monthly averaged atmospheric water vapor content (black circles: 0-10 km, open sircles: 0-2 km) in 2005 and 2006.

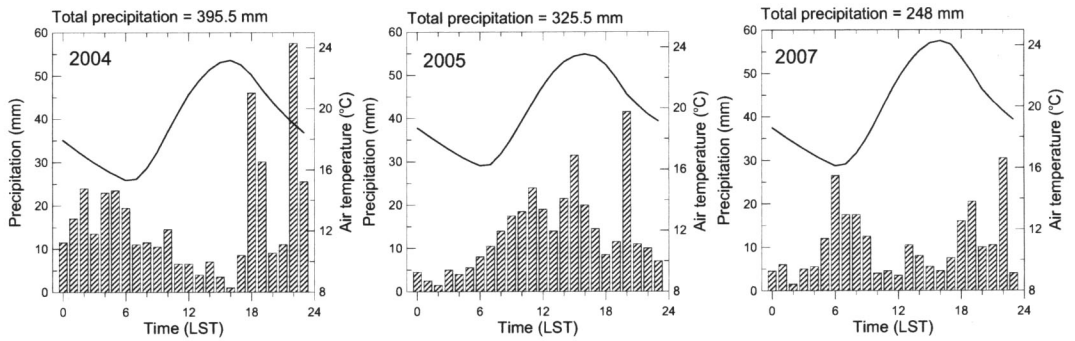

Fig. 3. Hourly precipitation accumulated over four months from June to September (bars with oblique), and mean diurnal variation of air temperature (solid lines) in 2004, 2005, and 2007.

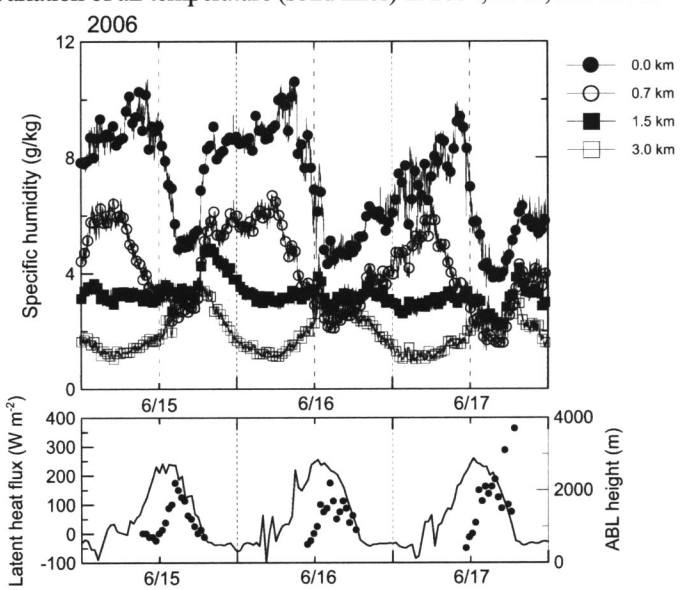

Fig. 4. Diurnal variation of specific humidity at four heights (see legend beside the upper figure to see the meanings of each symbol), latent heat flux (solid lines), and the heights of the atmospheric boundary layer (black circles) on 15, 16, and 17 June 2006.

References

Fujita, M., T. Sasaki, and F. Kimura (2006): A dramatic daytime decrease in water vapor over coastal Thailand, *SOLA*, 2, 49-52.

Nishikawa, M., T. Hiyama, A.Takahashi, W. Li, A. Higuchi, W. Liu, and Y. Fukushima (2005): Characteristics of vertical wind observed within and over the convective boundary layer on the Loess Plateau, China. *Proceedings of the Third Japan–China Joint Workshop on Lower Atmosphere and Precipitation Study (LAPS), Nagoya, Japan*, 105–106.

Owada, H., H. Ohmori, and J. Matsumoto (2005): Seasonal changes in wind systems relating to precipitation during the rainy season in the Loess Plateau, China. *Geographycal Review of Japan*, 78-8, 534-541.

Takagi, T., F. Kimura, and S. Kono (2000): Diurnal variation of GPS precipitable water at Lhasa in premonsoon and monsoon period, *J. Meteor. Soc. Japan*, 25, 175-180.

Takahashi, A., T. Hiyama, M. Nishikawa, A. Higuchi, W. Li, W. Liu, and Y. Fukushima (2007): Vertical mixing of water between the atmospheric boundary layer and free atmosphere overChangwu, the Loess Plateau of China. Proceedings of 3rd International Workshop on Yellow River Studies, February 14-15, 2007 Kyoto, 73-76.

Wu, P., S. Hamada, S. Mori, Yudi I. Tauhid, M. D. Yamanaka, and F. Kimura (2003): Diurnal variation of precipitable water over a mountainous area of Sumatra Island, *J. Appl. Meteor.*, 42, 1107-1115.

Zängle, G. and S. G. Chico (2006): The thermal circulation of a grand plateau: sensitivity to the height, width, and shape of the plateau. Mon. Wea. Rev., 134, 2581-2600.

Seasonal changes in the conditions of atmospheric boundary layer, land surface, and synoptic field over the Loess Plateau in China

Masanori NISHIKAWA[1)], Tetsuya HIYAMA[2)], Atsuhiro TAKAHASHI[3)],
Wei LI[4)], Hatsuki FUJINAMI[2)], Atsushi HIGUCHI[5)] and Yoshihiro FUKUSHIMA[3)]

1) Graduate School of Environmental Studies, Nagoya University, Japan
2) Hydrospheric Atmospheric Research Center (HyARC), Nagoya University, Japan
3) Research Institute for Humanity and Nature (RIHN), Japan
4) Department of Civil & Environmental Engineering, Duke University, U.S.A.
5) Center for Environmental Remote Sensing (CEReS), Chiba University, Japan

1. Introduction

Atmospheric boundary layer (ABL) plays an important role on the heat and water vapor exchanges between land surface and the free atmosphere (FA). Diurnal change of ABL transports water vapor from land surface to ABL and FA, which often induces generations of cumulus clouds near the top of the ABL. Diurnal change of ABL also changes the stratification of daytime lower atmosphere into near-neutral. However the interaction between ABL and convective precipitation has not been investigated over the Loess Plateau in China, previously.

On sunny days in the early summer of 2005 and 2006, we showed fair-weather cumulus have frequently generated over the Loess Plateau in China [*Nishikawa et al.*, 2007]. When active cumulus developed, water vapor exchanged diurnally between the ABL and FA [*Takahashi et al.*, 2007]. However the detailed structures of cumulus generation and relation to surface and ABL features over the Loess Plateau have not been investigated. Based on this background, we investigate seasonal changes in ABL, land surface and synoptic field over Changwu, the Loess Plateau in China, using the data obtained from April to July in 2005. Moreover the effect of ABL to the synoptic-scale disturbance is discussed.

2. Observation and data set

The study site is located at the research field of Changwu Agro-Ecological Experimental Station on the Loess Plateau (35.24°N, 107.68°E, 1224 m a.s.l.). We analyzed vertical profiles of three-dimensional wind velocity and those of echo intensity measured by a Wind Profiler Radar (WPR, L-28H, Sumitomo Electric Industries, Japan). We also determined surface heat fluxes and radiation fluxes using data obtained by a Flux & Radiation Observation System (FROS, Climatec, Japan). Details of the study site and the instrumentation at this site were shown in *Hiyama et al.*, [2005].

In order to investigate synoptic conditions, we used 6-hourly reanalysis data produced by National Center for Environmental Prediction (NCEP) / National Center for Atmospheric Research (NCAR) [*Kalnay et al.*, 1996]. We also used hourly IR-Tbb data derived from GOES-9. Spatial resolutions of the reanalysis and Tbb data are 2.5° x 2.5° and 1° x 1°, respectively.

3. Results and discussion

3.1 Seasonal changes in ABL, land surface, and synoptic field

Figure 1 shows seasonal changes in meteorological elements and surface conditions. Specific humidity was gradually increased from April to July. Broad areas of the Plateau tableland were occupied by agricultural fields planted with wheat, maize and apples. Maize was seeded in the middle of April, and wheat was harvested in the end of June.

Figure 2 shows seasonal changes in daytime mean surface heat fluxes and daily maximum ABL heights. From the spectral analysis of daily precipitation, the power spectral peak of daily precipitation appeared in 3 - 5 days (figure not shown). This means the precipitation occurred with 3 - 5 days intervals in this season. In the same way, from the spectral analysis of latent heat flux, the power spectral peak of latent heat flux appeared in 2 – 5 days (figure not shown). The power spectral peak of latent heat flux corresponded to that of precipitation. This means latent heat flux became higher after precipitation event, then before the precipitation event, i.e. after a long no-rain period, latent heat flux gradually decreased due to decreasing surface soil moisture. On the other hand, the power spectral peak of sensible heat flux has not been appeared in any intervals. This indicates that the seasonal change of sensible heat flux was unclear.

Figure 2-(c) shows seasonal changes in ABL heights on sunny days. A green bar represents the daily maximum ABL height determined by the median filtering method [*Angevine et al.*, 1994]. A black bar represents the daily maximum ABL height estimated by a slab model [*Tennekes*, 1973; *Garratt*, 1992]. The seasonal change in ABL height determined by the median filtering method was unclear. When the ABL height of the median filtering method was large as well as the difference of ABL heights determined by both methods was large, cumulus clouds have been frequently generated in the daytime. Thus, when this difference was large, we assumed cumulus clouds have been generated and developed from April to July in 2005.

When cumulus clouds generated, the atmospheric stability became near-neutral from 600 hPa to 700 hPa. At the study site, 600 - 700 hPa corresponds to 2 - 3 km height in which cumulus clouds appeared. Moreover, the seasonal change in the potential temperature gradient between 600 hPa and 700 hPa showed good agreement with the seasonal change of the difference in ABL heights determined by two methods (figure not shown). Therefore, it could be concluded that generations of cumulus clouds were strongly related to the atmospheric stability.

3.2 Effect of ABL on the synoptic scale disturbance

Before the effect of ABL to the synoptic scale disturbance is discussed, we show the synoptic conditions during a precipitation event over the Loess Plateau. Figure 3 shows longitude-time section of Tbb along 35.25°N from 13 to 19 May. The southern part of the Loess Plateau located in the middle latitude, which is affected by the subtropical jet. Thus the precipitation, which was observed at the study site on 15 - 16 May, resulted from the eastward transportation of the disturbance from the Tibetan Plateau. Moreover we confirmed all precipitation events have been resulted from eastward transportations of disturbances.

Figure 4 shows longitude-time section of Tbb along 35.25°N from 17 to 23 June. At the study site, the precipitation was observed at 19 BST (Beijing Standard Time) on 19 June. This precipitation occurred due to the synoptic disturbance. When the disturbance approached to the southern part of the Loess Plateau, the convective activity was intensified. Then the disturbance was decayed around there. In the daytime of 19 June over the study site, it was sunny and fair-weather cumulus clouds generated, and ABL developed up to around 3 km height. This means a neutral stratification was formed up to 3 km height due to the ABL development. Before and after the precipitation event, the synoptic-scale water vapor advection has been kept constant over this area (figures not shown). Therefore it could be concluded that ABL intensified the disturbance in this case.

4. Summary

In order to clarify effect of ABL to cumulus clouds generation and precipitation, we investigated seasonal changes in ABL, land surface and synoptic field over Changwu, the Loess Plateau in China, using the data obtained from April to July in 2005. Especially the effect of ABL to the synoptic scale disturbance was discussed.

Latent heat flux became higher after the precipitation event, then after a long no-rain period, latent heat flux became lower due to decreasing surface soil moisture. The interval was 2 - 5 days, which corresponded to intervals of precipitation. On the other hand, seasonal change of sensible heat flux was unclear, and thus seasonal change of ABL height was also unclear. This is because cumulus clouds were frequently appeared from spring to summer. Generation of cumulus clouds were related not only to surface fluxes but also to the atmospheric stability.

The precipitation which was observed at the study site resulted from the eastward transportation of the disturbance. One of the cases which ABL affected to the synoptic scale disturbance was shown. In the daytime of 19 June, ABL developed up to about 3 km height and this made fair-weather cumulus to develop. Because synoptic-scale water vapor advection has been kept constant over the area, it could be concluded that ABL intensified the disturbance in this case.

References

Angevine, W. M., A. B White, and S. K. Avery (1994), Boundary-layer depth and entrainment zone characterization with a boundary-layer profiler, *Bound.-Layer Meteor.*, *68*, 375-385.

Garratt, J. R. (1992), *The Atmospheric Boundary Layer*, 316 pp., Cambridge Univ. Press, New York.

Hiyama, T., A. Takahashi, A. Higuchi, M. Nishikawa, W. Li, W. Liu, and Y. Fukushima (2005), Atmospheric Boundary Layer (ABL) observations on the "Changwu Agro-Ecological Experimental Station" over the Loess Plateau, China.. *AsiaFlux Newsletter*, *16*, 5-9.

Kalnay, E., M. Kanamitsu, R. Kistler, W. Collins, D. Deaven, L. Gandin, M. Iredell, S. Saha, G. White, J. Woollen, Y. Zhu, M. Chelliah, W. Ebisuzaki, W. Higgins, J. Janowiak, K.C. Mo, C. Ropelewski, J. Wang, A. Leetmaa, R. Reynolds, R. Jenne, and D. Joseph, (1996), The NCEP/NCAR 40-year reanalysis project. *Bull. Amer. Meteorol. Soc.*, *77*, 437 - 471.

Nishikawa, M., T. Hiyama, A. Takahashi, W. Li, A. Higuchi, W. Liu, and Y. Fukushima, (2007),

Seasonal and diurnal changes of atmospheric boundary layer heights over Changwu, the Loess Plateau of China. *Proc. The Third International Workshop on Yellow River Studies*, 69-72.

Takahashi, A., T. Hiyama, M. Nishikawa, A. Higuchi, W. Li, W. Liu, and Y. Fukushima, (2007), Vertical mixing of water vapor between the atmospheric boundary layer and free atmosphere over Changwu, the Loess Plateau of China. *Proc. The Third International Workshop on Yellow River Studies*, 73-76.

Tennekes, H. (1973), A model for the dynamics of inversion above a convective boundary layer. *J. Atmos. Sci.*, *30*, 558-567.

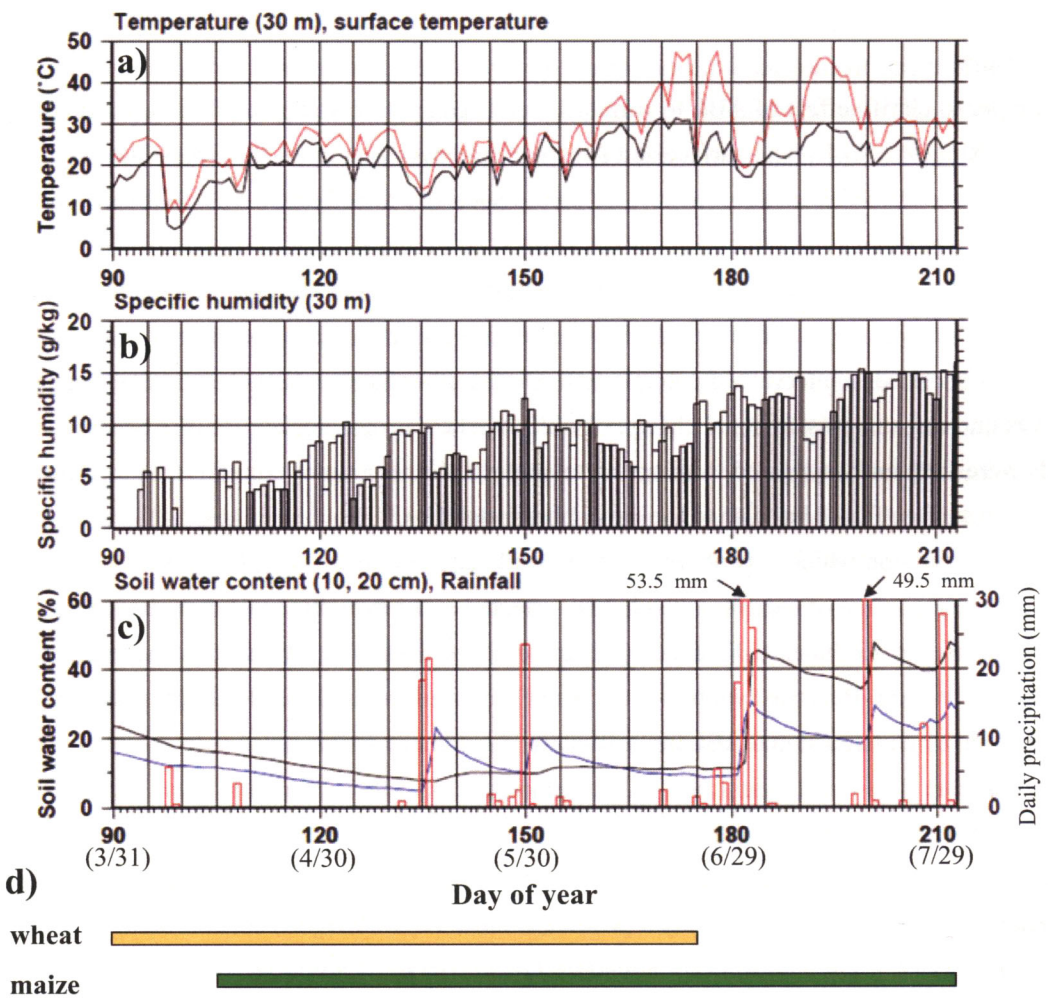

Figure 1. Seasonal changes in a) daytime mean surface temperature (red) and daytime mean air temperature at 30 m (black), b) daytime mean specific humidity at 30 m (black bars), c) daily precipitation (red bars) and daily soil water content at 10 cm depth (blue line) and 20 cm depth (black line), and d) growing season of wheat (yellow bar) and maize (green bar).

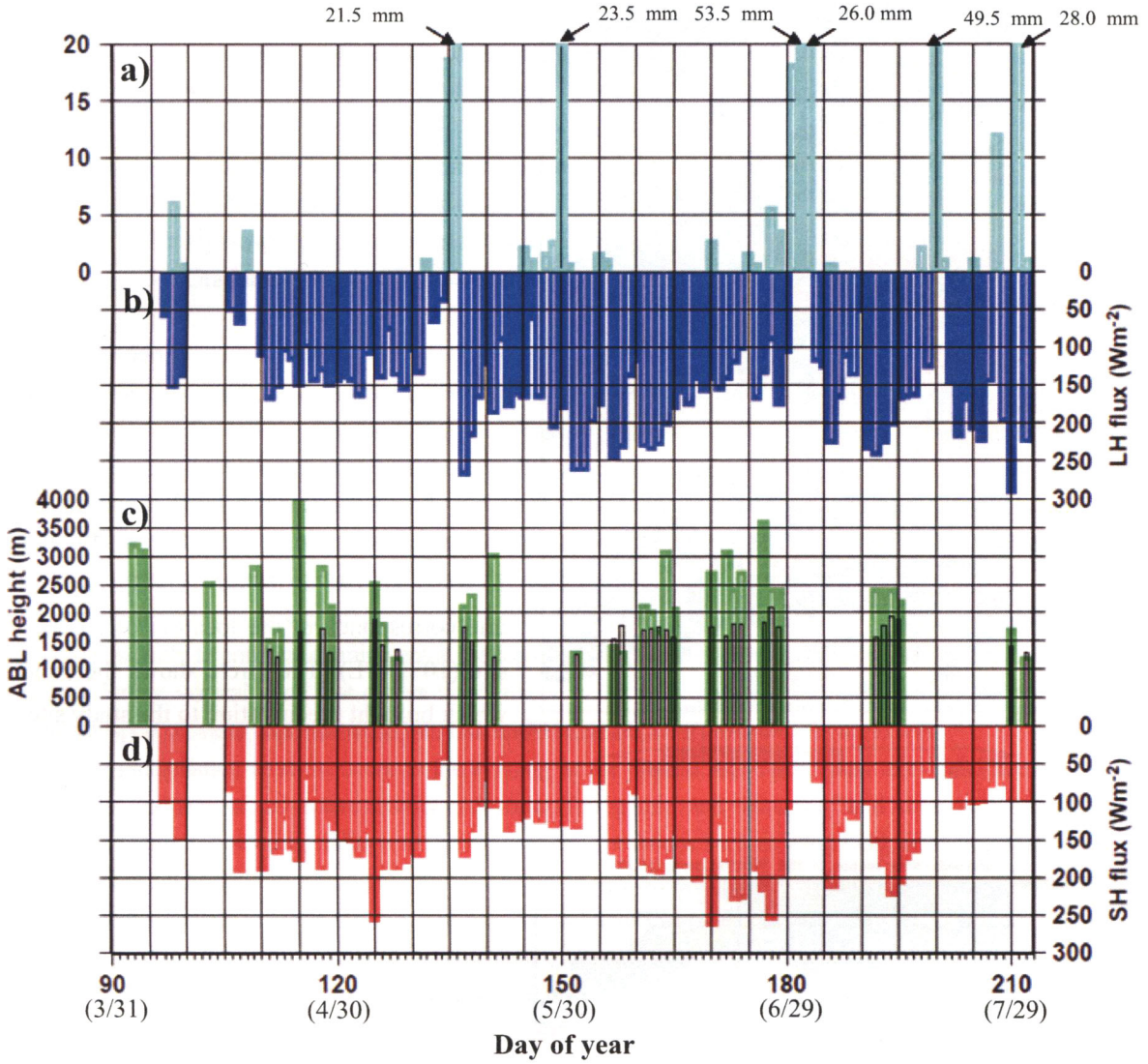

Figure 2. Seasonal changes in a) daily precipitation, b) daytime mean latent heat flux (LH flux), c) daily maximum ABL height determined by the median filtering method (green bars) [*Angevine et al.*, 1994] and that estimated by a slab model (black bars) [*Tennekes*, 1973; *Garratt*, 1992], and d) daytime mean sensible heat flux (SH flux).

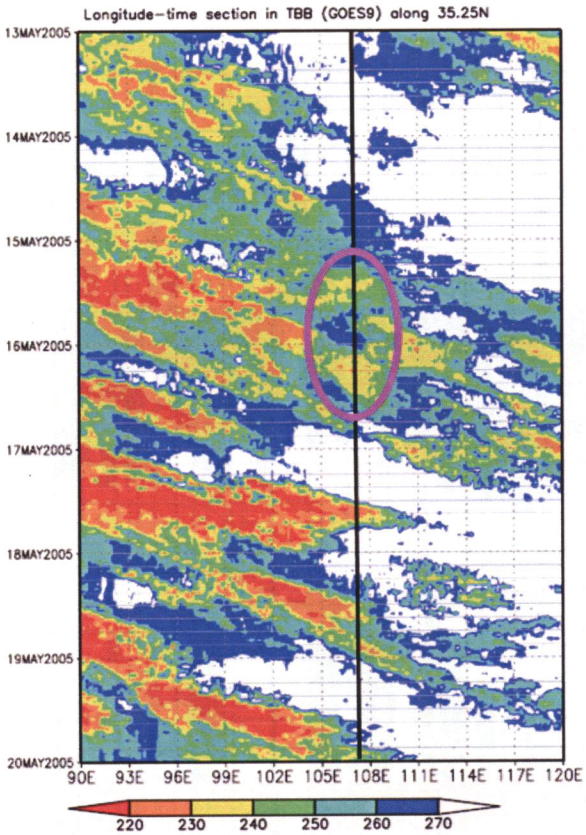

Figure 3.Longitude-time section of Tbb along 35.25°N from 13 to 19 May (UTC). The black line corresponds to the location of the study site (107.68°E). The circle shows the clouds which brought precipitation to the study site.

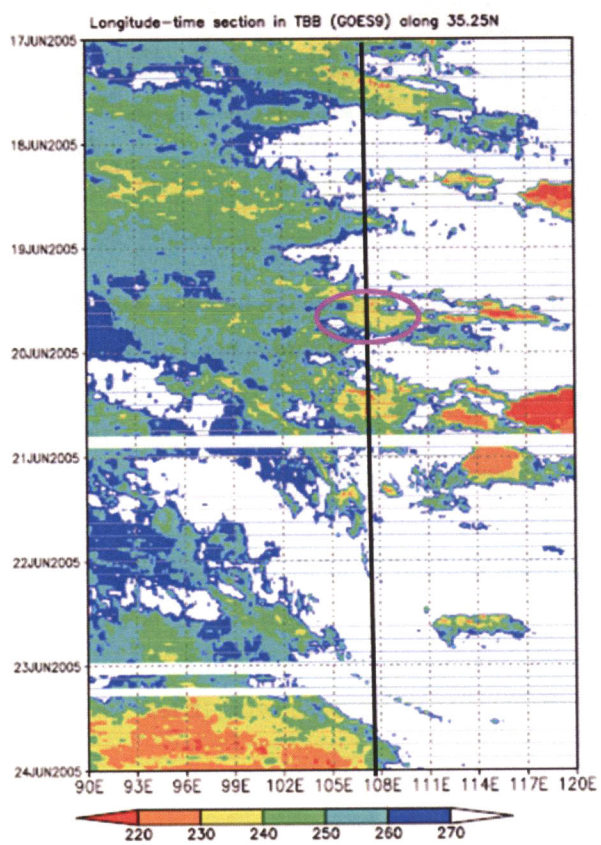

Figure 4. Same as Fig. 3 but from 17 to 23 June (UTC).

Impact of change in land surface condition on the development of the atmospheric boundary layer and cumulus clouds over the Loess Plateau in China
—Numerical experiment—

Atsuhiro Takahashi[1], Tetsuya Hiyama[2], Masanori Nishikawa[3], and Yoshihiro Fukushima[1]
1 : Research Institute for Humanity and Nature (RIHN)
2 : Hydrospheric Atmospheric Research Center (HyARC), Nagoya University
3 : Graduate School of Environmental Studies, Nagoya University

1. Introduction

A characteristic topographical terrain spreads over the southern part of the Loess Plateau in China. The plateau consists of flat tableland at the top of the plateau and steep gullies distributed with high complexity. No-irrigated agriculture has been conducted on the flat tableland. Large area was covered by fields of wheat, maize, and apple. Precipitation is significantly important to maintain agriculture in the plateau.

Most of annual precipitation occurs in five months from May to September (Owada et al., 2005). Cumulus clouds generated frequently during these period. Cumulus clouds that developed to a high altitude in the afternoon were observed in late of June in 2005 and 2006 (Takahashi et al, 2007). In such cases, cumulus convection is likely to enhance entrainment at the top of the atmospheric boundary layer (ABL) (Nishikawa et al, 2007). Strong vertical wind that occurs interactively in the ABL and cumulus clouds might enhance the vertical transport of water vapor between the ABL and free atmosphere (Takahashi et al., 2007).

Intense precipitation tends to occur in the evening in the plateau. Such precipitation is considered to be related to development of convective activity in daytime. Topography and wetness of land surface can influence generation of cumulus cloud in addition to the atmospheric conditions such as wind field, air temperature, and humidity. This study aims to investigate the sensitivity of ABL development and cloud activity to the land surface conditions over the Loess Plateau. Numerical experiments were conducted in order to clarify the extent of influence of the land surface wetness to generation of cumulus cloud over the ABL. The land surface was treated as a completely flat and homogeneous terrain in order to exclude any topological effects in this study.

2. Model description

CReSS (Cloud Resolving Storm Simulator) (Tsuboki and Sakakibara, 2001) was used for our numerical experiment in this study. Table 1 shows the initial and boundary conditions, parameters, and some physical schemes adopted in CReSS in this study. The model domain is the area of 20 km × 20 km with 12,824 m depth in the vertical domain in this numerical experiment. The Changwu Agro-Ecological Experimental Station is located at the center of the domain. The model domain contains 200 grid points in each horizontal direction and 120 layers in the vertical direction that is stretched according to the function of hyperbolic tangent for the layers above a height of 4.2 km. The boundary conditions of shortwave radiation and the initial profiles of air temperature, humidity, and wind velocity were input as the meteorological conditions observed on 19 June 2005, when strong vertical winds were observed in the afternoon. The time domain of the simulations was set to daytime from 8:00 local standard time (LST) to 18:00 LST with time step of 1 second.

We conducted numerical experiments under several conditions, i.e. changing the evaporation efficiency β at the land surface and the vertical profiles of relative humidity (RH) in the atmosphere. (β, RH) of each experiment are Exp. 1: (0.05, obs), Exp. 2: (0.05, obs+5%), Exp. 3: (0.2, obs), and Exp. 4: (0.2, obs+5%). Here, 'obs' means the observed profile of RH. The conditions of $\beta = 0.05$ and 0.2 correspond to dry and wet surface conditions, respectively.

3. Results and discussion

Figure 1 shows the horizontal distributions of wind velocity at heights of 1.2 km and 2.5 km in the case of Exp. 1 and Exp. 3. Colors mean the vertical wind velocity. Vectors mean horizontal wind vectors. Under the condition of dry land surface ($\beta = 0.05$), strong upwind appeared at a height of 2.5 km, while the vertical wind velocity was weak at the same height under condition of wet land surface ($\beta = 0.2$). This is due to the fact that the ABL was enhanced by much amount of sensible heat from the land surface to the atmosphere in the case of $\beta = 0.05$. The ABL developed to height of about 3 km, where strong upwind reached around there. Organized structures consisting of convective cells developed and generated upward wind as shown in Fig. 1(b) and (d).

Figure 2 shows time-height sections of the vertical wind velocity and specific humidity for each case of the experiment. We can see that the ABL developed relatively rapidly to higher altitudes with strong vertical winds in the case of $\beta = 0.05$. The influences of RH on development of the ABL were relatively small in both cases of $\beta = 0.05$ and $\beta = 0.2$.

Figure 3 shows time-height sections of specific humidity and the cloud liquid water content for each case of the experiment. Increase of RH by 5% caused increase in emergence of cloud liquid water in both cases of $\beta = 0.05$ and $\beta = 0.2$. This means that the slight increase of RH can stimulate generation of cumulus cloud, especially in the case of wet surface conditions, $\beta = 0.2$, in which supply of water vapor from the land surface is larger than dry surface conditions, $\beta = 0.05$.

Precipitation that reaches to the ground surface did not occur in all of the cases of the experiments in this study. However, we could confirm that generation of cumulus cloud is sensitive to vivid increase of relative humidity. Therefore, advection of convective activity would enhance generation of active cloud convection that can produce precipitation. In the observation on 19 June 2005, precipitation occurred in the evening on that day. At that time, the convective activity might be stimulated by the ABL then developed over the plateau.

4. Conclusions

This study conducted numerical experiments using cloud-resolving model for the purposes to clarify the factors that influence effectively the generation of cumulus cloud over the Loess Plateau in China. Especially, this study focused on the influence of the land surface wetness to generation of cumulus cloud. Thus, completely flat and homogeneous land surface was assumed in order to avoid any topological effects on generation of cumulus cloud. The meteorological conditions on 19 June 2005 were used in the experiments, since strong vertical winds were observed in the ABL especially in the afternoon.

The obtained results are summarized as follows. Under the condition of dry land surface, strong upwind developed especially and reached to a height of about 3 km. On the other hand, under wet surface condition, the development of the ABL and the vertical wind velocity in the ABL were relatively weaker than those under dry surface condition. Organized structures of convective cells developed. In both of the cases of dry and wet surface conditions, circular upwind areas developed at the edge of each cell. Such structure developed stronger under dry surface condition. If the vertical profile of relative humidity increases by 5%, generation of cumulus cloud was activated in both of the cases of dry and wet surface conditions. Especially, enhancement of generation of cumulus cloud was more prominent under wet surface condition.

Further study will be needed to clarify the mechanism of the interaction between the ABL and the active cloud convections in synoptic scale that have potential to cause precipitation, in order to understand the land-atmosphere interaction and the water circulation in the Yellow River basin.

Table 1. Boundary conditions, parameters, and various physical schemes in CReSS used in this study

Model	Cloud Resolving Storm Simulator (CReSS) version 2.1
Turbulence scheme	1.5 order closure scheme
Cloud physics	Warm rain
Land surface flux	Bulk method
Soil layers	0.1 m × 30 layes
Radiation	Energy budget at land surface
Model domain	Horizontal 200 × 200 (20 km × 20 km)
	Vertical 120 layers (12824.0 m)
Resolution	Horizontal 100 m
	Vertical 50 m (Stretching by function (tanh) above 4.2 km)
Time-step	1 second, Totally 36000 seconds (10hours)
Lateral condition	Periodic condition
Upper boundary	Non-slip condition
Lower boundary	flat surface (1224 m a.s.l.)
Forcing	Diurnal variation of shortwave radiation
Initial condition	Lower layer: Microwave radiometer and wind profiler radar
	Upper layer: radiosonde data 00Z (8BST) at Pingliang
Albedo	0.156
Evaporation efficiency	0.05, 0.2
Surface roughness	0.47 m
Temperature at bottom soil	293.0 K
Soil heat capacity	2.3×10^{6} J m^{-3} K^{-1}
Thermal diffusivity of soil	7.0×10^{-7} m^{2} s^{-1}

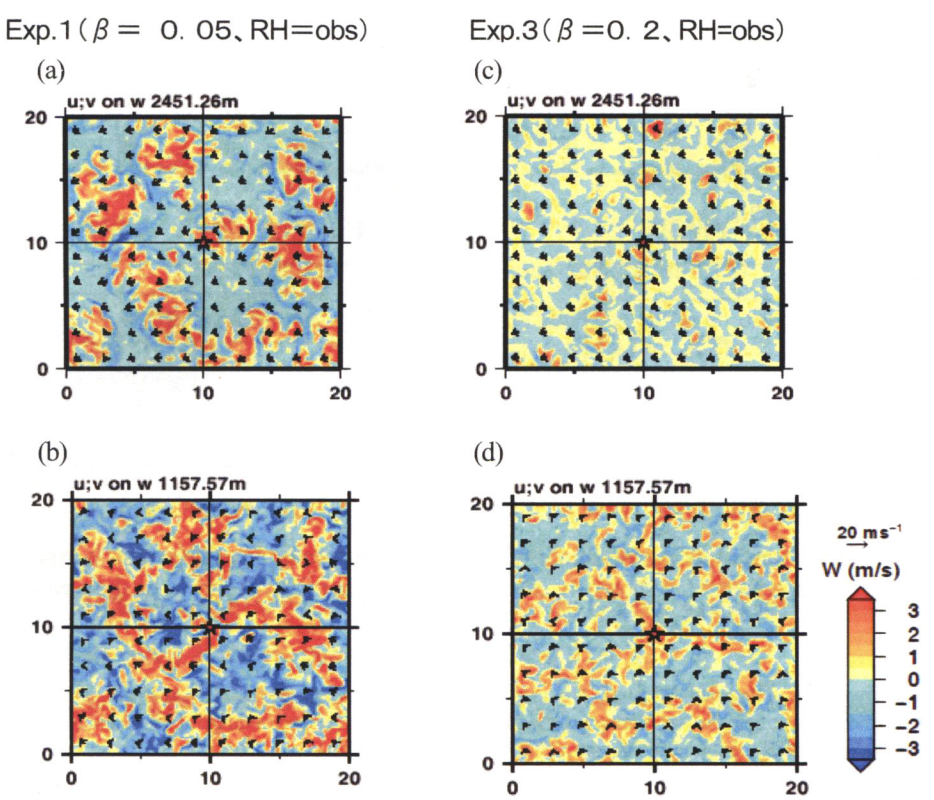

Fig. 1. Horizontal sections of wind velocity for Exp. 1 and Exp. 3. The vertical velocities are shown by colors. The horizontal wind velocities are shown by the vectors. The upper figures are wind velocities at a height of about 2.5 km and the lower figures are those at a height of about 1.2 km.

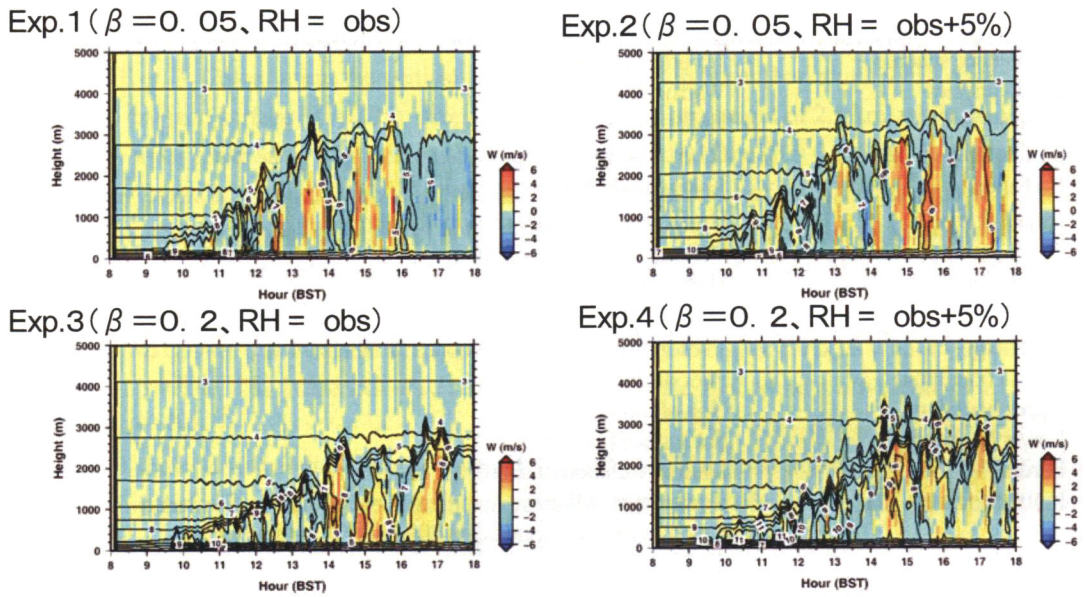

Fig. 2. Time-height sections of the vertical wind velocities and specific humidity in each experiment. The vertical wind velocities are shown by the colors and specific humidity is shown by the contour.

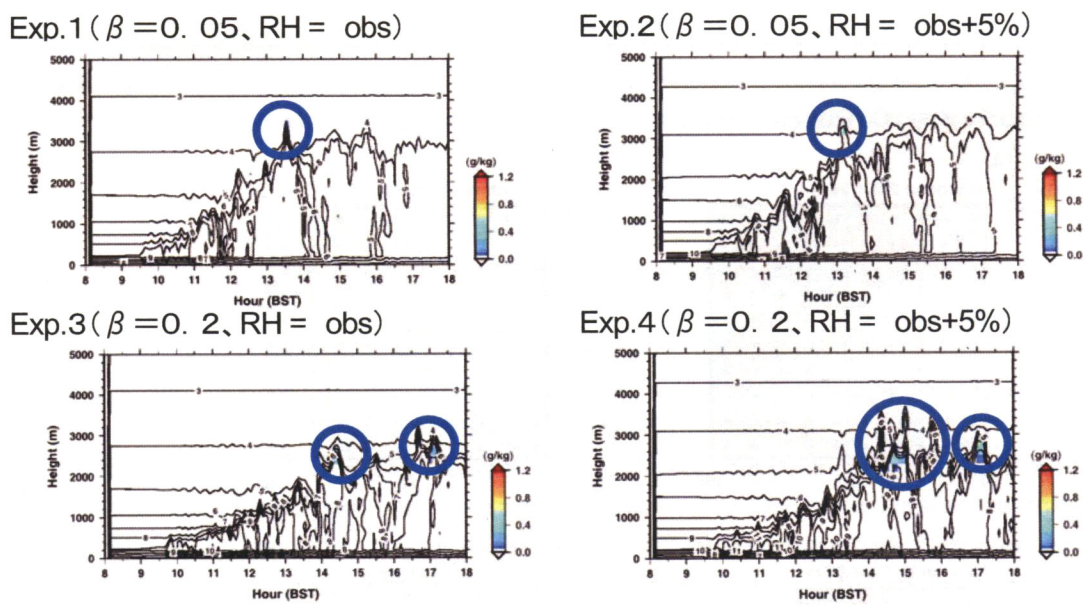

Fig. 3. Time-height sections of the cloud liquid water content and specific humidity in each experiment. The cloud liquid water contents are shown by colors and specific humidity is shown by the contour.

References

Nishikawa, M., T. Hiyama, A. Takahashi, W. Li, A. Higuchi, W. Liu, and Y. Fukushima (2007): Seasonal and diurnal changes of atmospheric boundary layer heights over Changwu, the Loess Plateau of China, Proceedings of 3rd International Workshop on Yellow River Studies, February 14-15, 2007 Kyoto, 69-72.

Owada, H., H. Ohmori, and J. Matsumoto (2005): Seasonal changes in wind systems relating to precipitation during the rainy season in the Loess Plateau, China, Geographycal Review of Japan, 78-8, 534-541.

Takahashi, A., T. Hiyama, M. Nishikawa, A. Higuchi, W. Li, W. Liu, and Y. Fukushima (2007): Vertical mixing of water vapor between the atmospheric boundary layer and free atmosphere over Changwu, the Loess Plateau of China, Proceedings of 3rd International Workshop on Yellow River Studies, February 14-15, 2007 Kyoto, 73-76.

Tsuboki, K. and A. Sakakibara (2001): Cloud resolving storm simulator, User's guide, 210pp.

Numerical simulations on local circulation and cumulus generation over the Loess Plateau in China

Masanori NISHIKAWA[1], Tetsuya HIYAMA[2], Kazuhisa TSUBOKI[2] and Yoshihiro FUKUSHIMA[3]

1) Graduate School of Environmental Studies, Nagoya University, Japan

2) Hydrospheric Atmospheric Research Center (HyARC), Nagoya University, Japan

3) Research Institute for Humanity and Nature (RIHN), Japan

1. Introduction

The previous study showed both surface wetness and vertical profiles of relative humidity affected cumulus generation using a numerical large eddy simulation (LES) of the atmospheric boundary layer (ABL) under a flat and homogeneous surface [*Takahashi* et al., 2007; this issue]. However, the Loess Plateau in China consists of dissected flat tablelands with steep gullies. Thus, the topographical effect on cumulus generation should be considered. Therefore, in order to estimate the topographical effect on cumulus generation, we conduct numerical simulation on the ABL development under the bottom boundary condition being the real-terrain. In this study, we describe the difference in the cumulus generation between under the flat-terrain and under the real-terrain. Then the structure of the local circulation induced by the ABL development is presented.

2. Model description

Four cases in numerical experiments conducted in this study are shown in Table 1. The bottom boundary conditions applied in the experiments were either the real-terrain or the flat-terrain. The flat-terrain condition means the flat and homogeneous surface at 1224 m a.s.l., and this altitude corresponds to the altitude of the tableland at the study site. Based on an observational study over the Loess Plateau [*Li et al.*, 2008], the evaporation efficiency (β) was set to 0.05 assuming a dry case, and 0.2 assuming a wet case. The topography of the real-terrain is depicted in Figure 1. The green area corresponds to the flat tableland ranging from 1200 to 1224 m a.s.l.. The tableland extends from northwest to southeast directions, and gullies whose depth is about 200 m existed northern and southern parts of the tableland. We set the center of the simulation domain as the observational site (35.24°N, 107.68°E) located on the tableland of the Loess Plateau. Hereafter we refer to flat-terrain run for Case 1 and Case 3, real-terrain run for Case 2 and Case 4.

The numerical model used for the experiment is the Cloud Resolving Storm Simulator (CReSS) which uses a 1.5-order turbulence kinetic energy (TKE) closure scheme [*Tsuboki and Sakakibara*, 2003]. Because the bottom boundary applies the real-terrain, we changed the settings from the previous report [*Takahashi* et al., 2007; this issue]. The major changes are as follows. The lateral boundary was set open boundary conditions. In order to take wide buffer region, the simulation

domain was spanned 50,000 m × 50,000 m × 11,292 m with a mesh of 500 × 500 × 110 points. In this study, the center domain of 20,000 m × 20,000 m × 11,292 m is used. Time step is set to be 0.5 s.

3. Results and discussion

Figure 2 shows the distribution of vertical integrated cloud liquid water over all integrated time. Cumulus clouds were generated near the top of updrafts. For flat-terrain run (Case 1, 3), small amount of cumulus clouds were generated. However, for real-terrain run (Case 2, 4), large amount of cumulus clouds were generated. If the evaporation efficiency was changed from 0.05 to 0.2 under the same bottom boundary (Case 1 → Case 3, Case 2 → Case 4), cloud liquid water increased. If the bottom boundary was changed from the flat-terrain to the real-terrain under the same evaporation efficiency (Case 1 → Case 2, Case 3 → Case 4), cloud liquid water drastically increased. The increment of cloud liquid water in the latter change was more than that in the former change. For real-terrain run, more cloud water appeared around the edge of the tableland, and thus cumulus clouds were generated in the upwind side of the edge of the tableland.

Structure of a local circulation induced by ABL development was investigated. Figure 3 shows horizontal cross-section of vertical and horizontal wind velocities for Case 1 and Case 2 obtained at 13:20 BST (Beijing Standard Time). For Case 1, updrafts showed the systematical distribution which had Bénard-Rayleigh type cellular convective structures, and compensated downdrafts appeared around the updrafts. For Case 2, updrafts developed around the edge of the tableland, and compensated downdrafts appeared around the gullies. In order to describe the detail structure of ABL, Figure 4 shows x-z cross-section of vertical wind velocity at 13:20 BST. At 0 km in the x axis, an updraft developed, and compensated downdrafts appeared at around the upwind or downwind. At 3 km height of upwind side of the updraft, weak return flow developed. This means a local circulation developed. The horizontal and vertical scales of the local circulation are about 2 km. The vertical scale could be corresponded to the ABL height.

4. Summary

In order to evaluate topographical effect on cumulus generations over the Loess Plateau in China, numerical simulations of ABL are conducted using CReSS. For real-terrain run, large amount of cumulus clouds were generated over the edge of the tableland. This process is explained as follows. Updrafts clearly developed around the edge of the tableland. Local circulations whose vertical scale corresponded to the ABL height were also developed. Because water vapor was accumulated on the tableland by local circulations and thermals, cumulus clouds clearly developed near the top of the updraft. It is concluded that the topography over the Loess Plateau plays an important role on small-scale cumulus generations. These simulation results also showed the topography is more crucial for cumulus generation than surface wetness.

References

Li, W., T. Hiyama, A. Takahashi, M. Nishikawa, N. Kobayashi, A. Higuchi, W. Liu and Y. Fukushima (2008), Seasonal variations in the surface fluxes and surface parameters over Loess Plateau in China, *Hydro. Process.*, revised.

Takahashi, A., T. Hiyama, M. Nishikawa and Y. Fukushima (2007), Impact of change in land surface condition on the development of the atmospheric boundary layer and cumulus clouds over the Loess Plateau in China －Numerical experiment－, Proceedings of YRiS meeting October 2007 (Ishikawa), (this issue).

Tsuboki, K. and A. Sakakibara (2003), Large-scale parallel compuing of cloud resolving storm simulator, *High Peformance Computing*, 243-359, Springer.

Table 1. Summary of the numerical simulation. β is evaporation efficiency.

Case	Case 1	Case 2	Case 3	Case 4
bottom boundary	flat-terrain	real-terrain	flat-terrain	real-terrain
β	0.05	0.05	0.2	0.2

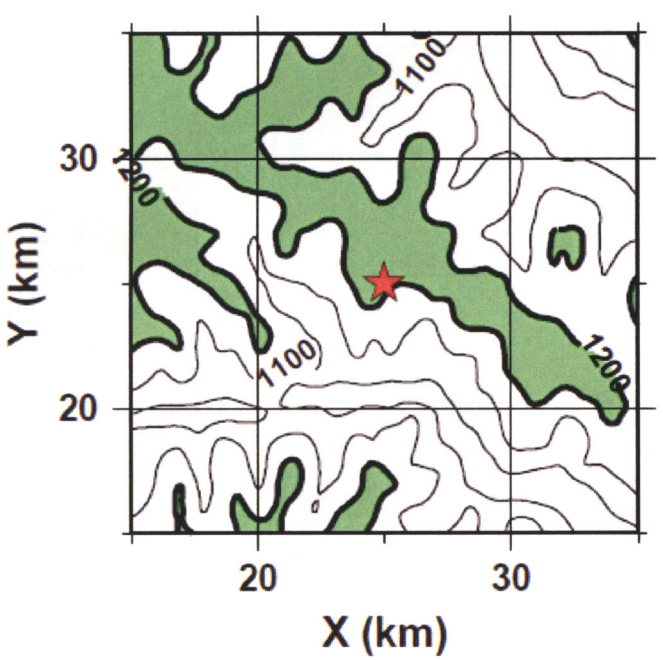

Figure 1. The topography of the real-terrain which is applied to bottom boundary conditions. The green area corresponds to the flat tableland of 1200 - 1224 m a.s.l. The red star represents the center of the simulation domain. (http://www2.jpl.nasa.gov/srtm/)

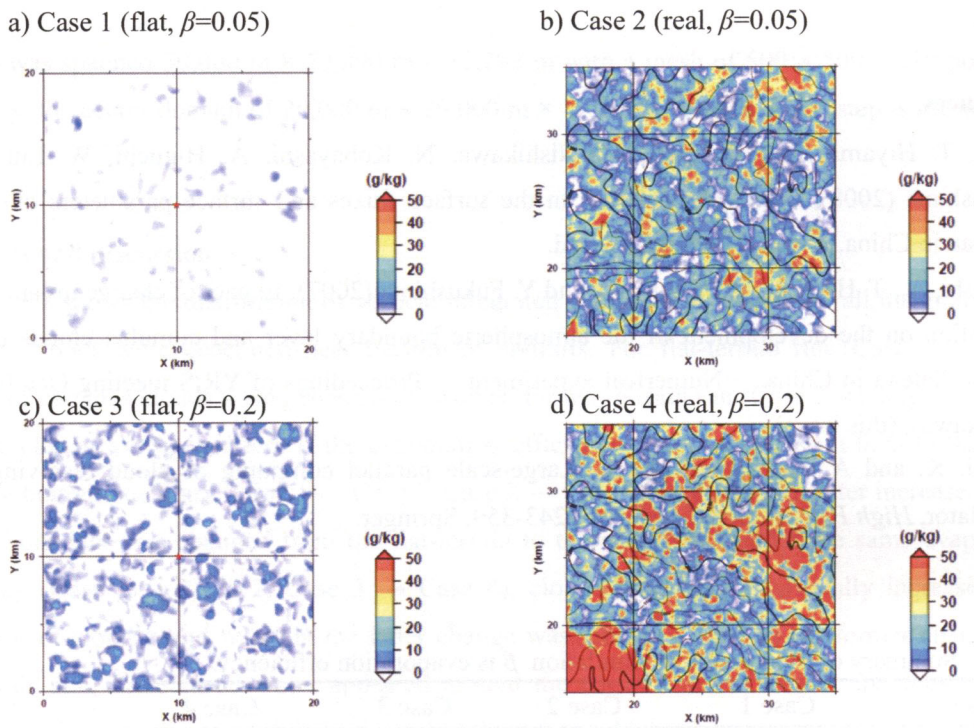

Figure 2. The distribution of vertical integrated cloud liquid water over all integrated time. The contour for real-terrain run is represented every 100 m.

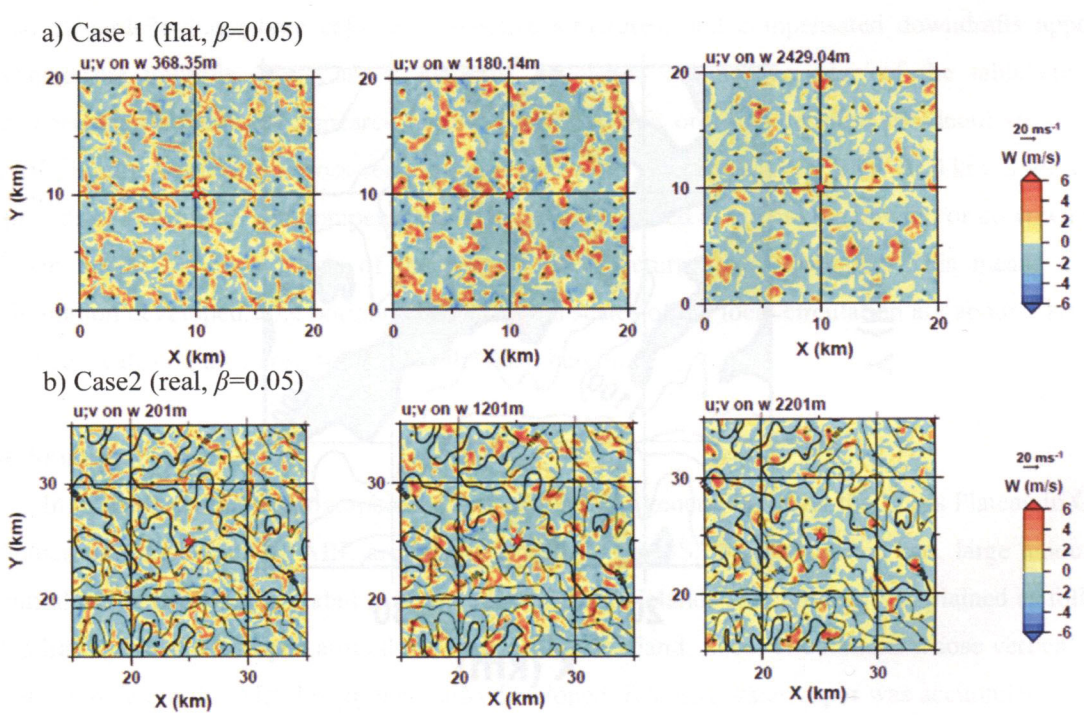

Figure 3. Horizontal section of vertical and horizontal wind velocities at 13:20 BST for a) Case 1 at 368.35 m height (left), 1180.14 m height (middle) and 2429.04 m height (right), b) Case 2 at 201 m height (left), 1201 m height (middle) and 2201 m height (right). Those heights stand for the heights from the tableland surface (1224 a.s.l.) The color represents vertical wind and the vector represents

horizontal wind.

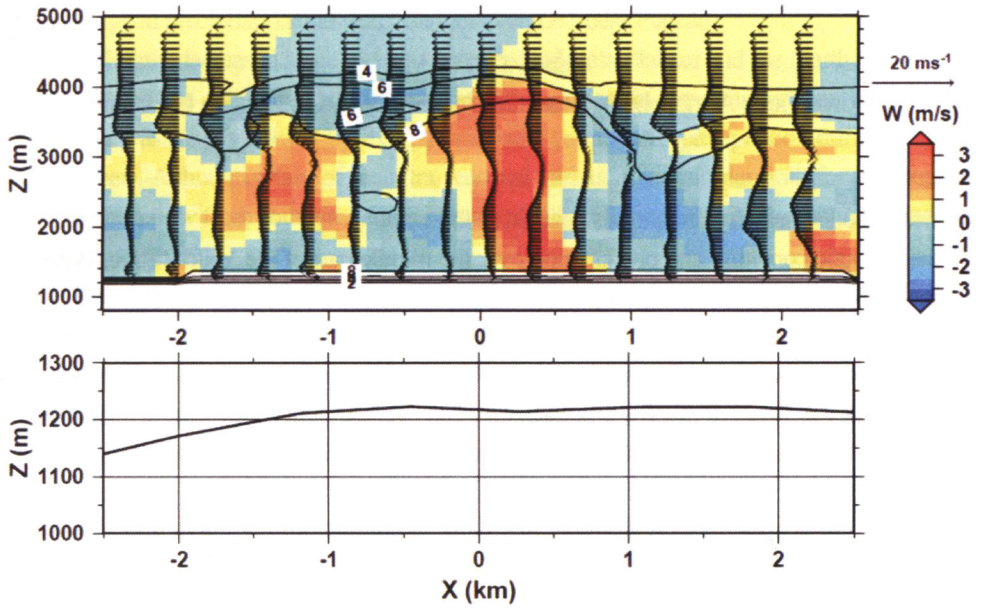

Figure 4. x-z cross-section of vertical and horizontal wind velocities at 13:20 BST for Case 2 (top), x-z cross-section of the altitude (bottom). The color represents vertical wind and vector represents horizontal wind. The contour line represents mixing ratio of every 2 g/kg. The value of 0 km in x-axis is the center of the simulation domain. z-axis is represented as a.s.l..

Research Activities of the ABL Team

Tetsuya HIYAMA
Hydrospheric Atmospheric Research Center (HyARC), Nagoya University

1. Motivations

The motivations of our research team are summarized as follows.

1) How did the synoptic condition and precipitation over the middle part of the Yellow River Basin change in the recent decades?
2) How did the land surface change in China affect for the synoptic condition and precipitation over the region?
3) Did the land surface and atmospheric boundary layer (ABL) actively influence for the precipitation system?
4) What are the primary differences of ABL processes between over the humid and semi-dry regions?
5) How does a sharp topography affect for the atmospheric turbulence within the atmospheric surface layer (ASL)?

2. Objectives

The ABL team established the following four objectives in order to attack the motivations described above.

1) To reveal inter-annual and intra-seasonal changes in precipitation amount and related convective activities over the Loess Plateau and the North China Plain.
2) To find any convective activities and precipitation systems affected by land surface and ABL processes over the Loess Plateau or the North China Plain.
3) To compare the diurnal and seasonal changes in the ABL developments over the humid and semi-arid regions.
4) To investigate topographical effects on the atmospheric turbulence and the local circulations appeared within the ABL over the Loess Plateau in China.

3. Observations and Data

3.1. Observations

We established an ABL observation system on a research field of the "Changwu Agro-Ecological Experimental Station over the Loess Plateau", which is located in southern part of the Loess Plateau in China (35.24 °N and 107.68 °E). The altitude of the station is 1224 m. The observation system consists of the following device (Hiyama et al., 2005):

1) Flux and Radiation Observation System (FROS), manufactured by Climatec, Inc., Japan.
2) Wind Profiler Radar (WPR), manufactured by Sumitomo Electric Industries, Ltd., Japan.
3) Microwave Radiometer (MR), manufactured by Radiometrics Corporation, USA.

The FROS provides turbulent fluctuations of three-dimensional wind speed, air temperature and humidity at the height of 2 m, 12 m, and 32 m. From these turbulent data, we evaluated surface sensible and latent heat fluxes. We selected those fluxes at 12 m and 32 m as regional values over this area. The WPR provides vertical profiles of mean wind velocity and wind direction together with those of echo intensity and Doppler spectral width. The MR provides vertical profiles of air temperature, relative humidity, and liquid water content.

3.2. Data

The following data were also used in this study.

1) NCEP/NCAR re-analysis data set.
2) Outgoing long-wave radiation (OLR) data set obtained from geostationary meteorological satellite (GOES 9).
3) Sounding data observed at Pingliang, which located at around 100 km northwest from Changwu station.

4. Results

4.1. Time-series change in precipitation and water budget over the Loess Plateau

Precipitation has slightly decreased since 1950s both over the Loess Plateau and the North China Plain, but it has no significant trend. On the other hands, the inter-annual variation in precipitation has been very large. This inter-annual variation was mainly caused by the intra-seasonal variation of precipitation during rainy season (July, August and September). Although phase of the intra-seasonal variation was similar both for wet year and dry year, amount of water vapor inflow from southern region was drastically different from each other (see details in the report of Fujinami, 2007; this issue).

The precipitation during rainy season is important for agricultural activities over the Loess Plateau. The available water (P – E), namely, difference in precipitation (P) and evapotranspiration (E), is positive during three months but negative in the others (see details in the report of Takahashi et al., 2007a; this issue). The amount of the available water (P – E) during the rainy season is much affected by that of precipitation (P), because E is conserved effectively by the dry surface layer of the loess.

4.2. Effects of land surface and ABL processes on the large-scale convective activities or precipitation systems

Variations in the latent heat flux over the plateau corresponded to those in precipitation during rainy season. Those dominant frequencies were around 4 or 5 days. This means that the overpass of cyclonic (disturbance) precipitation occur around 4 or 5 days intervals in the region. On the contrary, variations in the sensible heat flux had unclear and the dominant frequency was less than 4 days (see details in the report of Nishikawa et al., 2007a; this issue). This might be correlated with instantaneous formation of the dry surface layer of loess, as described above.

The daily maximum height of ABL was both affected by the surface sensible heat flux and the atmospheric stability in the middle and lower troposphere, which were the product of surface heating as well as intrusion of cold air mass over the region. Thus variations in the daily maximum height of ABL were affected by surface sensible heat flux as well as synoptic conditions (see also section 4.4).

Both in pre-rainy season and in rainy season (from April to July), land surface has occasionally enhanced cyclonic precipitation (or meso-scale convective activities). In 2005, the region has experienced 4 times in heavy rainfall at late afternoon, all of which exceeded 10 mm/hour in rainfall intensity. These heavy rainfalls have been brought by overpass of cold front. The cloud top height (i.e., brightness temperature) of the cold front, derived from a geostationary meteorological satellite (GOES 9), clearly showed diurnal variation (see details in the report of Nishikawa et al., 2007a; this issue).

4.3. Effects of land surface wetness and topography on regional-scale ABL development and cumulus generation

We employed a cloud resolving model (Cloud Resolving Storm Simulator; CReSS) developed in HyARC, Nagoya University, to perform sensitivity analyses of ABL and cumulus developments. In order to reveal effect of surface wetness on the ABL and cloud generation, we referred observed evapotranspiration efficiency using FROS (Li et al., 2008).

Over a virtually homogeneous flat terrain, surface wetness (or evapotranspiration efficiency) as well as relative humidity within the ABL are important for ABL and cloud generations. Lower surface wetness made mature ABL higher but generated cumulus less effective due to shortage of water vapor supply from the land surface. If the relative humidity was higher, cumulus generated more effectively (see details in the report of Takahashi et al., 2007b; this issue).

In contrast to this, over the real topography of the Loess Plateau, topographical effect is much higher than the effect of surface wetness for ABL development and cumulus generation. Topography of this region generates small-scale local circulation, in which vertical and horizontal scales are around a few kilometers (see details in the report of Nishikawa et al., 2007b; this issue). This scale might be correlated to the ABL height scale over the region.

4.4. Comparison of ABL processes between over a humid region and over the Loess Plateau

We compared seasonal ABL processes between over a Chinese humid region (Shouxian, Anhui province) and over the Loess Plateau (Changwu, Shaanxi province). Briefly, seasonal change in daily maximum height of ABL over the Loess Plateau was very unclear. This is mainly due to the following two reasons: 1) Land cover over tablelands of the plateau is very heterogeneous in addition to the existence of steep gullies. These land surface features contribute to complex seasonal march in the surface fluxes of sensible heat and latent heat, and thus to daily maximum height of ABL. 2) Weak subsidence (or capping inversion) appears during summer season over the area. This cooperates with thermals developing up to ABL tops or more (Hiyama et al., 2007). If atmospheric humidity became higher due to vertical or horizontal water vapor supplies, cumulus convection effectively enhanced.

4.5. Effect of topography on turbulence structures in atmospheric surface layer (ASL)

We present the power spectra of wind velocity and the cospectra of momentum and heat fluxes observed for different wind directions over flat terrain and a large valley on the Loess Plateau. The power spectra of vertical (w) wind speed downwind of the valley had similar shape as previous studies. Thus topographical effect for sensible and latent heat fluxes will not be large in the region (Li et al., 2007).

The power spectra of longitudinal (u) and lateral (v) wind speeds satisfy the -5/3 power law in the inertial subrange, but do not vary as observed in previous studies within the low frequency range. The u spectrum measured at 32m height for flow from the valley shows a power deficit at intermediate frequencies, while the v spectrum at 32m downwind of the valley reaches another peak in the low frequency range at the same frequency as the u spectrum. The corresponding peak wavelength is consistent with the observed length scale of the convective ABL at the site. The v spectrum for flat terrain shows a spectral gap at mid frequencies while obeying inner layer scaling in its inertial subrange, suggesting two sources of turbulence in the surface layer.

4.6. Studies on satellite remote sensing over the Loess Plateau

Surface heterogeneity induces uncertainty in pixel-wise land surface temperature (LST). Spatial scaling may account for the uncertainty, however, different approaches lead to differences in scaled values. Satellite-retrieved LST may be representative of the pixel-wise LST and useful for scaling analysis, but the limited accuracy of retrieved values adds uncertainty into the scaled values. Based on the Stefan-Boltzmann law, we proposed scaling approaches for LST over the Loess Plateau including flat and relief areas to explore the combined uncertainties in scaling using satellite-retrieved data. To take advantage of simultaneous, multi-resolution observations at coincident nadirs by the Advanced Spaceborne Thermal Emission Reflection Radiometer (ASTER) and the MODerate-resolution Imaging Spectroradiometer (MODIS), LST products from these two sensors were examined for part of the Loess Plateau. 90-m ASTER LST data were scaled up to 1 km using the proposed approaches, and variation in the LST was generally reduced after scaling. Amongst the sources of uncertainties, surface heterogeneity (emissivity) and different scaling approaches resulted in very minor differences. Terrain features, taken as an areal weighting factor, had negligible effects on the upscaled value. Limited accuracy of the retrieved LST was the major uncertainty. The overall LST increased 0.6 K on average with correction for terrain-induced angular effect and 0.4 K for both angular and adjacency effects over the study area. Accounting for terrain correction in scaling is necessary for rugged areas (Liu et al., 2006).

The ratio of latent heat flux to available energy, termed the evaporative fraction (EF), and the ratio of latent heat flux to downward shortwave radiation (ES), are two useful evaporative flux ratios (EFR) for estimating daily evaporation. Both EF and ES remain relatively constant during daytime, but their value varies from day to day. It is yet unclear if long-term change signals are detectable given the uncertainty associated with the diurnal variations. Using EF and ES data obtained during the major rainy seasons on a tableland of the Loess Plateau, we showed that day-to-day variability in the EF or ES was detectable given diurnal variation. The EF and ES showed slight increasing trends from midmorning to afternoon, but the ES was superior to the EF for satellite-based monitoring of

long-term evaporation trends (Liu and Hiyama, 2007) (Fig.1).

5. Unresolved issues

The effect of land surface change on the precipitation trend over the region could not be resolved in this study. This is mainly because of difficulty on separation of land surface effect from the other meteorological factors such as synoptic-scale influences and effects of meso-scale convective activities.

Use of AGCMs (Atmospheric General Circulation Models) has been employed to reveal the land surface effect on the precipitation feedbacks. However such previous studies mainly conducted numerical simulation virtually changing the whole (continental) land surface into the bare soil surface or deserts. Thus the scale issue should be governed in such land-atmosphere interactions. Additionally, previous AGCMs studies have ignored feedback processes of land-atmosphere interaction. Future studies will be encouraged involving such feedback processes of land-atmosphere interaction.

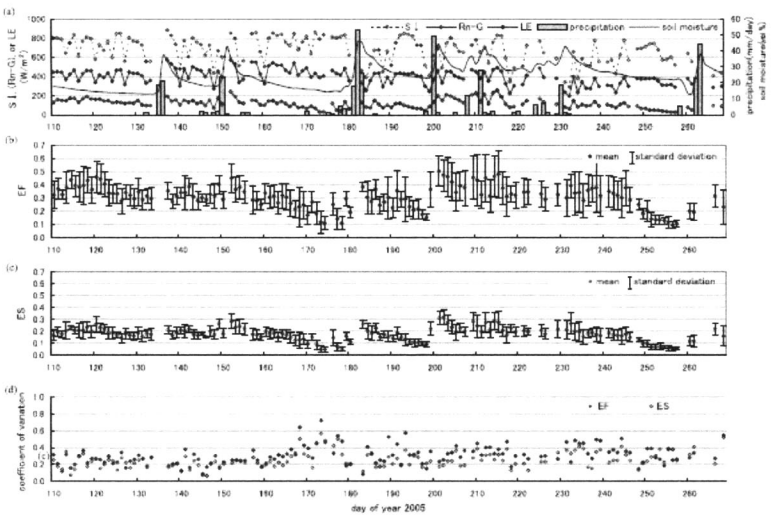

Fig. 1 Seasonal changes in a) downward short-wave radiation (S ↓), available energy (Rn – G), daily precipitation, surface soil moisture, b) EF, c) ES, and d) coefficient of variations of EF and ES, observed at the "Changwu Agro-Ecological Experimental Station over the Loess Plateau" from DOY (day of year) 110 to 270 in 2005. All of the values were daily-bases (Liu and Hiyama, 2007).

6. Publication list

The published papers obtained from the ABL team were listed below.

1) Hiyama, T., Takahashi, A., Higuchi, A., Nishikawa, M., Li, W., Liu, W. and Fukushima, Y. (2005): Atmospheric Boundary Layer (ABL) observations on the "Changwu Agro-Ecological Experimental Station" over the Loess Plateau, China. *AsiaFlux Newsletter*, **16**, 5-9.

2) Liu, Y., Hiyama, T. and Yamaguchi, Y. (2006): Scaling of land surface temperature using satellite data: A case examination on ASTER and MODIS products over a heterogeneous terrain area. *Remote Sensing of Environment*, **105**, 115-128.

3) Kobayashi, N., Hiyama, T., Fukushima, Y., Lopez, M.L., Hirano, T. and Fujinuma, Y. (2007): Nighttime transpiration observed over a larch forest in Hokkaido, Japan. *Water Resources Research*, **43**, W03407, doi:10.1029/2006WR005556.

4) Higuchi, A., Hiyama, T., Fukuta, Y., Suzuki, R. and Fukushima, Y. (2007): The behaviour of a surface temperature / vegetation index (TVX) matrix derived from 10-day composite AVHRR images over monsoon Asia. *Hydrological Processes*, **21**, 1157-1166.

5) Li, W., Hiyama, T. and Kobayashi, N. (2007): Turbulence spectra in the near-neutral surface layer over the Loess Plateau in China. *Boundary-Layer Meteorology*, **124**, 449-463.

6) Liu, Y. and Hiyama, T. (2007): Detectability of day-to-day variability in the evaporative flux ratio: A field examination in the Loess Plateau of China. *Water Resources Research*, **43**, W08503, doi:10.1029/2006WR005726.

7) Li, W., Hiyama, T., Takahashi, A., Nishikawa, M., Kobayashi, N., Higuchi, A., Liu W. and Fukushima, Y. (2008): Seasonal variations in the surface fluxes and surface parameters over the Loess Plateau in China. *Hydrological Processes*, (revised).

References

Fujinami, H. (2007): Synoptic-scale intraseasonal variation and its effect on interannual variation in precipitation over the middle-lower reaches of the Yellow River basin. Proceedings of YRiS meeting October 2007 (Ishikawa), (this issue).

Hiyama, T., Takahashi, A., Higuchi, A., Nishikawa, M., Li, W., Liu, W. and Fukushima, Y. (2005): Atmospheric Boundary Layer (ABL) observations on the "Changwu Agro-Ecological Experimental Station" over the Loess Plateau, China. *AsiaFlux Newsletter*, **16**, 5-9.

Hiyama, T., Takahashi, A., Nishikawa, M., Liu, Y., Tanaka, H., Higuchi, A., Liu, W. and Fukushima, Y. (2007): Progress in hydro-meteorological studies in Changwu, the Loess Plateau of China. Proceedings of third International Workshop on Yellow River Studies, Research Institute for Humanity and Nature, 61-64.

Li, W., Hiyama, T. and Kobayashi, N. (2007): Turbulence spectra in the near-neutral surface layer over the Loess Plateau in China. *Boundary-Layer Meteorology*, **124**, 449-463.

Li, W., Hiyama, T., Takahashi, A., Nishikawa, M., Kobayashi, N., Higuchi, A., Liu W. and Fukushima, Y. (2008): Seasonal variations in the surface fluxes and surface parameters over the Loess Plateau in China. *Hydrological Processes*, (revised).

Liu, Y., Hiyama, T. and Yamaguchi, Y. (2006): Scaling of land surface temperature using satellite data: A case examination on ASTER and MODIS products over a heterogeneous terrain area. *Remote Sensing of Environment*, **105**, 115-128.

Liu, Y. and Hiyama, T. (2007): Detectability of day-to-day variability in the evaporative flux ratio: A field examination in the Loess Plateau of China. *Water Resources Research*, **43**, W08503, doi:10.1029/2006WR005726.

Nishikawa, M., Hiyama, T., Takahashi, A., Li, W., Fujinami, H., Higuchi, A. and Fukushima, Y. (2007a): Seasonal changes in the conditions of atmospheric boundary layer, land surface, and synoptic field over the Loess Plateau in China. Proceedings of YRiS meeting October 2007 (Ishikawa), (this issue).

Nishikawa, M., Hiyama, T., Tsuboki, K. and Fukushima, Y. (2007b): Numerical simulations on local circulation and cumulus generation over the Loess Plateau in China. Proceedings of YRiS meeting October 2007 (Ishikawa), (this issue).

Takahashi, A., Hiyama, T., Nishikawa, M., Higuchi, A. and Fukushima, Y. (2007a): Vertical transport of water vapor and the atmospheric water budget over the Loess Plateau in China - Comparison of the cases in 2005 and 2006 -. Proceedings of YRiS meeting October 2007 (Ishikawa), (this issue).

Takahashi, A., Hiyama, T., Nishikawa, M. and Fukushima, Y. (2007b): Impact of change in land surface condition on the development of the atmospheric boundary layer and cumulus clouds over the Loess Plateau in China - Numerical experiment -. Proceedings of YRiS meeting October 2007 (Ishikawa), (this issue).

Relation of in situ Hyper-Spectral Radiometer Data with Phenomena Observed by Other Variables – Comparison of *in situ* data with MODIS images –

Atsushi Higuchi [1], Tetsuya Hiyama [2], Atsuhiro Takahashi [3], Masanori Nishikawa [2], Wei Li [4], Wenzhao Liu [5], and Yoshihiro Fukushima [3]

1: Center for Environmental Remote Sensing (CEReS), Chiba University, Japan

2: Hydrospheric Atmospheric Research Center (HyARC), Nagoya University, Japan

3: Research Institute for Humanity and Nature (RIHN), Japan

4: Department of Civil & Environmental Engineering, Duke University, USA

5: Institute of Soil and Water Conservation (ISWC), Chinese Academy of Sciences (CAS), China

1. Progress summary

In the one of activities in ABL team in YRiS (Hiyama et al., 2005), we installed in-situ type hyper-spectral radiometers in Changwu station, located on Loess Plateau, China. Observation started since May 2004, good quality of dataset was collected. We summarized the preliminary results derived from hyper-spectral radiometers and related variables as follows:

a. Seasonal variation in spectral radiance over the winter wheat represented well the seasonality of wheat phenology (stages of growth, mature, emergence, tillering and the end of wintering). In particular, red position moving to shorter wavelength (so-called blue shift of red edge) detected both years of 2005 and of 2006. Such phonological reaction of the winter wheat corresponded well the seasonality of NEP by eddy covariance variables.

b. Based on the time series of hyper-spectral radiometer's data, space-borne optical sensor's (e.g., NOAA/AVHRR, EOS/MODIS, Landsat/TM, ETM+) spectral reflectance could be simulated. We simulated each space-borne sensor's spectral reflectance and NDVI for the validation of NDVI obtained from different sensors. Intercomparisons of several NDVI did not show the significant differences based on spectral difference of each sensor, except AVHRR based NDVI (under-estimation compared with other NDVI). These results indicated that, at least NDVI based, observation wavelength differences among space-borne sensors are not critical than the effects of observation time (pre-noon or after-noon) and of bi-directional reflectance function, etc.

2. Comparison with MODIS

Based on previous our analysis, we focus on the spectral characteristics of MODIS. Usually, channels with spatial resolution of 250m and 500m (same as Landsat/ETM+) were used for the terrestrial studies (red lines in Fig. 1, blue, green, red and near-IR). MODIS is also sensible (more channels) in visible and near-IR wavelength (green lines in Fig. 1) with 1-km resolution for the target of ocean color and aerosol detection studies.

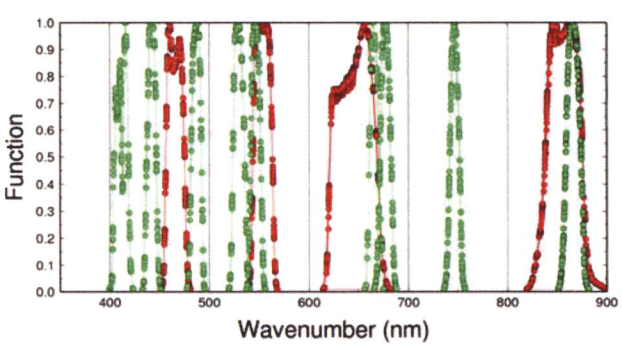

Fig.1 Weighting functions of Terra/MODIS in the wavelength of 350 – 900 nm. Red lines represent 250 & 500m res. Channels, green's are 1km res. Ch.

We simulated MODIS channels account for the weighting function of each channel from in situ

hyper-spectral data. Figure 2 shows seasonal variation in simulated MODIS Ch.13 (red1, 658 – 674 nm, a blue line), Ch. 14 (red2, 668 – 685 nm, a green line) and Ch.15 (near-IR, 739 – 754 nm, a red line) in 2005. Ch. 15's line in Fig. 2 had a peak around DOY120, decreased slightly until DOY150. However spectral radiance in Ch.15 was almost same during DOY150 to DOY 180.On the other hand, seasonal variation in Ch.13 and Ch. 14 (red) behaved quite similarly. To pay an attention of small difference in these two channels, Ch.14's value was slightly higher than that of Ch.13 during DOY150 to DOY180. Such small difference within the wavelength of red represents the phase change of winter wheat's phenology (blue shift of red edge). If MODIS's 1-km channel (Ch. 13 & 14) detectors measure correctly not only over the ocean also over the land, difference between Ch.13 and Ch.14 derived from in situ measurement is detectable (max. 7 W m^{-2} $microm^{-1}$). Thus we checked MODIS images during DOY150 to DOY160, particularly focus on 1-km resolution channels. Figure 3 shows examples of MODIS image including Changwu station (represented as star symbol). In the case of Ch. 8 (blue, 403 – 422 nm), images ware reflected day to day variance well (high spectral radiance captured clouds). Unfortunately, Ch.13's images (target channel) had almost same values over the whole of each image (both DOY153 and DOY158). Such responses imply that Ch.13 in MODIS could not capture the state of nature over the land. 1-km's red channels in MODIS specialized for monitoring ocean color, thus dynamic ranges in red are too narrow than that in other wavelength.

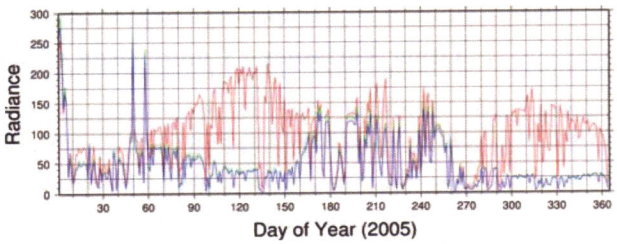

Fig. 2 Seasonal variation in estimated radiance of Terra/MODIS Ch.13 (blue line), Ch.14 (green line) and Ch. 15 (red line), derived from *in situ* hyper-spectral radiometer

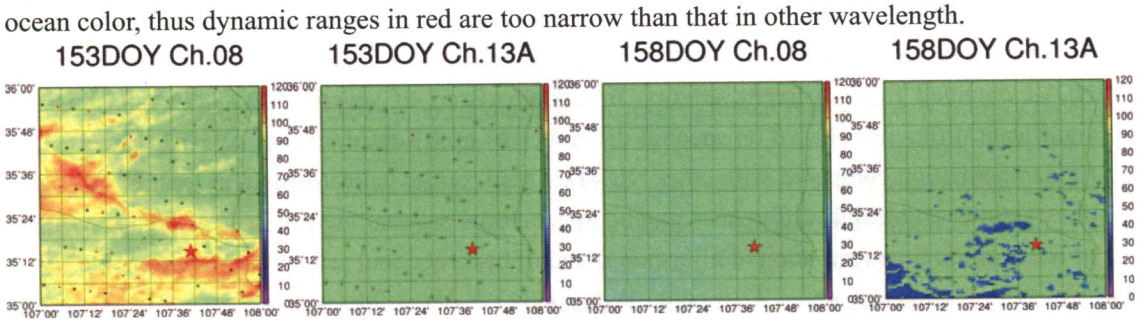

Fig. 3 Examples of Terra/MODIS images in Ch.08 (blue), Ch.13A (red) over Changwu station (marked red star symbol).

3. Concluding Remarks

Under the current situation, unfortunately, difference within red wavelength can not apply the space-borne sensor's study. In addition, next operational polar orbit satellites (NPOESS) plan only one channel will sensible within red. However, on the research objective bases, possibility of fine spectral observation on the visible wavelength are still remained. We need more efforts to recognize the efficiency of red channels by the accumulations of ground-based studies.

References

Hiyama, T., A. Takahashi, A. Higuchi, M. Nishikawa, W. Li, Y. Fukushima (2005): Atmospheric boundary layer (ABL) observations on the "Changwu Agro-Ecological Experimental Station" over the Loess Plateau, China, AsiaFlux Newsletter, No.16, 5-9.

Land Cover Change Analysis over Yellow River Basin by Remote Sensing

Masayuki MATSUOKA (Faculty of Agriculture, Kochi University)
Yoshihiro FUKUSHIMA, Tadahiro HAYASAKA (RIHN)
Taikan OKI (Institute of Industrial Science, University of Tokyo)
Yoshiaki HONDA (Center for Environmental Remote Sensing, Chiba University)

1. Introduction

Remote sensing is efficient tool for consecutive monitoring the wide region such as whole basin of the Yellow River in China in this study. The purpose of this study is to analyze the change of land cover on the Yellow River basin for two decades since 1980 using several kind of remote sensing data. This report gives three relevant topics: increase of agricultural area in Qingtongxia irrigation district, change of vegetation in tributary of the Yellow River, and change of land cover in Loess Plateau.

2. Methodology

2.1 Increase of agricultural area in Qingtongxia irrigation district

The time series of AVHRR onboard NOAA satellite were mainly used to detect the change of agricultural area. The spatial resolution of AVHRR is relatively low as one kilometer compared to scale of agricultural field, however, the pseudo improvement of spatial resolution was applied by means of high resolution (30 meters) sensor of ETM+ onboard Landsat. The outline of the method is shown in figure 1. Annual maximum value of Normalized Difference Vegetation Index (NDVI) derived from AVHRR showed positive correlation with fraction of agricultural area in one square kilometer calculated from land cover map generated from ETM+. This means that percentage of agricultural area within one AVHRR pixel is able to estimated, and the change of agricultural area could be detected from time series of annual maximum NDVI. Time series of annual maximum NDVI were generated from original raw data for 17 years from 1984 to 2000. Every two years of data are shown in figure 2. Linear relation between annual maximum NDVI and fraction of agricultural area, [fraction of agricultural area] = 2.54 * [annual maximum NDVI] - 0.33, was applied to this time series. The result was compared to county based agricultural area derived from census in yearbook of Ningxia Hui Autonomous Region.

2.2 Change of vegetation in tributary of the Yellow River

It was suggested by previous results in hydrological simulation in this study that vegetation, mainly grass or shrub type vegetation, has been increased in Loess Plateau. Therefore, it has been checked using time series of AVHRR data. The Pathfinder AVHRR Land dataset, which has spatial resolution of eight kilometer, was used in this analysis. The annual maximum NDVI was generated from daily product by averaging of five samples from second to sixth maximum NDVI in a year because erroneous high NDVI exist in the dataset. The four sample area, which is shown in figure 3, were extracted from the data along the major tributaries of the Yellow River, Wuding, Fen, Luo, and Qin river.

2.3 Change of vegetation in Loess Plateau

Land cover classification was applied using four kilometer AVHRR data, which were generated from original raw data, for the years of 1982, 1991, and 2000. Only three land cover categories, barren, open shrubland, and grassland, were extracted on the Loess Plateau. Other land cover was followed the other classification result derived using MODIS data. The detail of the classification method is included in the reference [1].

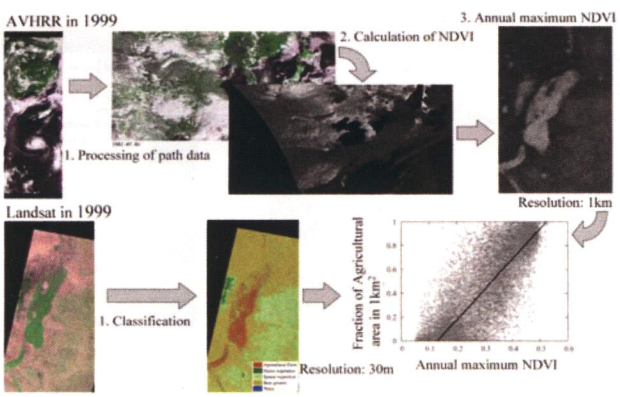

Fig. 1 Methodology of pseudo improvement of resolution

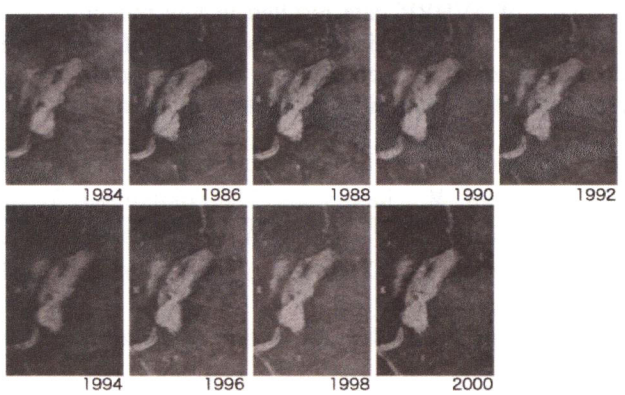

Fig, 2 Time series of annual maximum NDVI

3. Results and discussions

3.1 Increase of agricultural area in Qingtongxia irrigation district

Estimated time series of agricultural area is shown in figure 4, top figure is estimation using AVHRR and bottom is census value. Estimated time series has unrealistic fluctuation by year, compared to census value. Since the linear

equation was derived from the data in 1999, good agreement was appeared in this year. On the other hand, the other years especially from 1993 to 1995 showed large decrease of the area. This is mainly due to the fluctuation of annual maximum NDVI, rather than due to the true variation of the agricultural area. Annual maximum NDVI has large inter-annual variation owing to the following two reasons. One reason is shortage of the sample. The AVHRR used in this analysis was received by University of Tokyo receiving station located in Tokyo, that is, Qingtongxia is western border of the receivable coverage. The enough sample for annual maximum calculation is not received for this region. The other reason is poor accuracy of geometric correction. The low geometric accuracy resulted in low contrast of the annual maximum NDVI image. Therefore, extremely low agricultural area was estimated especially in the years around 1994.

3.2 Change of vegetation in tributary of the Yellow River

The time series of annual maximum NDVI over four tributaries of the Yellow River, which was extracted from Pathfinder dataset, is shown in figure 5. Five lines in each figure indicates the NDVI value for the sample of 10, 30, 50, 70, 90 percent in the region. All figures indicates large inter-annual variation of NDVI, it is same as previous analysis. Continuous increase of NDVI is appeared only in Wuding river region, but almost stable (except inter-annual variation) for other region, in the broad view.

3.3 Change of land cover in Loess Plateau

Land cover classification over Loess Plateau in 1982, 1991, and 2000 are shown in figure 6. Relatively larger increase of grassland is appeared in northern part of Loess Plateau between 1982 and 1991. This suggest the possibility of the increase of the vegetation mainly due to the reforestation implemented in 1970s and 80s, even though the inter-annual variation of the vegetation is larger in this region. The further analysis is needed for this point.

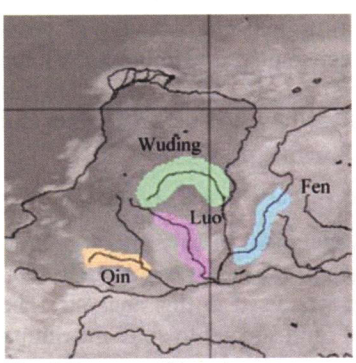

Fig. 3 Four sample region

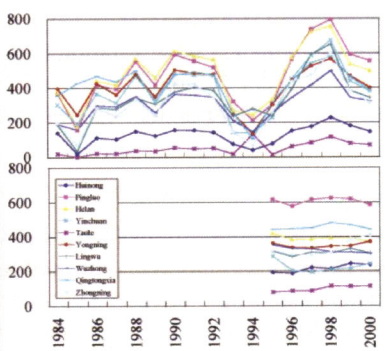

Fig. 4 Time series of Agricultural area (top: this study, bottom: census)

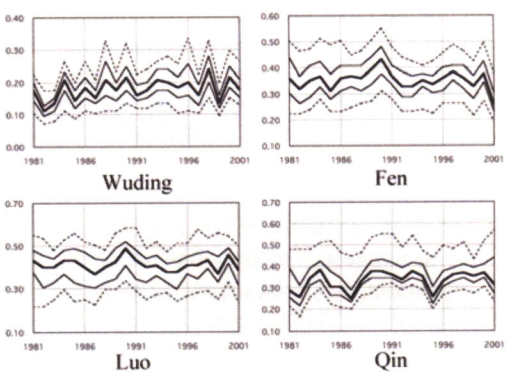

Fig. 5 Time series of annual maximum NDVI

4. Conclusion

Three topics, Increase of agricultural area in Qingtongxia irrigation district, change of vegetation in tributary of the Yellow River, and change of land cover in Loess Plateau, were reported concerning the land cover change of the Yellow River basin. Though the large inter-annual variation of vegetation and low processing accuracy of AVHRR data resulted in low reliability of land cover change in both analysis, Obvious change of land cover was not detected from all of three analyses. The result of hydrological model reported in this symposium shows similar conclusion.

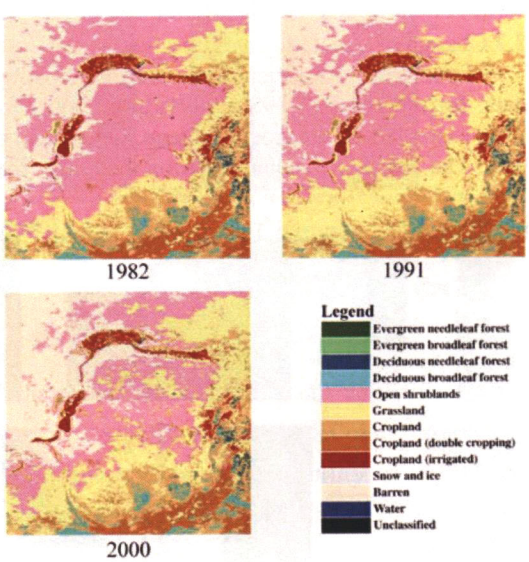

Fig. 6 Land cover map of Loess Plateau

Reference:

[1] Matsuoka, M., Hayasaka, T., Fukushima, Y., and Honda, Y., "Land cover in East Asia classified using Terra MODIS and DMSP OLS products", International Journal of Remote Sensing, Vol. 28, Nos. 1-2, pp. 221-248, 2007.

The Climate Change of Yellow River Basin in recent years

Jianqing Xu (E-mail: jxu@jamstec.go.jp)

Frontier Research Center for Global Change

Japan Agency for Marine-Earth Science and Technology

1. Precipitation

The climate of the Yellow River basin is complicated due to its complex topography. The area from the water resources (34°N, 97°E, altitude 4500m) in the Tibet Plateau to Lanzhou(36°N, 104°E, altitude 1560m) belongs to Tibet monsoon climatic zone. From Lanzhou to its east, the climate type is the North temperate or subtropical monsoon zone. Siberian high controls the whole area in the winter season, and it prevails westerlies with few precipitation, dry and cold temperature. In the summer time, the subtropical high becomes strong in this area, leads to plenty of water vapor blowing from the ocean, and results in the intensive rainfall. Headwater area of high-altitude Tibetan Plateau has a lot of snowfall, the snow is an important water resources. The water from headwater area covers 56% runoff of the entire basin. From the northwest to the southeast, the Precipitation decreases gradually. The largest precipitation area is located in the north side of the Qinling mountains, and its average annual precipitation is 800 mm. The smallest precipitation area is the south side of Yinshan mountains, and its annual precipitation averaged as 100 to 200 mm. Other places is around 400 to 600 mm. Half amount of those precipitation occurs in June, Sept. and Aug. Meanwhile, the lowest precipitation season is in Dec. Jan., and Nov., only 3% of annual precipitation occurs in this period. Other characteristic of the precipitation in the Yellow River basin is its large fluctuations from year to year. The ratio of the maximum to minimum values is 1.7 to 7.5.

2. Temperature

From southeast to northwest of the Yellow River basin, the air temperature decreases gradually while the daily range of the temperature becomes larger. The annual mean surface air temperature in the water resource area of the Yellow River is 1 - 8℃, from the water source area to Lanzhou is 8 - 14℃, Lanzhou to the Loess Plateau area of Taihang Mountains (35-37° N, 114° E) ranges 12-14℃, and from Taihang Mountains to the Bohai estuary of the Yellow River shows 12 - 14℃. The highest temperatures are happened in July, and ranges 20 - 29℃ depending on the location. The minimum temperatures is in January, monthly mean temperatures are lower than 0 ℃ in most part of the

Yellow River basin. Daily range of temperature is 10 - 15 ℃. It becomes dry from Lanzhou to the west, and the daily range shows 13 - 16.5℃.

3. Wetness

From the water resource area of the Yellow River to Lanzhou, the precipitation is small, relative humidity is around 60%, it is dry and the potential evaporation (Kondo and Xu, 1997) is large. The potential evaporation is 800-1300mm (Xu et al 2005), this value is lager than that of Japan, the potential evaporation is 600-1100mm in Japan. The potential evaporation is small in the Qinling mountains area, and increases to northwest and northeast gradually. This distribution of the potential evaporation is as similar as the distribution of observed pan evaporation (Xu et al 2005). Pan evaporation ranges 1000-2000mm in the basin. In the northwest part of the Yellow River basin, the precipitation is as small as 100-200mm, solar radiation is large, landsurface covers with desert and bare soil. Most part of the energy of the net radiation flux is consumed by sensible heat flux, and the boundary layer is heated in this region (Kondo and Xu, 1997).

The ratio of potential evaporation to precipitation was defined as the wetness index (Kondo and Xu, 1997. Xu, 2001. Xu et al., 2005). Humid areas are where the wetness index lager than 1.0, semi-humid areas the wetness index range 0.3-1.0, semi-arid 0.1-0.3, arid areas are less than 0.1. The southeast part of the basin belongs to humid or semi-humid area, and it becomes arid from southeast to northwest gradually. The vegetation corresponds with the distribution of wetness index very well (Xu et al 2005, Suzuki et al 2006).

4. The climate change in recent years

Figure 1 shows the temperature change in the Yellow River basin during 1960-2001.Just like other regions of the world, the temperature on the basin is increased in recent years too. Maximum and minimum temperatures also show increasing trends. Except the part of the areas in Shanxi and Shan'xi provinces, the daily ranges became small in the period.

The changes of precipitation show decreasing trend excepting a small area in the Yellow River resource. Cloud amount also decreased. From resources area to the Loess Plateau area of Taihang Mountains, the potential evaporation deceased and it increased from the eastside of the Taihang Mountains to the Bohai estuary of the Yellow River.

The change of the wetness index summarized the all of the change items mentioned above. From the water resource area to Lanzhou, the climate became humid in recent years. Humid or arid

changings in the other regions has influenced by two reasons, one is natural variability and the other is human activity. The situation is different from area to area. It is reported that the LAI became larger in the irrigation areas of the Yellow River basin, this kind of change may due to the economic development in recent years in China.

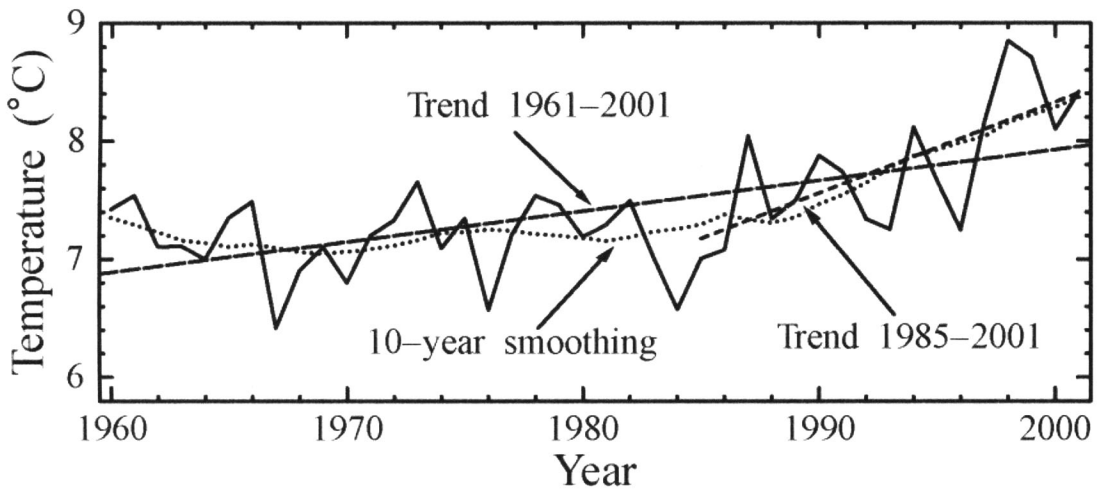

Fig. 1 The temperature change in the Yellow River basin during 1960-2001. Solid line is the temperature change from 1960 to 2001. Long broken line the trend during 1960-2001, short broken line the trend in 1985-2001. Dotted line is the 10-year smoothing average during the whole period.

Reference

China Meteorological Agency, Monthly data report of the surface observation, 1960-2000

Kondo, J., (1997), Hydrological meteorology in Japan (5) potential evaporation and wetness index. J. Japanese Soc. Hydrol. Water Resour., 10(5), 450-457.

Kondo, J., and J. Xu, (1997a), Seasonal variations in the heat and water balances for non-vegetated surfaces. J. Appl. Meteor., 36, 1676-1695.

Kondo, J., and J. Xu, (1997b), Potential evaporation and climatological wetness index, Tenki, 44(12), 875～883.

Suzuki, R., J. Xu, and K. Motoya (2006) Global Analyses of satellite-derived vegetation index related to climatological wetness and warmth, International Journal of Climatology, 26, 425-438.

Xu, J., S. Haginoya, K. Saito, and K. Motoya (2005) Surface heat balance and pan evaporation trends in Eastern Asia in the period 1971-2000. Hydrological Processes, vol. 19, 2161-2186, DOI:10.1002/hyp.5668.

Xu, J., (2001), An analysis of the climatic changes in Eastern Asia using the potential evaporation. J. Japanese Soc. Hydrol. Water Resour., 14(2),151～170.

Impact of Hetao Irrigation District on the Formation of Clouds in the Vicinity of the Yellow River in Summer

Hiroaki Kawase, Takao Yoshikane, Masayuki Hara (FRCGC), Tomonori Sato (CCSR), Shingo Ohsawa (Weathernews Inc.), and Fujio Kimura (University of Tsukuba/FRCGC)

1. Introduction

Land use sometimes changes rapidly due to the effects of natural processes as well as anthropogenic forcing. Irrigated farmlands are one of the most important anthropogenic land use changes. The Hetao Irrigation District in western Inner Mongolia, China, is one of the most extensive irrigations in Asia (Figure 1). It is surrounded by the Langshan Mountains, the northern Loess Plateau, and the Ulan Buh Desert. Most of the cultivated land is irrigated using the water resources of the Yellow River. The irrigation district creates a prominent heat contrast along its boundary.

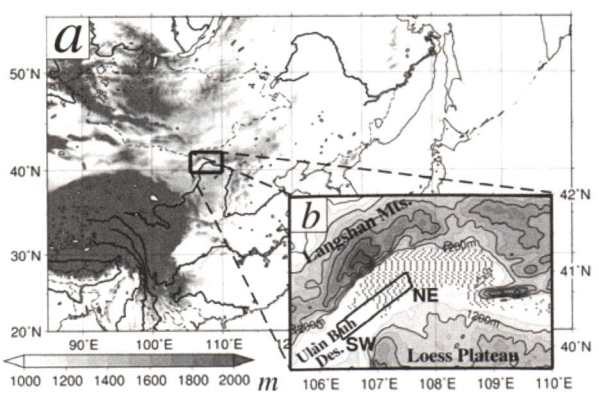

Fig. 1 (a) Map of East Asia. (b) Topography around the Hetao Irrigation District and a simplified irrigated area (dotted area) in the simulation.

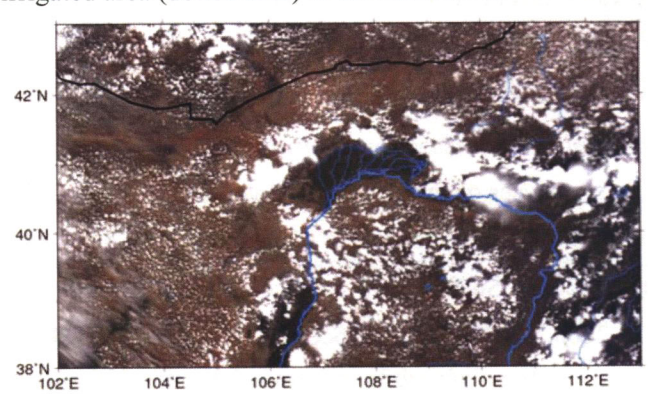

Fig. 2 True color satellite snapshots observed by MODIS/AQUA at 14:10 LST on 4 August 2005. Hetao Irrigation District is located at the center of the figure. Blue lines show rivers and blue thick line shows the Yellow River.

By a statistical analysis of satellite images, Sato et al. [2007] indicated that the frequency of cloud formation is lower over the Hetao Irrigation District than over the surrounding area. Figure 2 shows a true color snapshot on 4 August 2005 obtained with the Moderate Resolution Imaging Spectroradiometer (MODIS) on the Aqua satellite. Numerous clouds are evident around the Hetao Irrigation District although almost no clouds appear there. Sato et al. [2007] speculated that a mesoscale circulation induced by the land surface contrast is attributed to form the cloud near the irrigation district.

A contrast of land use often induces clouds and precipitation as pointed out in many studies [e.g., Chen and Avisser, 1994; Avissar and Liu, 1996; Lee and Kimura, 2001]. The clear contrast of land use around the Hetao Irrigation District may induce convective clouds. The objective of this study is to reveal the impact of the Hetao Irrigation District on cloud formation using a mesoscale numerical model. We focus on 4 August 2005 when the typical cloud distribution was observed (Figure 2).

2. Design of numerical experiments

Numerical experiments were conducted using a non-hydrostatic numerical model, Advanced Research Weather Research and Forecasting (WRF) modeling system Version 2.2 [Skamarock et al., 2005]. Two-way nested grid systems were adopted. The coarse grid system and the nested fine grid system have grid intervals of 15 km and 3 km, respectively. The initial and lateral boundary conditions for the coarse grid system are interpolated from the 6-hourly NCEP global tropospheric analysis data (1x1 degree grids). Two sensitivity experiments are conducted, i.e., experiments assuming and not assuming the Hetao Irrigation District (hereafter, SFC-WET run and SFC-DRY run, respectively). To evaluate the surface condition of the Hetao irrigation, we assume a distribution of simplified irrigated farm lands (hereafter, the irrigated area) in the SFC-WET run. The volumetric soil water content (hereafter, soil water content) is artificially kept at 0.4 in all soil layers within the irrigated area throughout the simulation, which corresponds to about 85 % of the saturated soil water content there. Besides the irrigated area, the soil water content derived from the NCEP global tropospheric analysis data is adopted as an initial value, and then the soil water content is predicted every time step. These experiments were conducted from 00 UTC 1 July 2005 to stabilize the surface soil conditions.

3. Results and Speculations

Figures 3a and 3b show the distributions of cloud water simulated by the SFC-WET run and the SFC-DRY run at 14 LST on 4 August 2005, respectively. The SFC-WET run simulates numerous clouds over the dry flat area and mountains (Figure 3a). In contrast, almost no clouds are simulated

over the irrigated area. The distribution of clouds is similar to the observation (Figure 2). In contrast, the SFC-DRY run simulates clouds not only over the dry area but also over the irrigated area (Figure 3b). The distribution of clouds in the SFC-DRY run differs from the observation.

Figures 3c and 3d show the land surface temperatures at 12 LST on 4 August 2005 simulated by the SFC-WET run and the SFC-DRY run, respectively. The low surface temperature over the mountains corresponds to the decrease of solar radiation by clouds and the cooling by rainfall. A clear contrast of the surface temperature is found between the irrigated area and the surrounding dry area in the SFC-WET run (Figure 3c). In the SFC-DRY run, the contrast of the surface temperature is quite small (less than 5 K) except for the northern mountain area which is covered by the clouds. These results suggest that the contrast of the surface temperature can affect cloud formation around the irrigated area.

Figure 4 illustrates vertical cross sections of simulated wind velocity and water vapor mixing ratio along the SW-NE section in Figure 1b at 14 LST on 4 August 2005. The altitude is almost 1,000 m along the SW-NE section. In the SFC-WET run, the southwestern component of wind is predominant over the southwestern dry area, while the northeastern component of wind is predominant over the northeastern irrigated area at the layers below 1,500 m (Figure 4a). The low surface temperature on the irrigated area (Figure 3c) produces wind that blows toward the dry area with high surface temperature. The two different winds at the lower level cause the convergence over the boundary between the dry area and irrigated area. Prominent upward and downward flows are found over the boundary of the dry area and the irrigated area, respectively. Therefore the SFC-WET run simulates a clear mesoscale circulation between the dry area and the irrigated area (hereafter, land-use-induced circulation) at the lower layer. The ascending flow of the land-use-induced circulation produces clouds without mountains and hills (clouds shown by vectors in Figure 3a). On the other hand, no significant circulations are simulated in the SFC-DRY run (Figure 4b).

Moreover, the irrigated area supplies much water vapor to the lower atmosphere in Figure 4a. The moist air goes toward the dry area and then ascends above the boundary between the irrigated area and the dry area. The land-use-induced circulation also transports the evapotranspired water vapor to the dry area and then helps the cloud forming.

The Hetao Irrigation District is surrounded by the Langshan Mountains and the Loess Plateau. During daytime, the mountain-valley circulation is predominant between the Hetao Irrigation District and the mountains. The circulation also induces the downward flow over the irrigated area and transports water vapor evapotranspired from the irrigated area to the mountainous area as well as the land-use-induced circulation (figure not shown). Therefore, the land-use-induced circulation and mountain-valley circulation inhibit cloud formation over the Hetao Irrigation District and transport water vapor from the irrigated area to the surrounding dry area.

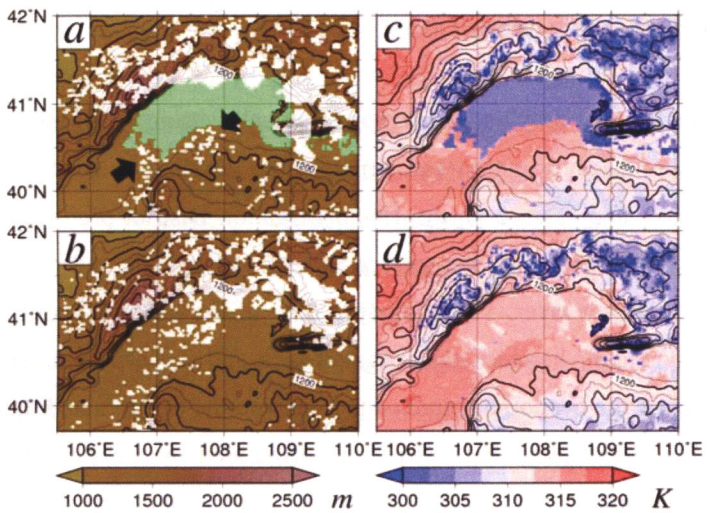

Fig. 3 Distributions of clouds at 14 LST (left) and surface temperature at 12 LST (right) simulated by the SFC-WET (top) and SFC-DRY (bottom) on 4 August 2005. The green area in Figure 3a shows the irrigated area.

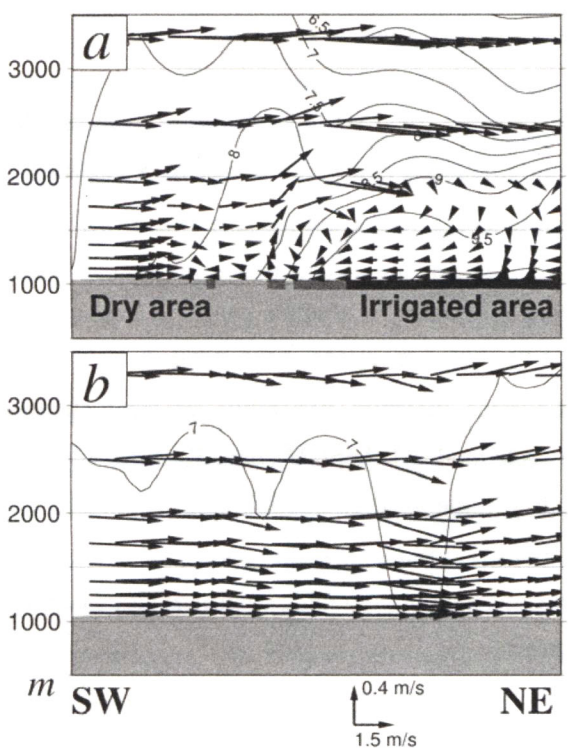

Fig.4 Vertical cross sections of wind velocity (vector) and water vapor mixing ratio [g/kg] (contour) along SW-NE in Figure 1b at 14 LST. (a) SFC-WET and (b) SFC-DRY. The winds are averaged across section SW-NE. A simple moving average is taken for five grids. Vectors are plotted every three grids in horizontal. The light-gray indicates topography. The black area shows that all of the averaged grids are the irrigated area. The dark-gray shows that the averaged grids include parts of the irrigated area.

5. Summary

An impact of the Hetao Irrigation District on cloud formation is revealed using WRF model. The numerical experiment assuming simplified irrigation can simulate the distribution of clouds observed by the satellite. The low surface temperature on the Hetao Irrigation District produces a wind that blows toward the surrounding dry area, where the surface temperature is high, and results in the land-use-induced circulation at the lower layer. The ascending flow of the land-use-induced circulation generates clouds over the boundary between the irrigated area and the dry area. The land-use-induced circulation also transports the evapotranspired water vapor to the dry area and then helps the cloud forming. Moreover, the Hetao Irrigation District is surrounded by the Langshan Mountains and the Loess Plateau. The mountain-valley circulation is also predominant between the Hetao Irrigation District and the mountains. The land-use-induced circulation and mountain-valley circulation inhibit cloud formations over the Hetao Irrigation District and transport water vapor from the irrigated area to the surrounding dry area.

Acknowledgments

This work was supported by Global Environment Research Fund (B-061) of the Ministry of the Environment and Ministry of Education, Culture, Sports, Science, and Technology (MEXT), Japan.

References

Avissar, R., and Y. Liu (1996), Three-dimensional numerical study of shallow convective clouds and precipitation induced by land surface forcing, J. Geophys. Res., 101, 7499-7518.

Chen, F and R. Avissar (1994), Impact of land-surface moisture variability on local shallow convective cumulus and precipitation in large-scale model, J. Appl. Meteor., 33, 1382-1401.

Lee, S. H., and F. Kimura (2001), Comparative studies in the local circulation induced by land-use and by topography, Bound. Layer Meteorol., 101, 157-182.

Sato, T., F. Kimura, and A. S. Hasegawa (2007), Vegetation and topographic control of cloud activity over arid/semiarid Asia, J. Geophys. Res., in press.

Skamarock, W. C., J. Dudhia, D. O. Gill, D. M. Barker, W. Wang, and J. G. Powers (2005), A description of the Advanced Research WRF version 2, NCAR Tech. Rep. TN-468, 100 pp.

Analysis of long-term water balance of the Yellow River basin
-Mechanisms of the drying-up-

Yoshinobu SATO[1], Akio Onishi[1], Yoshihiro Fukushima[1], Xieyao Ma[2], Jianqing Xu[2], Masayuki Matsuoka[3], Hongxing Zheng[4], Jianyao Chen[5]

[1]Research Institute for Humanity and Nature (RIHN)

[2]Frontier Research Center for Global Change (FRCGC)

[3]Kochi University

[4]Chinese Academy of Sciences (CAS)

[5]Zhongshan University

1. Introduction

In recent years, the river discharge in the lower reach of the Yellow River basin had decreased rapidly due to dry climate condition and heavy water demands. The river discharges observed at Huayuankou of the 1990s decreased almost half of the 1960s, and observed discharge at Lijin of the 1990s decreased less than one third of 1960s. Accordingly, the drying-up in the lower reach of the Yellow River basin occurred since 1972. The main factors to induce water shortage in the lower reach of the Yellow River basin are recognized as the increase in water consumption within the lower reach and decrease of river water supplied from its upstream. However, the contributions of these two factors had not been clarified quantitatively in the previous studies. Thus, in the present study, we attempted to clarify the mechanism of the drying-up of the Yellow River basin by long-term water balance analysis and several hydrological model simulations.

2. Data and Method

For the long-term analysis, we used 41 years (1960-2000) of daily observation data from 128 meteorological stations and interpolated them into 0.1° × 0.1° degree grid scales as the input parameters for the semi-distributed hydrological model. Then, to predict the evapotranspiration loss from various land use types, we applied a high resolution satellite remote sensing data as another input parameters. The remote sensing data includes the elevation, land surface classification map, and normalized difference vegetation index (NDVI) data sets, which were also converted into 0.1° × 0.1° degree grid scales. The hydrological model used in this study is based on the soil-vegetation-atmosphere transfer (SVAT) and hydrological cycle (HYCY) model, which is composed of the following three sub-models: a one dimensional heat balance model on the land surface, a runoff formation model and a river-routing network model. To understand the heat and water balances more precisely, the original model was modified as follows. First, the land surface was classified into five land-use types (bare, grassland, forest, irrigation area, and water surface). Then, potential evaporation was calculated using the heat balance models. The evapotranspiration

without soil water deficit from each vegetation surfaces was calculated from the potential evaporation using functions of the leaf area index (LAI). The LAI of each vegetation type was derived from monthly NDVI data set. Thus, seasonal and spatial variations of vegetation were considered in this model. Finally, actual evapotranspiration was estimated by regulating the evapotranspiration using functions of soil moisture content. However, this hydrological model could not predict long-term water balance of the Yellow River basin as it includes a lot of anthropogenic factors such as irrigation water intake, large reservoir operation, and human-induced land-use changes. Thus, in the present study, we considered these artificial factors in our model by applying simple sub-models for irrigation water intake, reservoir operation and land-use change. The details of model structure and parameters used in this study are summarized in Sato *et al.* (2007b).

3. Results and discussion

3.1. Performance of model simulation

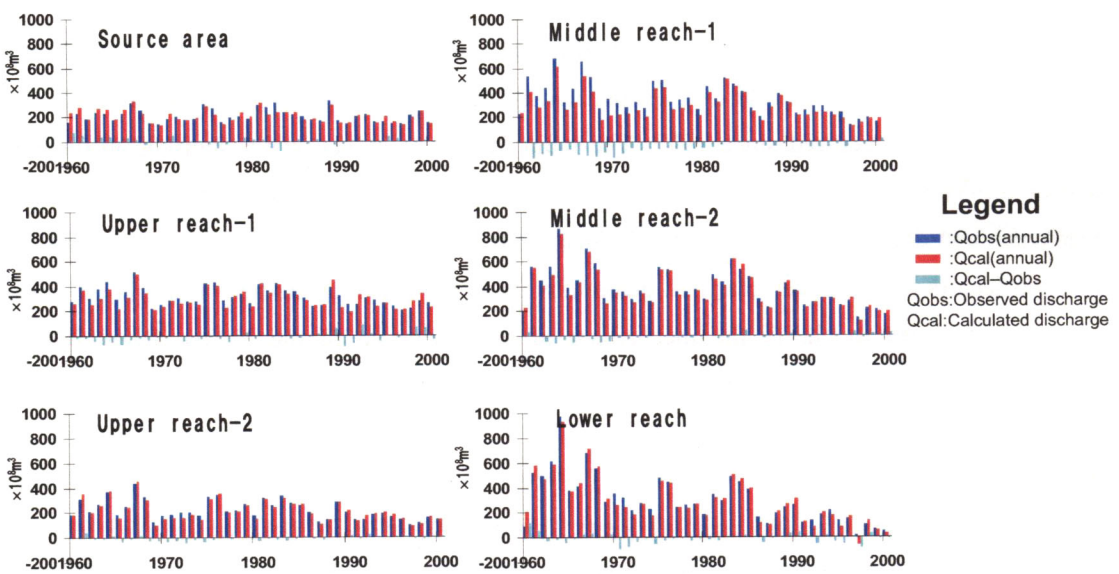

Figure 1 Performance of model simulation

The performances of the hydrological model applied in this study are shown in Figure 1. These figures indicate that the annual discharges from source area to lower reach during the past 40 years (1960 to 2000) estimated by the model (red bars) and observed results (blue bars). In this study, the Yellow River basin was divided into the following six sub-basins: (1) Source area (upstream of Tangnaihai), (2) Upper reach-1 (Tangnaihai to Lanzhou), (3) Upper reach-2 (Lanzhou to Toudaoguai), (4) Middle reach-1 (Toudaoguai to Sanmenxia), (5) Middle reach-2 (Sanmenxia to Huayuankou), and (6) Lower reach (downstream of Huayuankou). Although, we did not consider the influence of long-term land-use change in this model simulation, the observed discharges were reasonably captured by the model except for the Middle reach-1. Therefore, the influence of land-use

change on long-term water balance of the Yellow River basin will not be so severe. During the past several decades, natural vegetations on the Loess Plateau located in the middle reaches have been severely destroyed due to human activities. Thus, the soil and water conservation measures (massive vegetation recovery and land surface engineering) become effective since 1970s. And then, the water balance in the middle reach of the Yellow River basin had clearly changed since 1980s. However, the long-term changes of NDVI did not change significantly since 1980s. Therefore, we assumed that the land-use (vegetation) condition in the Loess Plateau had changed drastically until the 1980s. Thus, the underestimation of river discharge from the 1960s to 1970s in the middle reach of the Yellow River basin (Figure 1) was assumed to be overestimation of the evapotranspiration by the model. Then, to reduce the evapotranspiration from the Middle reach-1, we modified (reduced) the model parameter of vegetation cover ratio (VCR). The details of modification procedures of VCR are described in Sato *et al.* (2007a). After that, the estimation error decreased significantly (Figure 2). Therefore, we found that it is necessary to consider the influence of land-use change for estimating long-term water balance in the middle reach of the Yellow River basin.

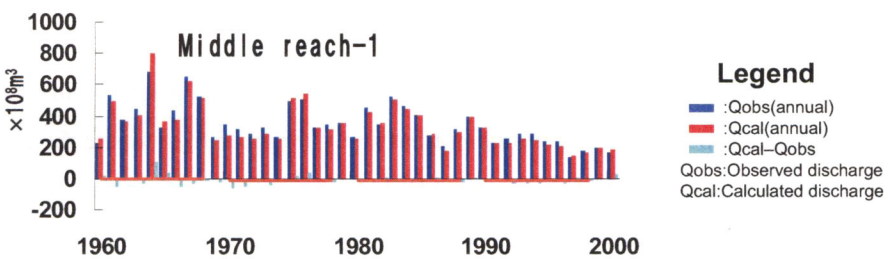

Figure 2 The results of modified model considering the land-use change in the middle reach of the Yellow River basin

3.2. Hydrological impact of soil and water conservation in the Loess Plateau

The massive land-use changes in the middle reach of the Yellow River basin also include "Land terracing", "Afforestation (tree and grass planting)", and "Silt-control" (check dam building) in the Loess Plateau. These land surface engineering will increase the amount of rainfall infiltration by reducing surface overland flow. Thus, to clarify the influence of the land-use change (soil and water conservation) more precisely, we considered the influence of the rainfall infiltration (soil permeability) as well as vegetation changes.

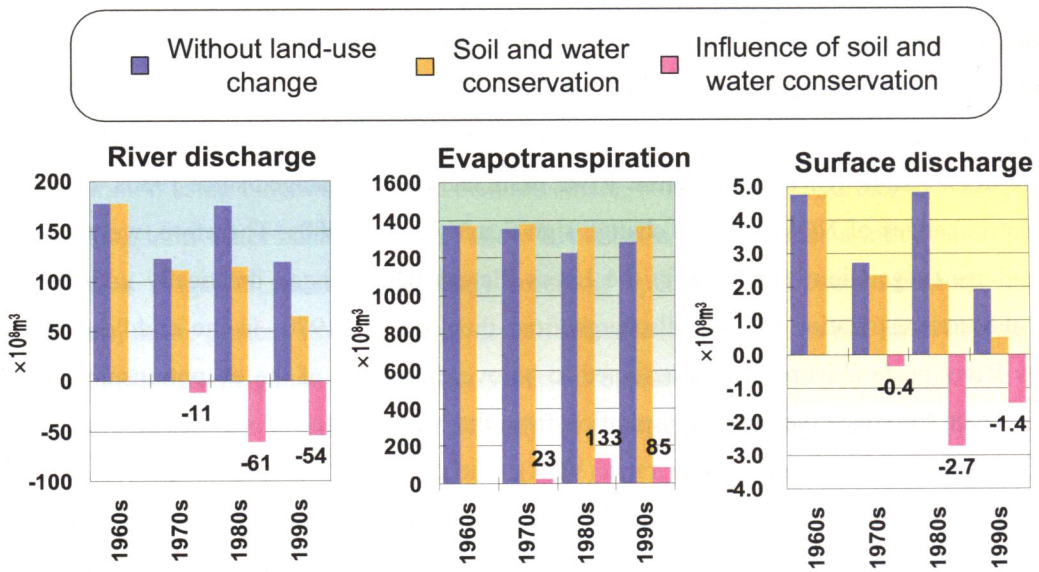

Figure 3 The influence of soil and water conservation in the Loess Plateau simulated by the model

Figure 3 indicates the influence of soil and water conservation on long-term water balance in the middle reach of the Yellow River basin. In the present study, we tried to compare the change of river discharge, evapotranspiration and surface (overland) flows due to soil and water conservation by the model simulation (Sato *et al.*, 2007a). According to these results, we can find that the model used in this study can simulate hydrological impact of soil and water conservation quantitatively as follows: The soil and water conservation will decrease the river discharge about 10-50%, and increase the evapotranspiration about 2-13%, and on the other hand, decrease the surface overland flow about 14-74%. These results suggested that the soil and water conservation will decrease not only soil erosions by decreasing surface (overland) flow, but also will decrease available water resources in the middle reach of the Yellow River basin by increasing evapotranspiration loss with the vegetation recovery.

3.3. Analysis of long-term water balance of the Yellow River basin

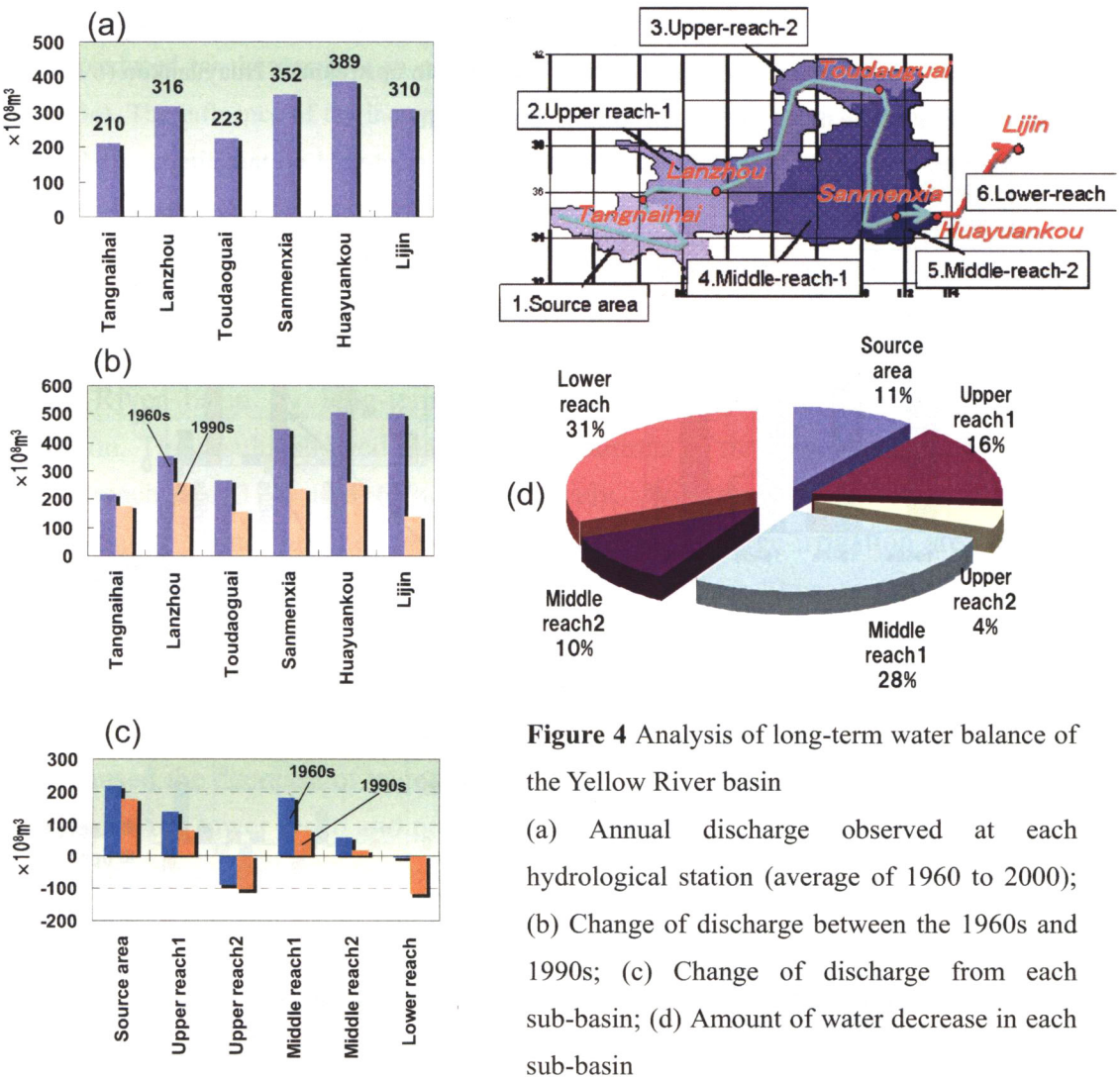

Figure 4 Analysis of long-term water balance of the Yellow River basin

(a) Annual discharge observed at each hydrological station (average of 1960 to 2000); (b) Change of discharge between the 1960s and 1990s; (c) Change of discharge from each sub-basin; (d) Amount of water decrease in each sub-basin

Figure 4a shows annual river discharge observed at each major hydrological station located in the main stream of the Yellow River. From this figure, we can find that there are two sinks in observed river discharge at Toudaoguai and Lijin. It is probably because large amounts of water intake from river channel to the large irrigation areas located in these relatively dry regions. According to the Figure 4b, we can notice that all the hydrological station's discharges had decreased, and consequently, the discharge near the river mouth (observed discharge at Lijin) had decreased almost 36 billion m^3 during the past 40 years. Figure 4c also indicates that there are 'source' and 'sink' in the Yellow River basin. From this figure, we can find that most of river water supplied from source area and middle reach-1. However, the amount of water supplied from middle reach had decreased drastically during the past 40 years. On the other hand, in spite of the amount of water consumption in the upper reach-2 had not changed so much, the rapid increase in water consumption had occurred in the lower reach (Figure 4c). Finally, from the result of figure 4d, we can see that the water

shortage in the lower reach of the Yellow River basin (decrease of observed river discharge at Lijin: 36 billion m^3) was induced by the following two factors: (1) increase in water consumption within the lower reaches (31%) and (2) decrease in water supply from upstream of Huayuankou (69%).

3.4. Mechanisms of the drying up of the Yellow River basin

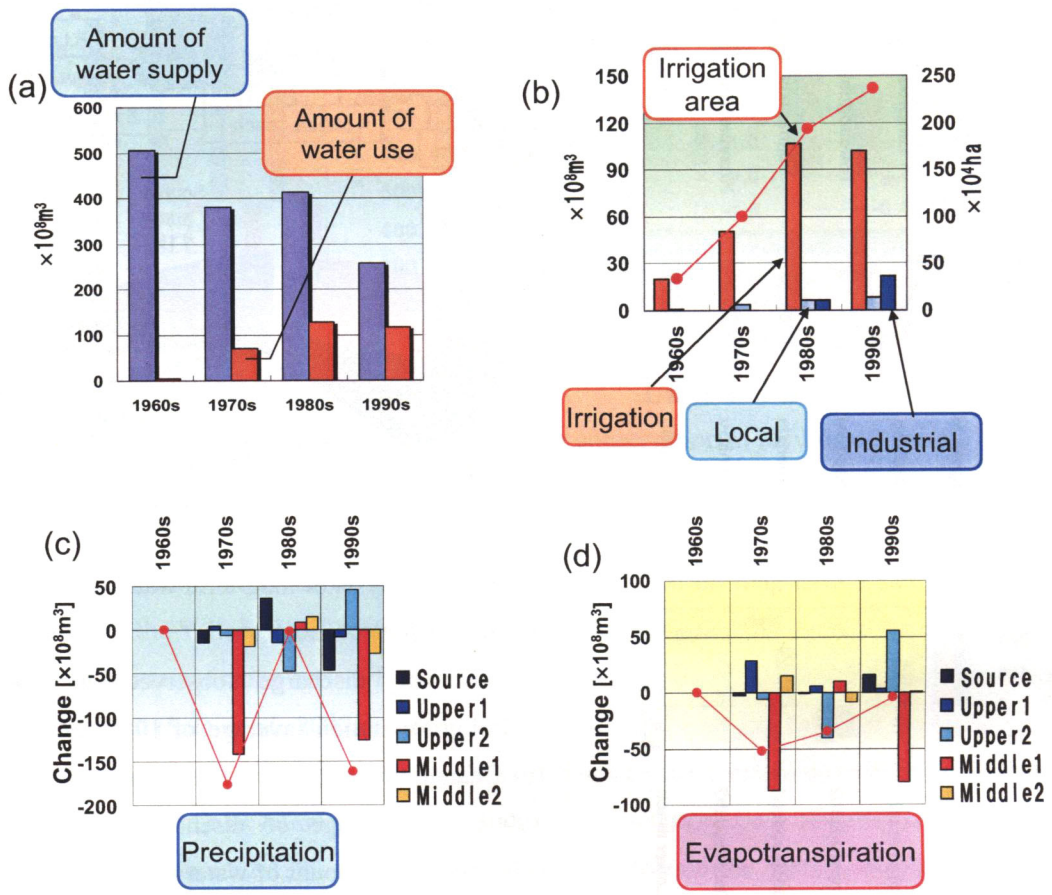

Figure 5 Mechanisms of the drying-up of the Yellow River basin

(a) Decadal change of water supply for the lower reach and water use within the lower reach; (b) Decadal change of irrigation area, irrigation water use, local water use and industrial water use within the lower reach; (c) Decadal change of precipitation from source area to middle reach-2; (d) Decadal change of evapotranspiration from source area to middle reach-2

According to the decadal analysis of the water use within the lower reach and the water supply to the lower reach, we can find that the water use within lower reach increased between the 1960s to the 1980s and water supply to the lower reach decreased in the 1970s and the 1990s (Figure 5a). The major reason of the increase in water use within the lower reach can be due to the increase in irrigation water use with the increase of irrigation areas from the 1960s to the 1980s (Figure 5b). However, despite of the increase in irrigation area from the 1980s to 1990s, the amount of irrigation water use did not change. This is probably because the influence of climate conditions (i.e. decrease

in sunshine duration) will decrease the amount of potential evaporation or the efficiency of water use might improved in the lower reach after the 1980s. The decrease in water supply to the lower reach must be induced by the decrease in precipitation in the middle reach-2 in the 1970s and 1980s (Figure 5c). The influence of the increase in evapotranspiration with the increase of air temperature will not be so significant on long-term water balance of the Yellow River basin compared with the influence of the precipitation change (Figure 5d).

4. Conclusion

In the present study, we attempted to clarify the mechanisms of the drying-up of the Yellow River basin by long-term water balance analysis and hydrological model simulation. The results showed that the contributions of the lower reach and upper and middle reach are 31% and 69%, respectively. According to the results of model simulation, we found that the water consumption in the large irrigation area located in the upper reach did not change significantly during the past 40 years. On the other hand, the water consumption in the irrigation area located around the lower reach had increased significantly during the period from 1960s to 1980s. Furthermore, it was found that the rapid decreases in precipitation in the middle reach-2 in the 1970s and the 1990s caused the decrease of water supply to the lower reach. Compared with irrigation water use in the lower reach and precipitation change in the middle reach, the impact of rise in temperature and vegetation change on long-term water balance were found to be negligible. These results will contribute to the integrated water resources management in the Yellow River basin, such as the more adequate water allocation or soil and water conservation.

REFERENCES

Sato *et al.* (2007a): Impacts of human activity on long-term water balance in the middle-reaches of the Yellow River basin. *IAHS Publication* 315: 85-88

Sato *et al.* (2007b): Analysis of long-term water balance in the source area of the Yellow River basin. *Hydrological Processes*, DOI: 10.1002/hyp.6730

Published by

Y R I S PROJECT Prof. Fukushima Yoshihiro

Inter-University Research Institute Corporatior
Research Institute for Humanity and Nature
457-4 Kamigamo Motoyama ,Kita-ku,Kyoto
603-8047 JAPAN
URL : http://www.chikyu.ac.jp/yris/
February 1, 2008